AN EXPERIMENTAL AND ANALYTICAL INVESTIGATION

OF THE

IOSIPESCU SHEAR TEST FOR COMPOSITE MATERIALS

by

Barry Stuart Spigel
B.S., December 1980
Virginia Polytechnic Institute and State University

A Thesis Submitted to the Faculty of
Old Dominion University in Partial Fulfillment of the
Requirements for the Degree of

MASTER OF SCIENCE

ENGINEERING MECHANICS

OLD DOMINION UNIVERSITY
August, 1984

Approved by:

_____

_____

_____

ABSTRACT

AN EXPERIMENTAL AND ANALYTICAL INVESTIGATION
OF THE
IOSIPESCU SHEAR TEST FOR COMPOSITE MATERIALS

Barry Stuart Spigel
Old Dominion University, 1984
Director: Dr. R. Prabhakaran

Mechanical properties of composite materials under shear loading are difficult to determine. The Iosipescu Shear test, originally proposed for metals, has in recent years been applied to composites. It has the advantages of small specimen size, simple loading and a reasonably uniform shear stress in the test section.

The purpose of this work is to study the validity of the Iosipescu test method for measuring the shear modulus and shear strength of composites. Finite element analyses indicate that optimum specimen geometry and load locations depend upon the degree of orthotropy of the composite. Test results for a quasi-isotropic graphite/epoxy laminate show that modifications in the notch geometry aimed at improving stress distributions result in unexpected changes in the failure mode. Thus, while the Iosipescu Shear test is valid for some composites with a suitable choice of test parameters, its validity for other composites, especially with a higher orthotropy, is doubtful.

ACKNOWLEDGMENTS

The author is grateful to Dr. James W. Sawyer of NASA's Langley Research Center and Drs. R. Prabhakaran and A. Sidney Roberts of Old Dominion University for their guidance and contributions to this work. This work was supported through the Old Dominion University Aeronautics Program sponsored by NASA Langley Research Center.

TABLE OF CONTENTS

LIST OF TABLES

LIST OF FIGURES

Chapter 1

INTRODUCTION

The increasing use of composites as high performance structural materials in modern aerospace vehicles necessitates the accurate determination of the composite material's response to thermal and mechanical loads. Testing provides the means to determine these characteristics of composite materials under controlled conditions. The tensile, compressive and shear properties, whether in-plane or interlaminar, are most often determined by materials testing and not from complex theoretical analyses. Design information for composite materials is also obtained from experimental testing.

Yet composite materials test techniques are plagued with certain limitations. Current test methods are largely based upon technology developed for wood, metals and adhesives. While the test techniques may be applicable to tensile and compressive tests of composites, it does not appear that a test method which induces a state of pure shear in metals or adhesives will induce a state of pure shear in a composite material. Coupling effects, nonlinear behavior of the matrix or the fiber/matrix interface, laminate geometry and the presence of normal stresses all conspire against a state of pure shear in a composite.

Pagano [1]* notes that a state of pure shear does not exist in any of the current test methods. It is pointed out that the complex, unknown stresses which occur in these tests render the application of the results fortuitous. Prosen [2] contends that even though pure shear does not occur in a test method, this does not mean that the test provides useless information. Many test methods have helped advance the state of the art in fibrous composites. Yet for the research and development engineer who is investigating interfacial adhesion, matrix failure or developing a design philosophy incorporating realistic failure criteria, a pure, uniform shear stress is desirable in a composite material shear test [3,4,5]. For him the ideal shear test should [4,6]:

1. Be mechanically simple and require no special equipment
2. Use small specimens with simple geometry and not require extensive specimen preparation
3. Provide reproducible results
4. Have a simple data reduction procedure
5. Produce an unambiguous state of pure shear

One or more of these requirements is lacking in current shear test methods.

Indeed, so many methods and variations of each method have been developed to measure the shear response to composites, that there is now much confusion as to which technique is applicable to a specific investigation. The following review of shear tests briefly describes the test technique and states whether the method determines the shear

---

*The numbers in brackets indicate references.

strength, the shear modulus or both. The advantages and disadvantages of each test are discussed and the usefulness of the test method for determining design data or quality control information is also mentioned.

Chapter 2

LITERATURE REVIEW OF SHEAR TEST METHODS

2.1 NOL Ring Test and Short Beam Shear

In the late 1940's and early 1950's, the advancements in manufacturing glass-fiber reinforced plastics made it necessary to devise a reliable test method in order to evaluate the effectiveness of various surface treatments. The Naval Ordnance Laboratory developed a simple, reproducible procedure known as the NOL Ring test. This method involved testing a six-inch diameter ring in tension or in flexure. Lyle [3] reports, however, that the NOL scientists determined that a ring tensile test or a ring flexure test did not differentiate between surface treatments of the fibers. The Naval Ordnance Laboratory then developed a horizontal shear test utilizing a one-inch convex specimen cut from a ring of material as shown on Fig. 2.1. This, they believed, would give an indication of the adhesion between the glass fibers and the resin. This test procedure, termed the Horizontal Ring Shear Method, would be the predecessor to what today is known as the Short Beam Shear test. Lyle presents a fascinating account on the development and history of the NOL Ring test and the Horizontal Ring Shear Method.

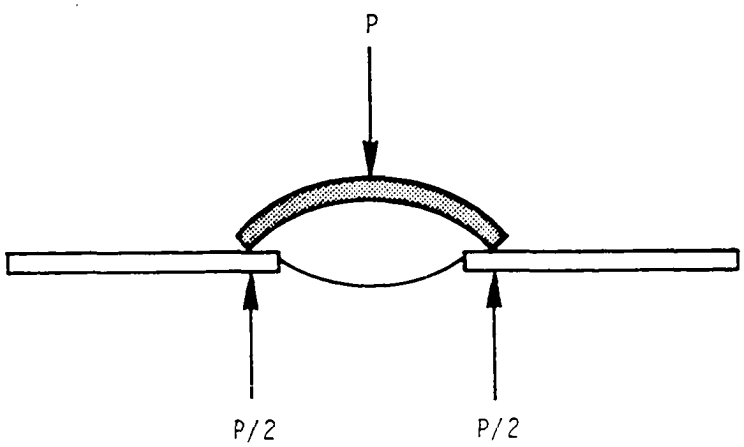

Fig. 2.1. The NOL Ring test.

As the potential use of composite materials increased during the mid-1960's, the Horizontal Ring/Short Beam Shear test was evaluated as a candidate test for determination of interlaminar shear strength. In 1965, the Short Beam Shear test was accepted as a standard test method (ASTM D2344-76).

Essentially, this test method is nothing more than a short beam supported by two rods with a third rod applying a small deflection to the beam's mid-section. A sketch is given on Fig. 2.2. Based upon elementary beam theory, the shear stress distribution through the thickness of the specimen is a parabolic function which is zero at the upper and lower surfaces and is a maximum at the center. The method's simplicity and economical use of material has led to its wide acceptance in the composite materials industry.

Lately, however, the Short Beam Shear test has been subjected to increasing criticism. Markham and Dawson [7] state that the ratio of beam length to thickness must be five or less, otherwise a bending failure may occur. Further, defects in the material may precipitate a failure other than pure shear along the mid-plane. The authors also state that the shear stress distribution is sensitive to minor eccentricities of the rollers used to apply the loads. Berg et al. [8] show that the shear stress varies along the length of the beam and that the maximum shear stress occurs off of the symmetry axis. Phillips and Scott [9], in addition to verifying a non-uniform stress state, point out other problems due to combined stress states and severe stress concentrations at loading points. Chiao, Moore and Chiao [4] state that Short Beam Shear test results are not always reproducible even when the

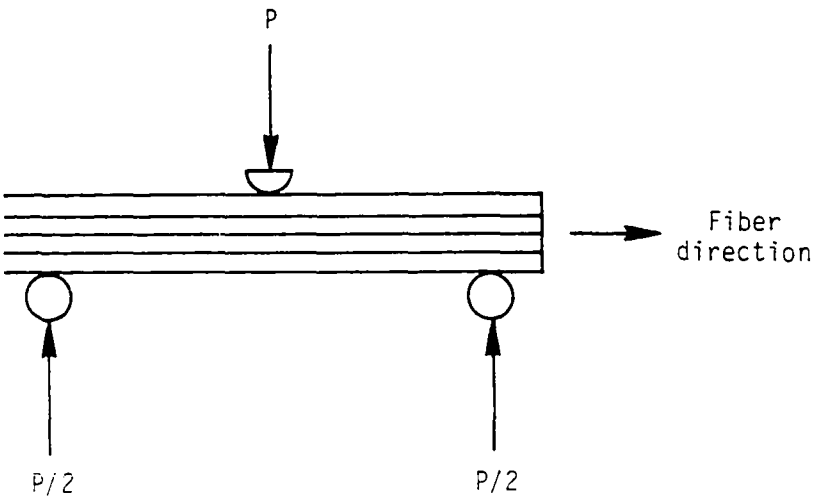

Fig. 2.2. The Short Beam Shear test.

material is made by the same process and specimens are tested by the same person.

The Short Beam Shear test is questionable for determining design data. Yet because of its simplicity and economy, the test procedure is frequently used to evaluate candidate composite materials and, as a comparative test method, to control material quality. Yet Stinchcomb et al. [10], found that the true shear strength of a good quality specimen could not be determined using the Short Beam Shear test since the specimen failed in some mode other than pure shear - in this case microbuckling or a combination of shear and microbuckling. Shear failure occurred only in specimens which had severe defects or poor quality bonding.

2.2 Block Shear

Originally developed to determine the shear strength of wood and the shear strength of a glue bond between blocks of wood, the Block Shear test was first examined as a possible interlaminar shear strength test for glass-fiber composites in the mid-1950's. In the basic Block Shear test, shown in Fig. 2.3, a part of the specimen is sheared-off under a compressive force. But due to the antisymmetric loading, an overturning moment is developed which must be counteracted. This requires rather bulky apparatus [11]. Another complication for this test method is that the end-bearing compressive strength is low for composite materials and the loading may tend to crush a specimen [12]. Also, another principal disadvantage of conducting this test is that the moments and compressive loads must be handled in the test section.

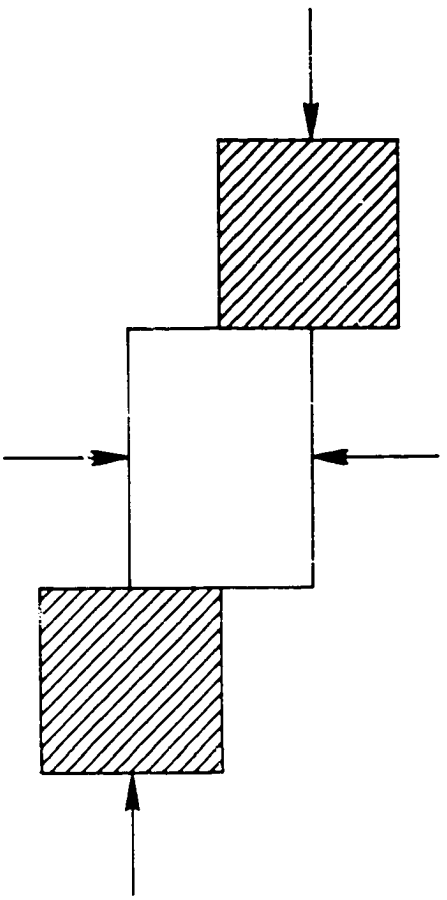

Fig. 2.3. The Block Shear test.

It was stated by Werren and Heebink [11] and Zabora and Bell [12] that the Block Shear test does not produce a state of pure shear. For example, the specimen rotation induced by the eccentric loads resulted in localized normal loading along the shear plane.

One method to eliminate the eccentric loading, and hence the overturning moment, is to utilize the Symmetric Block Shear fixture as depicted in Fig. 2.4. Also known as Johnson Shear or Punch Shear, the Symmetric Block Shear test employs two supporting blocks at the specimen ends as a third block cuts through the specimen in two parallel cross-sections similar to a punching device. Although the bending moment is eliminated, a pure shear stress state is still not obtained. Iosipescu [13] showed that stress concentrations are produced at the contact points between the punching tool and the test specimen. Flexure stresses, particularly in an interlaminar shear test, must also be taken into account.

Peters [14], however, determined that the Symmetric Block Shear test was useful under certain constraints. Basically, any differences in shear deformation between the two shear planes or any unequal shear deformation due to dimensional inaccuracies of the specimen was compensated by a matrix with high plasticity and the slow growth of shear cracks. Further, frictional forces resulting from the section of specimen being pushed into the fixture were not too high. The author found that the Symmetric Block Shear test resulted in better interlaminar shear strength data than the Short Beam Shear test.

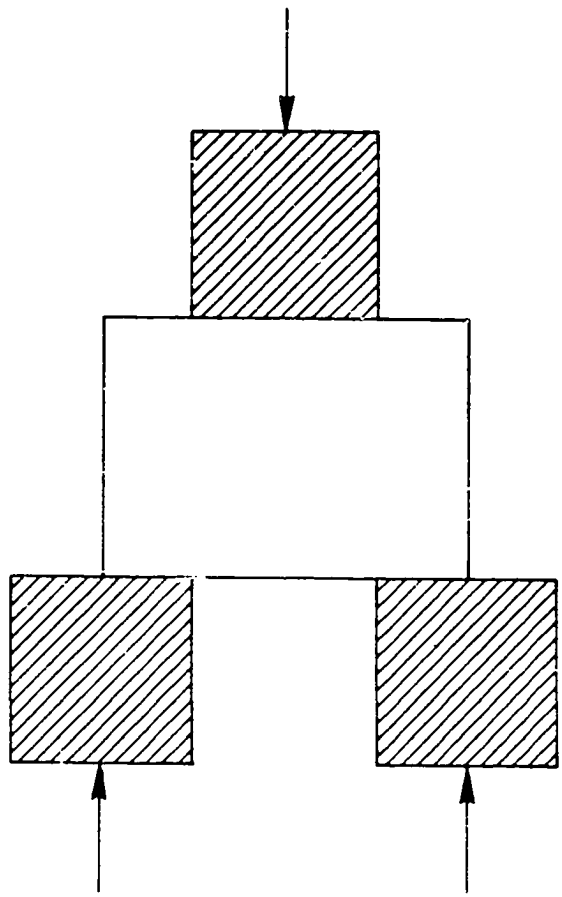

Fig. 2.4. The Symmetric Block Shear test.

The Symmetric Block Shear test serves the same purpose as the Short Beam Shear test. While the shear values are not the true shear strength of the material due to the presence of stress concentrations, this method can be expected to show the relative shear strength of different materials.

2.3 Torsional Shear of a Thin-Walled Tube

The torsional shear of a thin-walled circular tube is considered the most desirable method to obtain both the shear strength and the shear modulus of a material. It is accepted as an ASTM Standard (ASTM E143-61). Essentially, a torque is applied to a tube about its longitudinal axis, subjecting the walls of the cylinder to a state of pure shear stress as shown on Fig. 2.5. The shear strain gradient is considered negligible since the wall thickness is small compared to the tube's mean radius.

Though from the applied mechanics viewpoint this is the ideal shear test, the torsional tube presents many problems to the experimentalist. Cost of fabricating tubular specimens can be prohibitive. Preparation of a tube is time-intensive and requires more material than a flat specimen. Composite tubes can also be extremely fragile and difficult to handle. Further, the specimen must be mounted concentrically in the test apparatus to prevent the introduction of bending moments and the tube must be free to move axially to avoid introducing axial forces. Buckling of the tube must also be prevented. This requires special test equipment which can be expensive to manufacture.

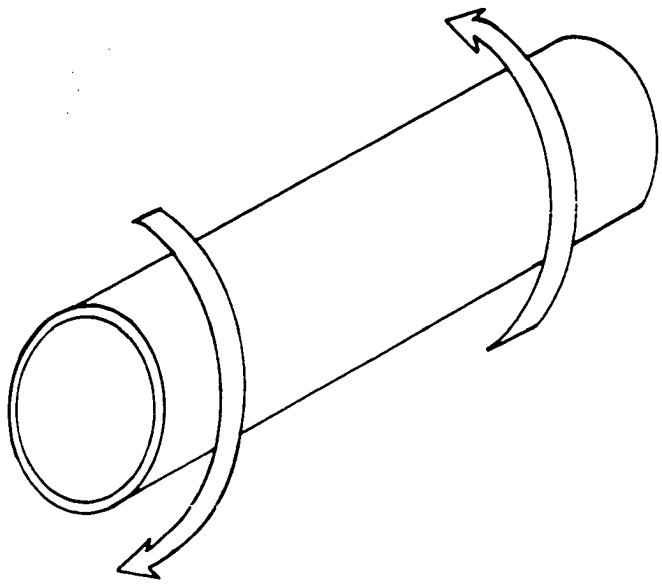

Fig. 2.5. Torsional shear of a thin-walled tube.

It is the exorbitant cost of performing a torsional tube test that forbids it from being a popular shear test for use in both the laboratory and industry. Yet when shear properties from this test are available, these values are the standard by which results from other shear tests are judged.

2.4 Torsional Shear of a Unidirectional Rod

The torsional shear of a unidirectional rod is similar to the torsional tube test except that a small molded rod is utilized instead of a hollow tube. The same restrictions that applied to the tube are also applicable to the rod. There are, however, additional advantages and disadvantages.

The most important distinction between the two tests is that the shear strain in the rod is not constant over the entire cross-section. A maximum shear strain occurs at the outer surface. Chiao, Moore and Chiao [4] found that the moduli calculated from strain gages mounted on the surface were 13 percent higher than the moduli determined from torsional tube tests. The authors also calculated the shear strains from the angle of twist and found these values to be consistently higher than the results from the strain gages. The failure stress for the torsional rod was similar to the failure stress for the torsional tube.

Another disadvantage of the torsional rod shear test is that if inelastic deformation occurs prior to failure, the results may be ambiguous. Yet Pagano [1] notes that the torsional rod is more economical than the torsional tube and is more representative of actual composite fabrication techniques. Further, the rod is insensitive to end effects.

But because the torsional rod shear test is also expensive to conduct, it has been necessary to search for other less costly shear tests.

2.5 Slotted Shear

The Slotted Shear specimen has been used to determine the shear properties of concrete, metals and composite materials. Various configurations are given in Fig. 2.6. There are, however, fundamental limitations to the specimen design which prevents this test method from becoming a viable, low-cost alternative to the torsional tube tests for accurately determining a material's shear properties. The very nature of a slot in the material produces stress concentrations which act at the ends of the test section. Iosipescu [13] determined that the fracture of the specimen was initiated by these stress concentrations. Bergner, Davis and Herakovich [15] showed that the stress concentrations also produce high normal stresses in the test section.

The Slotted Shear test does not produce nor even approximate a pure, uniform shear stress in the test section. Hence, this method is unacceptable for quantitatively determining the shear behavior of a material and is seldom used.

2.6 Double-Notched Laminate Shear

The Double-Notched Laminate Shear test is used for determining the interlaminar shear strength of composite materials. This shear test utilizes a flat-plate specimen which has one groove cut to half the thickness in each face. A typical specimen is shown on Fig. 2.7. Theoretically, a tensile load is distributed along the central section

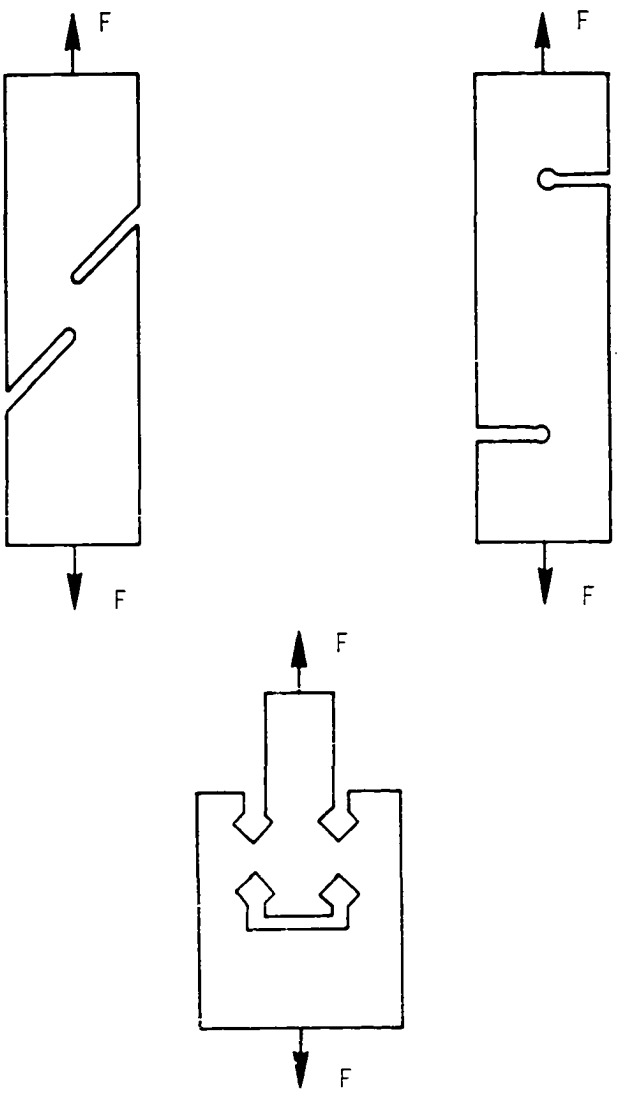

Fig. 2.6. Slotted Shear test specimens.

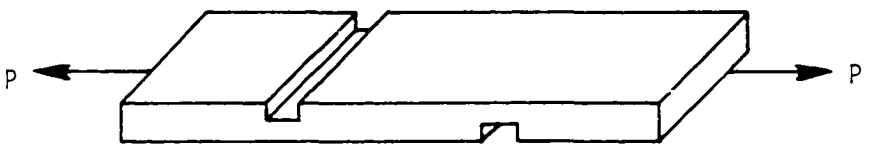

Fig. 2.7. Double-Notched Laminate Shear test.

between the grooves, resulting in pure shear on the central plane. This shear test is an ASTM standard (ASTM D3846-79) for determining the in-plane shear strength of thermosetting plastics. The double-notched specimen has also been adapted for determining the shear strength of pultruded, uniaxially aligned glass fiber/resin composites. In this case, small round specimens are loaded in compression as short columns to induce shear fractures between the notches [16].

Many researchers have found, however, that the Double-Notched Laminate test is dependent upon the specimen dimensions. Markham and Dawson [7] determined that the ratio of specimen thickness to the distance between notches was an important parameter for proper stress distribution. The mathematical theory developed by the authors allowed them to obtain consistent shear strength data from their experimental tests, even though their theory did not take into account the effects of bending or stress concentrations at the notches. Romstad [17] pointed out that longer shear lengths are influenced by large tensile stresses which develop at the ends of the shear area. With shorter shear lengths, it was difficult to notch the specimen accurately and the standard deviation of the data increased. Furthermore, any weaknesses along the shear plane had a pronounced effect on the shear strength.

Chiao, Moore and Chiao [4] found it very difficult to cut the grooves to precisely half the depth of the specimen. A slight undercut resulted in a higher shear strength than an overcut. Some tearing of fibers was noticed in undercut specimens whereas bending and peeling were observed in overcut specimens.

It is possible to use the Double-Notch Laminate Shear test for comparative purposes as long as standard test specimens are used. Yet

compared to the Short Beam Shear test, the precise machining of the specimens and the presence of stress concentrations would tend to limit the usefulness of the Double-Notched Laminate test.

2.7 Rail Shear

The Rail Shear test is one of the most analyzed and best accepted methods for determining the in-plane shear modulus of composite materials. Though design data is often quoted from the results of a Rail Shear experiment, the test method is not without its limitations.

Ideally, a plate specimen is gripped along each side of a long, narrow central region and a shear stress is applied by loading the grips in tension, as shown on Fig. 2.8. The central region is then assumed to be in a state of pure shear. Whitney, Stansbarger and Howell's [18] classic analysis of the Rail Shear test revealed that the ratio of length to width should be greater than ten. This ratio would achieve nearly uniform shear in the test section and would minimize any free edge effects. Yet Bergner, Davis and Herakovich [15] found that significant normal stresses were present in the test section and that these normal stresses were dependent upon the method by which the load was applied, the stiffness of the rails and the properties of the laminated composite. Indeed, a ±45-laminate with its inherent high Poisson's ratio made it particularly difficult to achieve a uniform shear stress. This laminate also gave rise to severe stress concentrations at the edges [6,18].

Duggan [19] also observed problems with the load fixtures. He remarked that "the bolts clamping the two sets of rails together required frequent retightening throughout the test, even in the case of low-strength materials and with high-friction gratings between the

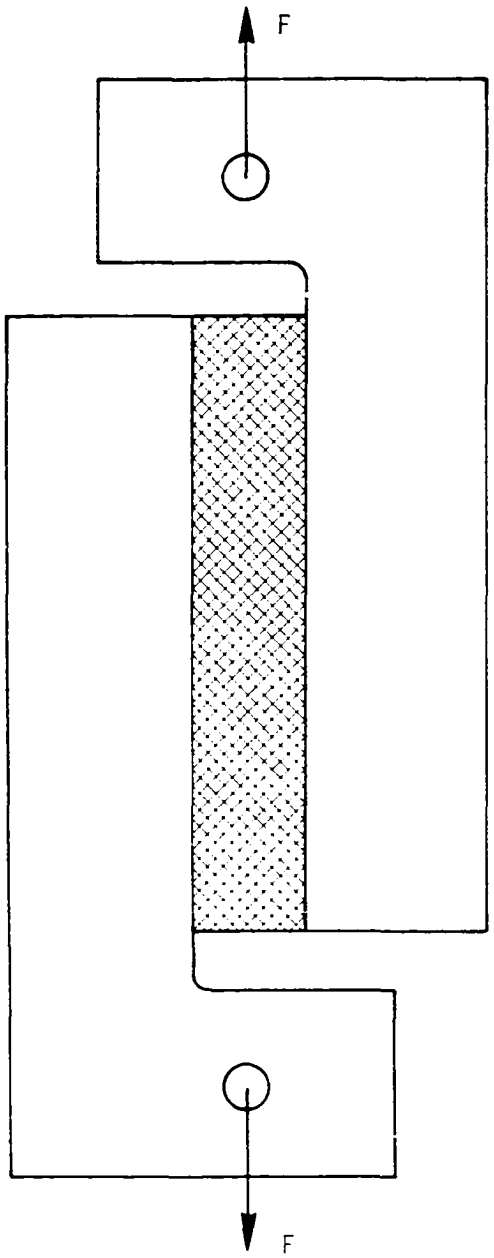

Fig. 2.8. The Rail shear test.

specimen and the steel rails. In most cases it proved impossible to fail the higher stiffness laminates because the steel rails could not be prevented from slipping on the specimen" [19].

The standard Rail Shear test is simple in application and specimen geometry, but the non-homogeneous state of stress caused by the grips, particularly at the corners [20] and free edges [15], makes this test applicable for determining only the shear modulus. Experimental results have shown excellent agreement with laminate theory for in-plane shear moduli [18]. Yet the material, fixture and labor costs and the unsymmetric loading (relative to the specimen) tend to make the Rail Shear test undesirable.

A modified Rail Shear method, the Symmetric or Double Rail Shear test, as shown on Fig. 2.9, avoids the unsymmetric load but does not solve the problems of high fixture and labor costs and the need for large amounts of material [21]. Sims' [22] modulus experiments with the Symmetric Rail Shear test were in good agreement with Torsion Tube tests and ±45-degree Shear tests.

2.8 Double-Lap Shear

The Double-Lap Shear or Modified-Lap Shear method is a hybrid between the Rail Shear test and the Lap-Shear test for adhesives (ASTM D4027-81). A unidirectional laminate is bonded, not clamped, between two metal bars and then loaded in a manner similar to the Rail Shear test as shown on Fig. 2.10.

With most laminates it is impossible to obtain a failure because the epoxy bonding the specimen to the bars is not as strong as the reinforced matrix. However, if the laminates are thick, say a few millimeters, it may be possible to obtain an interlaminar shear modulus

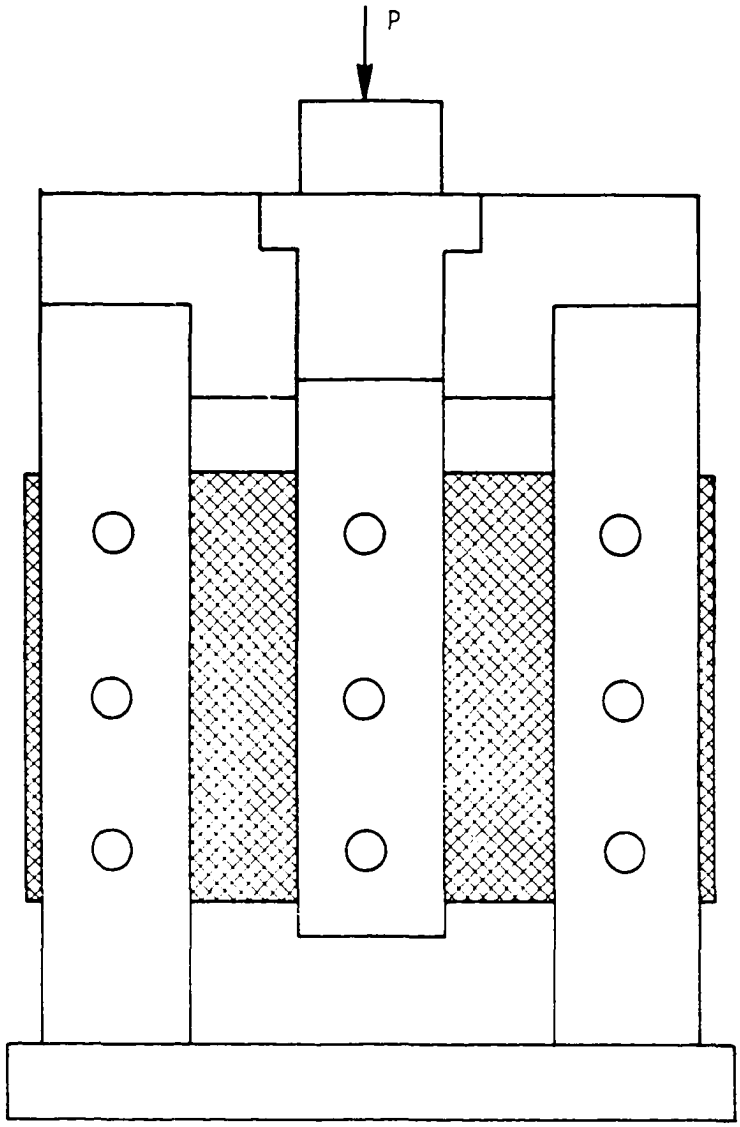

Fig. 2.9. The Symmetric Rail Shear test.

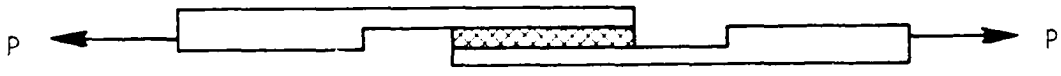

Fig. 2.10. The Double-Lap Shear test.

by orienting a strain gage to sense the normal strains at the midplane along the specimen's sides [19]. But the reliability of this modulus value must be questioned.

Adsit et al. [23] identified reasons why the Double-Lap Shear test cannot be used for determining material strengths. The authors stated that a pure shear stress was not even approximately produced in the material at critical points. Also, they could not determine if the failure was initiated by tensile or shear stresses and they felt that the failure was due to a combination of both forces.

Thus, based upon the fact that the stress state produced in a material by this method is not one of pure shear and that the failure mode is ambiguous, it is questionable if even an accurate shear modulus can be obtained.

2.9 Slant Shear

Kadotani and Aki [24] have suggested a new method for the determination of interlaminar shear strength called the Slant Shear test. Basically this method is an adaptation of the Lap Shear test. A sketch is given on Fig. 2.11.

The test apparatus consisted of three metal pieces and two specimens bonded together. The end pieces contained holes which were used to pull the fixture. Otherwise the fixture could be loaded in compression. Three fixtures were used in this first analysis, each having a different angle of inclination (27, 37 and 45 degrees). In this manner the specimens were subjected to a shear stress together with either a compressive or tensile stress. From the apparent shear strength obtained from the three sets of data, the authors were able to extrapolate the results and obtain the intrinsic shear strength.

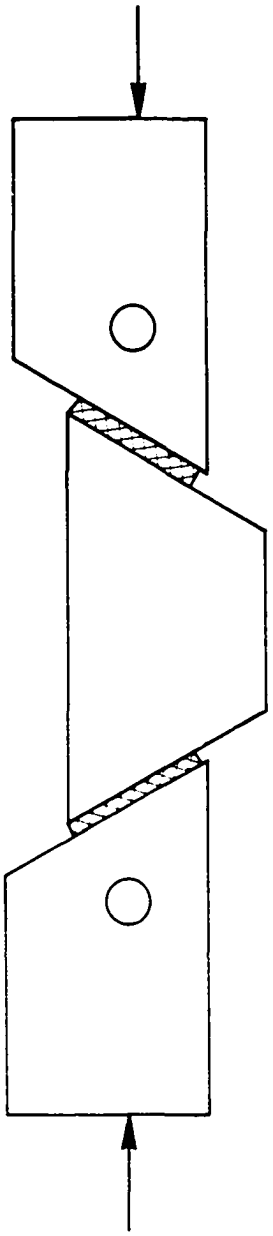

Fig. 2.11. The Slant Shear test.

Acknowledging that some stress concentrations could occur and thus affect the results, the authors compared their results to Lap Shear, Short Beam Shear and Torsional Shear tests. (Note that the Torsional Shear was not a tube test, rather it is another modification to a Lap Shear test. The test method is depicted on Fig. 2.12.) The authors compared the apparent strengths from the above three tests with the intrinsic strength determined by the Slant Shear, and they determined that the additional compressive or tensile stresses present in the tests had a considerable influence on the apparent shear strength. The authors listed the shear strengths in decreasing order: Lap Shear, Torsion Shear, intrinsic strength from Slant Shear and Short Beam Shear.

Since this was the first paper describing this shear test method, closer examination of this test is required. Its limitations, however, may be similar to those of the Double-Lap Shear test. Obviously, one must question the magnitude and extent of the stress concentrations and their effect on the test results as well as the failure mode of the test specimen. Also, it takes multiple tests to obtain one shear strength value.

2.10 Picture-Frame Shear

The Picture-Frame Shear test measures the in-plane shear response of a composite material. This test applies a uniaxial tensile or compressive load at two diagonally opposite corners of a rigid frame which is attached to the edges of a plate specimen, as shown on Fig. 2.13. In order to reduce high corner stresses, the frame is pinned to the specimen such that the shear deformation is not resisted by bending moments at the corners [25]. The corners are usually cutout and have

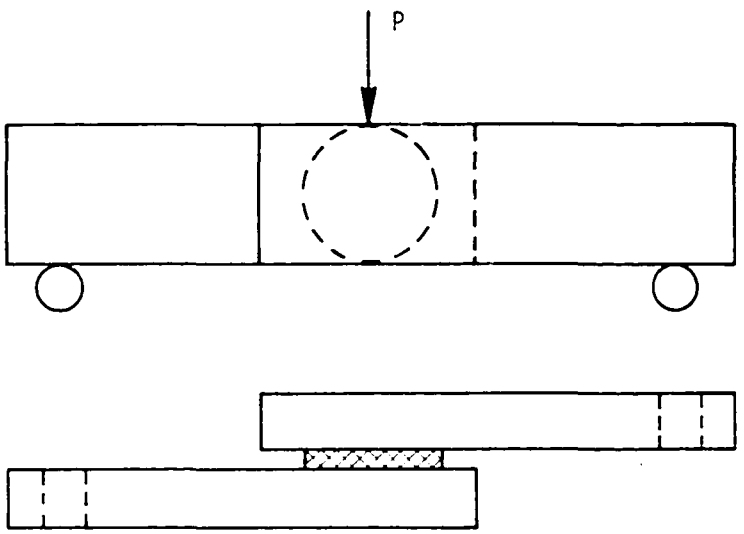

Fig. 2.12. Torsional shear of a thin disk.

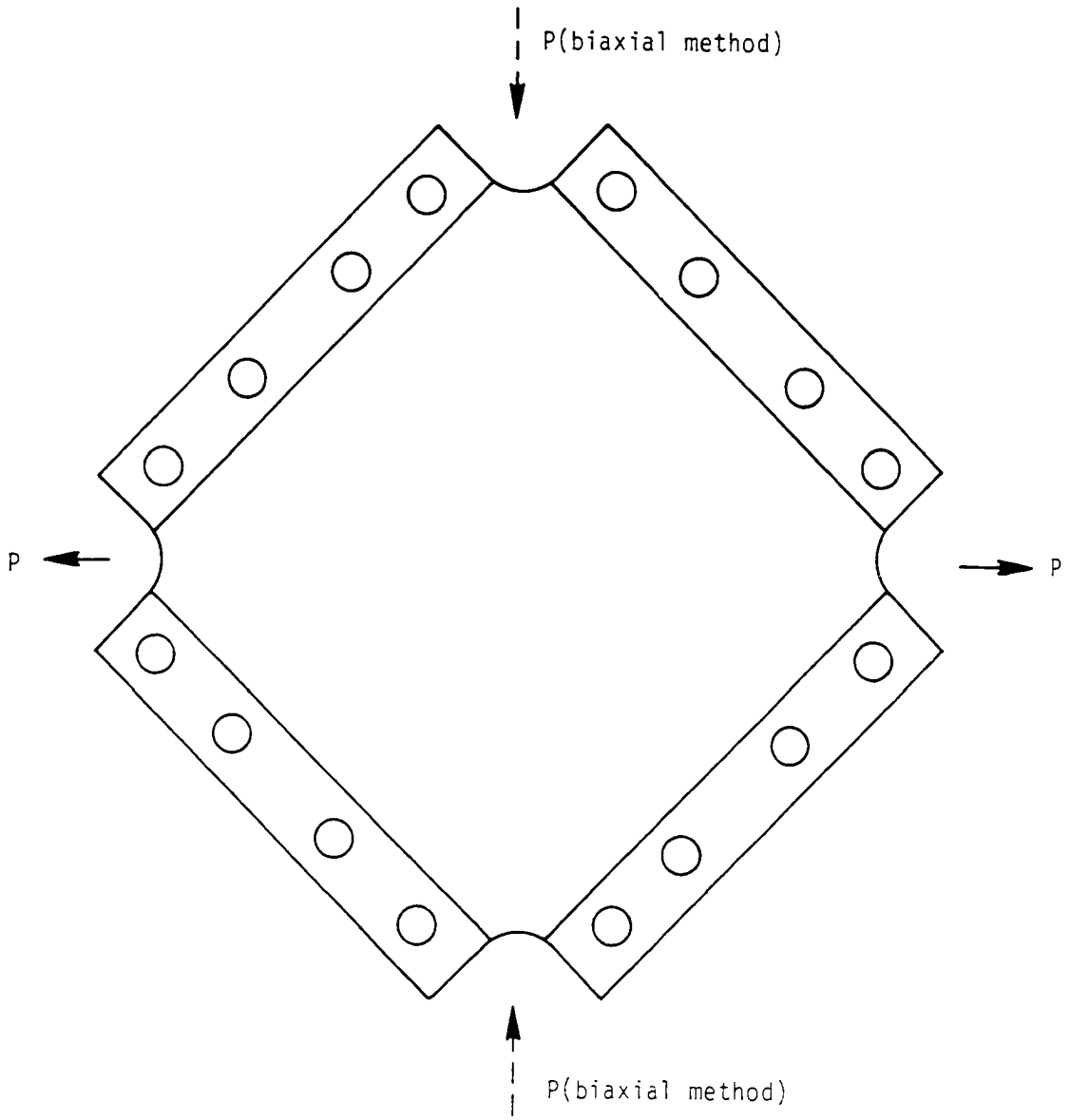

Fig. 2.13. Picture-Frame Shear test.

doublers bonded on or near the free edge to further reduce any high corner stresses [15].

The specimen can be either a plate or a honeycomb core sandwich. A sandwich configuration stabilizes the flat laminates against shear buckling at low loads, but it is necessary to account for the core stiffness. If the core is unattached to the face sheets, the core will not have a significant shear stiffness in a plane parallel to the face plates [25].

One of the problems with the uniaxial load Picture-Frame test is the bending and extension of the frame members. Bush and Weller [25] reported that attempts to eliminate these deformations had included oversizing the edge cross-sections to prevent bending and axial deformations or tapering the members to improve load transfer between the frame and specimen. Neither modification was completely successful in solving the problems.

Bush and Weller then devised the Biaxial Picture-Frame test which simultaneously applied equal tensile and compressive forces along the frame diagonals. The frame deformation would thus subject the specimen to a uniform shear strain. They found that this biaxial method applied a more uniform shear deformation to the specimen than did the uniaxial test. Frictional effects were found to be negligible. Also, doublers were placed at the corners where the compressive loads were applied in order to reduce any stress concentrations. The authors state that this prevented premature material failure without any detectable stiffening of the specimen.

Neither the biaxial method or the uniaxial method solve the overriding problem of the Picture-Frame test: material and equipment

expense. The test requires a significant amount of plate material and the frames can be rather expensive to manufacture [21]. Further, the state of stress is not homogeneous and this reduces the usefulness of the test method in determining a shear stress-strain response [6,26]. Experimental and finite element analyses have also shown that stress concentrations remain high even with the use of doublers or cutouts [27,28]. Unanticipated failure modes that are commonly found in the Picture-Frame test include folding or crimping of the panel in the corners of the tensile diagonal, in-plane failures due to normal stresses in the corners of the compressive diagonal and tearing of the specimen along the loading tabs [28].

Yet even with these problems, the Picture-Frame test is widely used to measure the response of composites to loads greater than the initial buckling load. Farley and Baker [28] performed an extensive analysis of the Picture-Frame method and found that the most significant parameter in reducing corner stress concentrations was the location of the corner pins. They concluded that if the corner pins were placed at the corners of the panel and not at the corners of the load frame, then the shear stress was nearly uniform and that normal stresses were negligible. Also, the ratio of load frame stiffness to specimen stiffness should be greater than 30 to further reduce the stress gradients. With the necessary modifications, the authors found that the Picture-Frame test yielded classical buckle failures.

2.11 Panel Shear

The Panel Shear test consists of loading a thin, square specimen in shear by adjustable loading links which are bolted to each side of the specimen. The loading links are placed in a pinned steel frame

which is loaded in tension along diagonal corners [5]. Figure 2.14 shows the test technique.

This method is obviously similar to the Picture-Frame method though the load introduction scheme is much more complex. The material costs are alleviated by the use of a smaller specimen, but the savings may be offset by the complexity of the load fixture. It may be assumed that the problems associated with the Picture-Frame method are also found in this test procedure. Further, experimental analysis [5] has shown that the Rail Shear and ±45 Shear tests yield similar results, thereby eliminating the need for a complex load frame in favor of simpler experimental methods.

2.12 Plate-Twist Shear

The Plate-Twist test is used for determining the in-plane shear modulus. A thin, flat plate is loaded upward along two diagonal corners and downward along the other two diagonal corners as shown on Fig. 2.15. Then, applying classical plate theory, the shear modulus can be determined.

The experimentalist must be careful to use the appropriate equations in converting the measured data into a shear modulus. If small deflection theory is used, then the geometry of the plate and the magnitude of the applied load must be such that the plate does indeed undergo small deflections. Careful specimen preparation is also necessary. The plate must be perfectly flat because any warpage of the specimen will affect the results. Further, it may be necessary to protect the specimen from crushing because of excessive local deformation where the loads are applied [29].

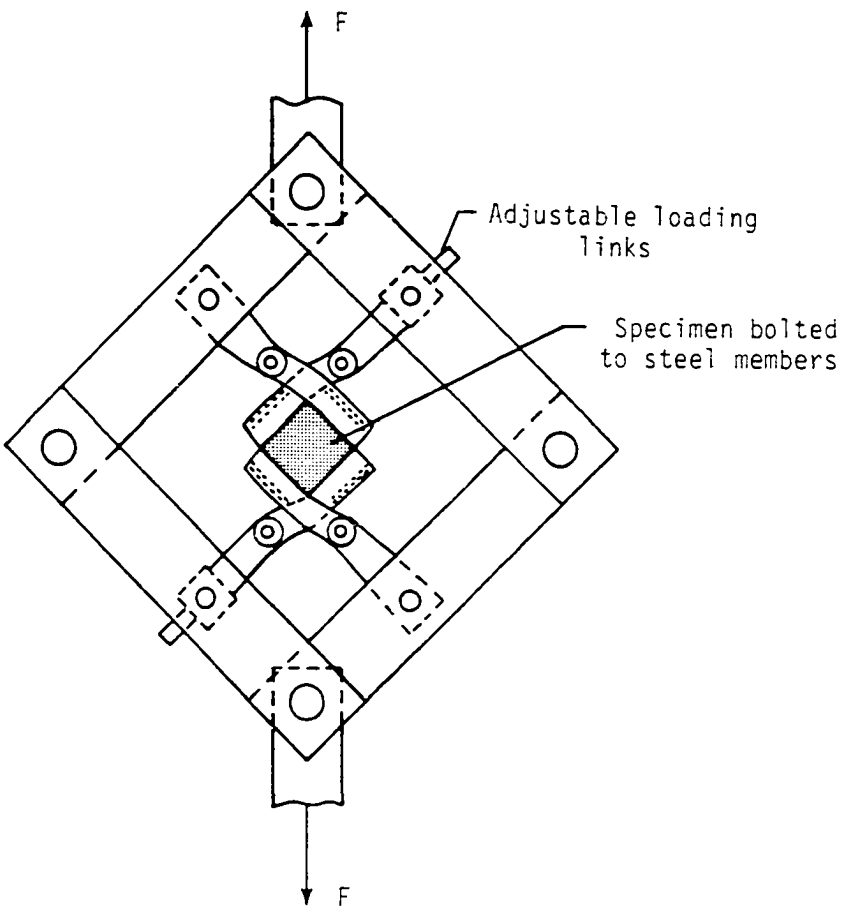

Fig. 2.14. The Panel Shear test.

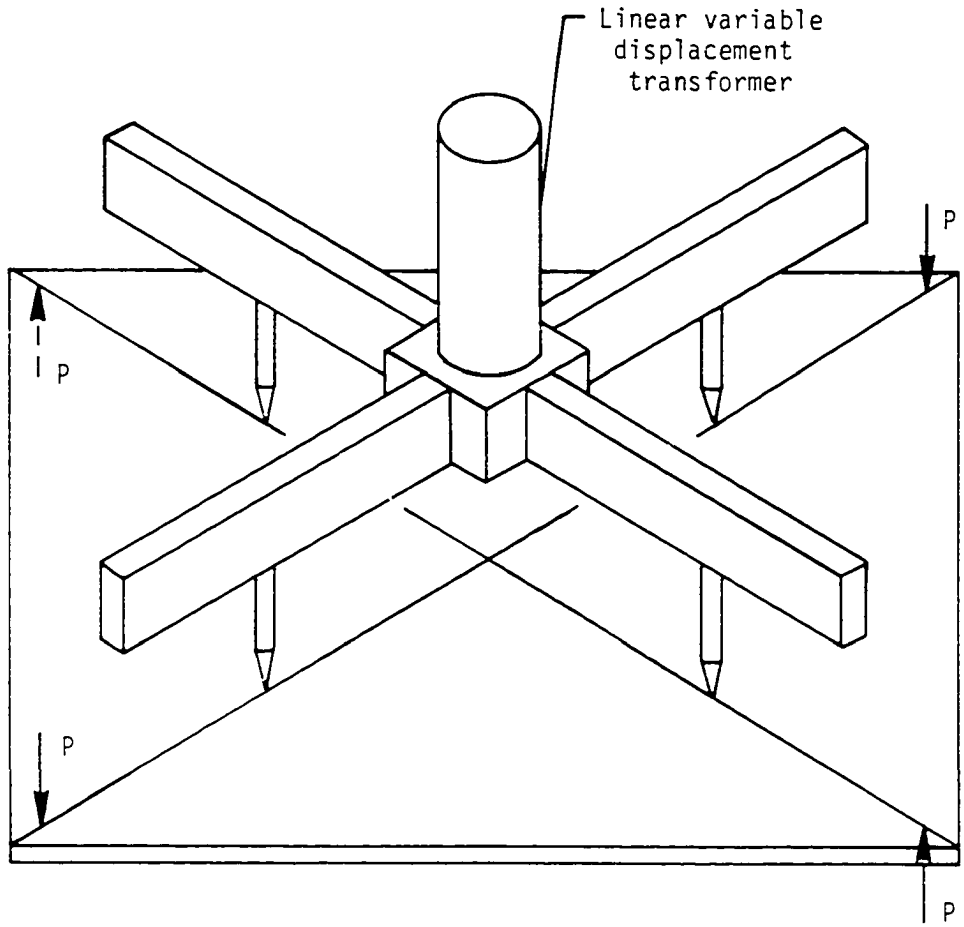

Fig. 2.15. The Plate-Twist Shear test.

Because the Plate-Twist test relies on small deflection theory and thus can only give the initial shear modulus, the values tend to be higher than the results from other shear tests. The nonlinearity of the shear stress-strain curves from other shear test methods demonstrate that the Plate-Twist test may be inadequate for determining the shear modulus [5].

2.13 Split-Ring Shear

The Split-Ring or Douglas Ring test consists of applying two equal but opposite loads acting normal to the plane of the ring at the points where the ring is split. Since the out-of-plane deflection is predominately due to shear deformation, this test may be useful in determining an in-plane shear modulus.

Greszczuk [29] performed an experimental investigation of this test method and he concluded that the ring test was simple, accurate and inexpensive. The test set-up is shown on Fig. 2.16. The load was applied through U-grips that were drilled radially into the ring and a pulley system was devised that counterbalanced the ring weight and allowed the ring to be horizontally suspended in air. During the experimental testing, Greszczuk noted that large deflections of the rings were necessary (in some cases up to one inch) and that there was some influence due to bending.

Because this test method can require a large amount of material and an elaborate set-up, the Split-Ring test does not appear to lend itself well to shear modulus testing of all laminated composites. More analysis of this shear test is required.

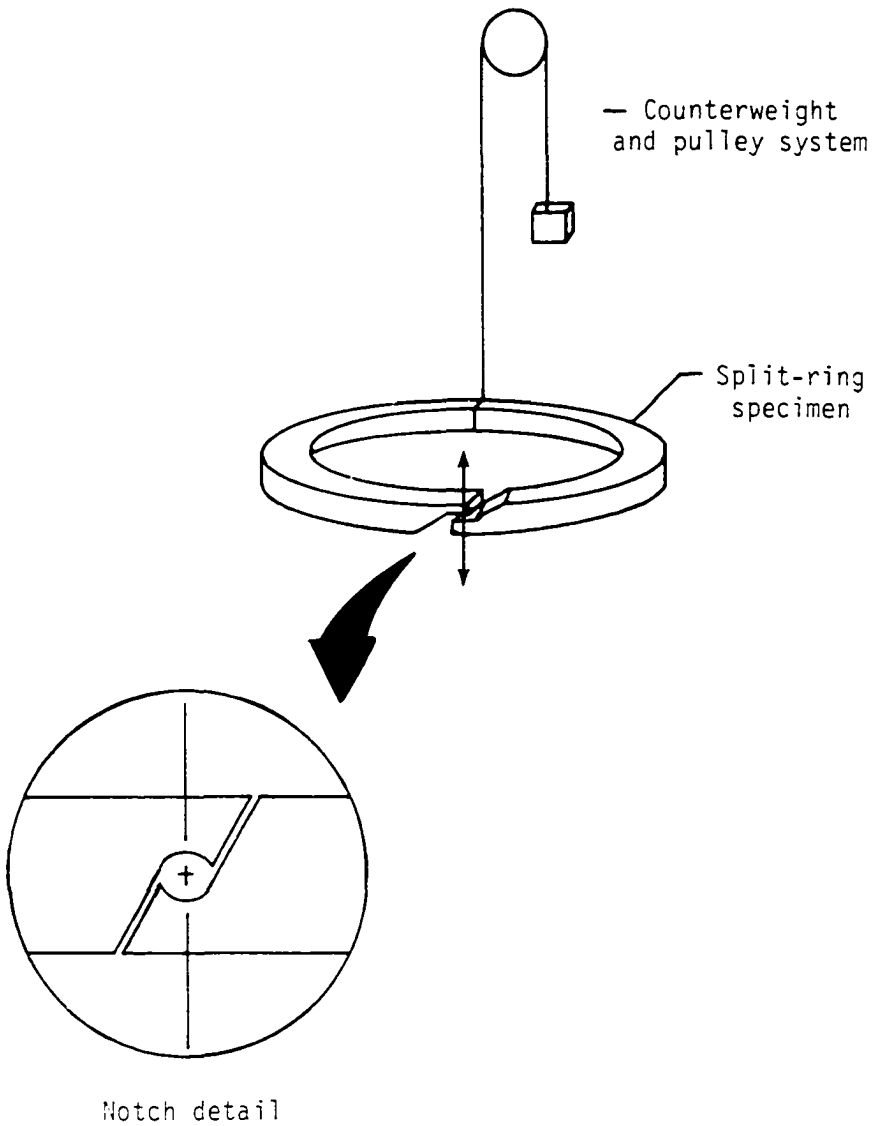

Fig. 2.16. The Split-Ring Shear test.

2.14 Cross-Beam Shear

The Cross-Beam Shear specimen is loaded in positive and negative bending such that a biaxial state of stress is produced over the center test area. A pure, uniform shear region is then oriented at ±45 degrees to the axes of the cruciform. In common usage a sandwich construction is used as depicted on Fig. 2.17.

This test method requires a considerable amount of material, much of which is wasted. Further, it has been found that the fiber orientation of the material and the core reinforcement in the sandwich may significantly influence the stress distribution in the test area. Duggan et al. [30] reported the stress state to be 13 to 20 percent greater in the test region than what is predicted by elementary beam theory. Slepetz, Zageski and Novello [6] noted that since pure shear is oriented at ±45 degrees to the axes of the cruciform, that if one wants the shear properties with respect to the material symmetry axes, the principal axes of the specimen must also be oriented at 45 degrees to the cruciform axes. This geometry can introduce in-plane shear coupling and edge effects which affect the test results.

Bergner et al. [15] performed an extensive finite element analysis of the Cross-Beam Shear test and found the stress distribution in a $[0/90]_s$ laminate to be nearly ideal with the exception of some high corner stresses. The shear stress in the center of a $[\pm 45]_s$ laminate was influenced by the core stiffness and was high because of low shear stresses away from the center.

The Cross-Beam Shear test can determine both the in-plane shear stress-strain response and the ultimate shear strength. Yet because of the presence of corner stress concentrations in most laminates and the

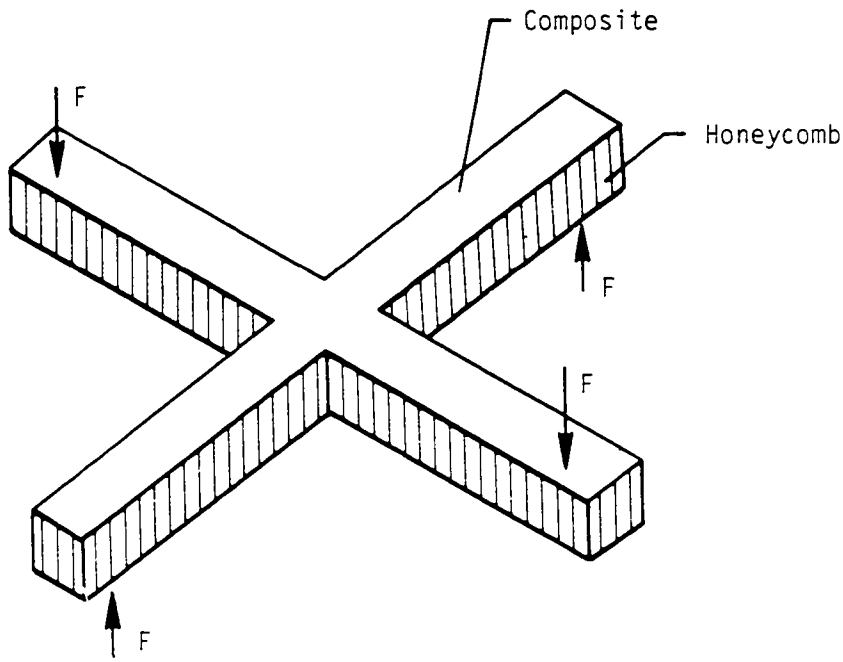

Fig. 2.17. The Cross Beam Shear test.

requirement for large amounts of material, the Cross-Beam Shear test has seen limited use.

2.15 ±45 Off-Axis Tensile Shear

This shear test consists of loading a ±45-degree symmetric laminate uniaxially in tension. A specimen lay-up is given on Fig. 2.18. The technique, originally proposed by Petit [31], was later simplified by Rosen [32]. Hahn [33] further verified and defined the conditions under which Rosen's simplified data reductions held.

This test has the advantages of being economical with material and time and it involves a simple test procedure [5]. Researchers have reported good correlation between the results of the ±45-degree Shear test and other shear test methods. Petit [31] obtained agreement between the ±45-degree Shear test and the Cross-Beam Shear test for boron/epoxy in the design area of the stress-strain curve. Sims [22] found good agreement with Torsion Tube tests using graphite/epoxy and with Rail Shear tests using glass/epoxy. Yeow and Brinson [21] also obtained satisfactory results between Rail Shear and ±45-degree Shear tests using graphite/epoxy. Chiao et al. [4] conducted Torsion Tube tests with aramid fiber/epoxy and also obtained good agreement with ±45-degree Shear tests. Finally, Terry [5] compared Panel Shear, Rail Shear and Short Beam Shear results with ±45-degree shear data and concluded that the ±45-degree Shear test produced acceptable results for design purposes as long as the layers were stacked in a homogeneous (symmetric) sequence.

Like all other shear test methods, this shear test is not without its problems. Terry points out that Petit's results were very reliable up to 1.3 percent shear strain but that the stiffness at higher stress

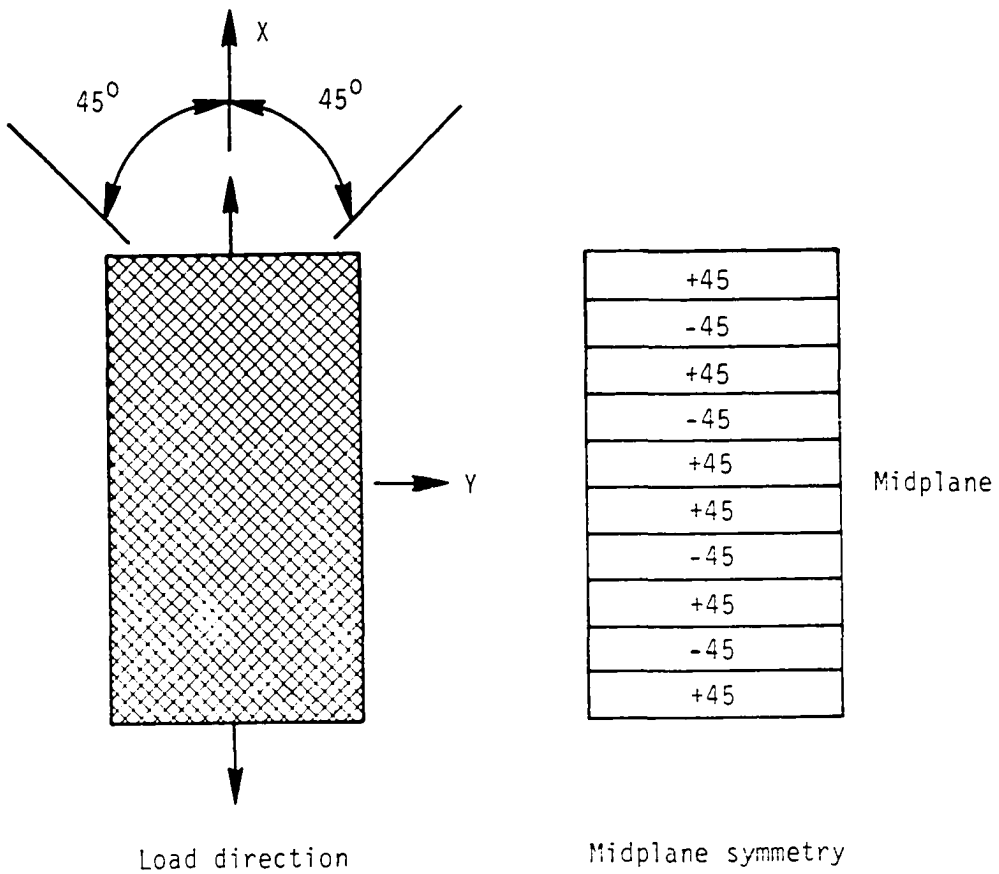

Fig. 2.18. A ±45-Degree Off-Axis Tensile Shear specimen.

levels was underestimated due to edge effects. Slepetz, Zageski and Novello [6] note that the tensile strength of the ±45-degree laminate is governed by free edge effects. Further, this test method does not provide shear data for laminates of arbitrary configurations. Yeow and Brinson state that the stress/strain response tended toward ductile characteristics as a result of interply effects, making the ±45-degree specimen a good test for the study of this phenomenon.

Duggan [19] and Arcan et al. [26] remarked that a combined stress state exists in the ±45-degree specimen. The planes of principal shear are subject to non-zero, statically indeterminate normal stresses. Duggan notes that the uncertain effect of this test method on the mean failure stress can be observed by loading specimens in compression instead of in tension. The values will be substantially different.

In conclusion, it appears that the ±45-degree Shear test will provide a reasonable in-plane shear modulus for design purposes though one must be aware of the limitations. The test's usefulness in determining shear strength or inelastic shear behavior is limited due to the interaction of normal and shear stresses on the shear planes.

2.16 Off-Axis Tensile Shear

The Off-Axis Tensile test has been accepted by many researchers as the basic test method for complete shear characterization of composite materials. It has the advantages of a familiar tensile test procedure, uniform shear stress through the thickness and ease of specimen manufacture. The test yields off-axis properties such as modulus, Poisson's ratio, fracture stress and coupling between extensional and shear deformations as well as the in-plane shear

properties. Further, the specimens are free of the residual stresses that can be found in ±45-degree specimens [34].

Essentially, a specimen is uniaxially loaded in a direction other than exactly coincident with the fiber orientation. A ten-degree orientation is commonly used. A biaxial state of stress is then produced in the material's principal coordinate system which makes the test useful for the study of stress interactions on nonlinear behavior and strength [35].

The Off-Axis test is not without its disadvantages, however. It is necessary to measure three strains at a point and to transform both the stresses and strains to another coordinate system. Care must also be taken in machining the specimen angle and aligning the strain gage on the specimen [34]. Perhaps the worst disadvantage is that a large aspect ratio of length to width is required. Nemeth et al. [35] suggests a ratio of 15 or greater. This aspect ratio provides a large region of uniform shear stress and low transverse stresses in the test section. The severe stress concentrations found in the corner of the specimen and the high strain gradients near the grips do not influence the state of stress in the test section when a large aspect ratio is utilized.

In comparison to other shear tests, Chamis and Sinclair [34] found the in-plane shear strain for graphite/epoxy laminates almost identical to that found in a Torsion Tube test. Yeow and Brinson [21] compared 10-degree and 15-degree Off-Axis specimens to ±45-degree and Symmetric Rail Shear specimens and found the Off-Axis test the best method for determining shear responses. Yet Chiao et al. [4] found that the 10-degree Off-Axis test for graphite/epoxy laminates resulted in a

higher shear modulus, lower failure strain, lower failure stress, and had more significant shear coupling effects than a ±45-degree Shear test.

Whatever the conclusions, it is important to note that the Off-Axis test provides only in-plane shear data of unidirectional composites. The data may be affected by shear coupling, though the magnitude of this effect is in question.

As an aside, in a 1967 paper, Greszczuk [36] derived a theoretical expression for determining the shear modulus of composite materials from an Off-Axis test using any fiber orientation angle. Though the effects of shear coupling were not accounted for in the derivation, the author's derived expressions agreed well with experimental results.

2.17 Slotted-Tension Shear

This shear test method is based on the principle that a uniform state of shear will exist in a region if equal orthogonal tensile and compressive stresses are imposed on the element's edges. Planes of pure shear will exist at 45 degrees to the load axes.

Duggan, McGrath and Murphy [30] proposed a statically determinate system to apply orthogonal tensile and compressive loads to a slotted specimen as shown on Fig. 2.19. The axial slots insured that the compressive forces were transmitted only to the rectangular gage section. The slots also minimized the diffusion of the compressive loads outside of the gage section [19].

This shear test provides both the shear modulus and the shear strength. It also has the advantage of not being restricted to specific ply orientations. The principal difficulty of this shear test is to

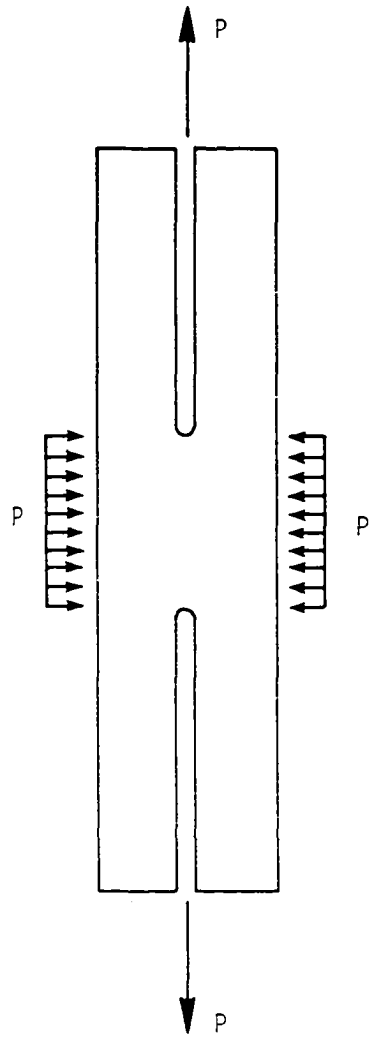

Fig. 2.19. The Slotted-Tension Shear test.

insure that the tensile and compressive stresses are equal. The loading apparatus appears to be quite complex and may not be possible without extensive modifications to a tensile test machine. More test results are necessary before any conclusions can be reached about this shear test method.

2.18 The Iosipescu Shear and Arcan Shear Tests

Originally developed by Iosipescu [13] in the early 1960's for determining the shear properties of metals, the Iosipescu Shear test has only recently been investigated for determining the shear properties of composite materials. The encouraging results from research with metals indicate that this test method has potential for use with composites [15].

In an isotropic material, the Iosipescu Shear test induces a state of pure shear at the specimen's midlength by applying two counteracting moments which are produced by two force couples. A 90-degree notch is cut completely around the cylindrical specimen. The test specimen and test fixture are given on Fig. 2.20. This geometry transforms the parabolic shear stress distribution found in beams of constant cross-section to a constant shear stress distribution in the area between the notches. The reduced area also ensures shear failure in that region. Note that the sides of the notch, when oriented at 45-degrees to the longitudinal axis, are isostatics of stress-free surfaces.

The Iosipescu Shear test for composite materials is similar, but the orthotropic properties of the materials necessitate modifications. For example, the flat, rectangular specimens are notched in one

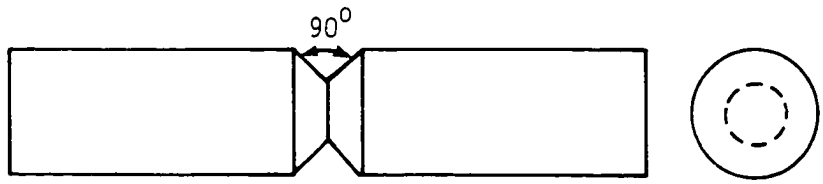

Iosipescu shear test specimen
for isotropic materials

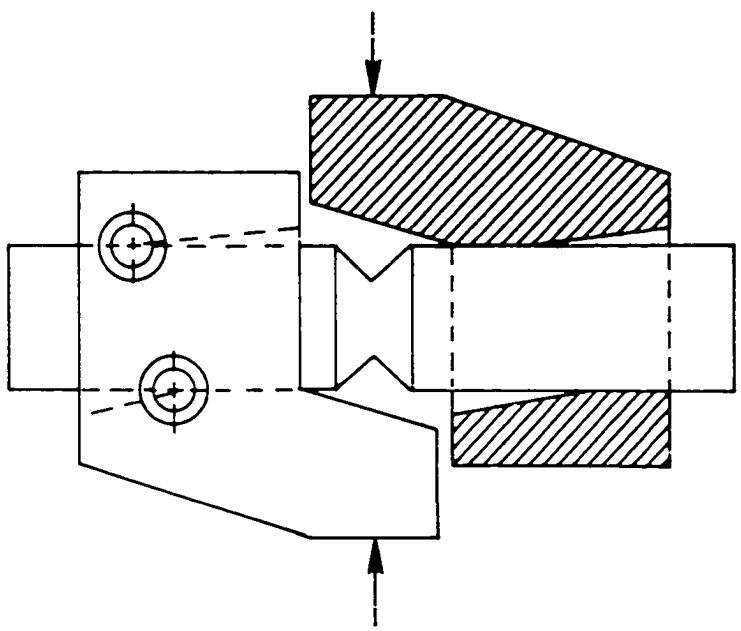

Iosipescu shear test fixture

Fig. 2.20. The Iosipescu Shear test for isotropic materials.

direction only as shown on Fig. 2.21. This geometry allows the laminate stiffness to be uniform in the test section and makes it possible to obtain strain measurements at the center. As in the case for isotropic materials, a pure, uniform shear stress is found between the notches, but the orthotropy of a composite produces stress concentrations at the notch tips. The minimization of these stress concentrations has been the subject of numerous investigations.

Bergner, Davis and Herakovich [15] conducted a finite element analysis of the Iosipescu Shear test and concluded that a uniform shear stress was found in the central region for all laminate configurations. Yet the degree of uniformity of the shear stress was found to be dependent upon the orthotropy of the laminate. The complex state of stress at the notch tips assuredly contributed to failure, so the authors recommended rounding the notch tips and bonding doublers to the corners.

Perhaps the most comprehensive investigations of the Iosipescu Shear test have been performed by Walrath and Adams [37]. The authors presented experimental results for five sheet-molding compound materials and showed that the Iosipescu Shear test was capable of testing composite materials in any one of the six shear loading modes (12,21,13,31,23,32) [38]. A separate finite element analysis [39] tried to perfect the specimen geometry and the Iosipescu Shear test fixture. The authors stated that an orthotropic specimen with a 120-degree notch angle, 0.05-inch notch radius and having a notch depth of 20 percent of the width would be the optimal test configuration. Walrath and Adams have called for further investigations into the Iosipescu Shear test [37].

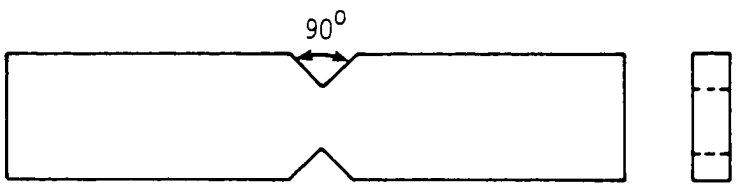

Fig. 2.21. Iosipescu Shear test specimen for composite materials.

Slepetz, Zageski and Novello [6] developed a test method that was essentially a modification of Iosipescu's original technique. Termed the Asymmetrical Four-Point Bend (AFPB) test, this shear test produced a constant shear stress distribution in a notched laminate by applying a concentrated load at four points. This differed from Iosipescu's test which applied a distributed load to a specimen at four locations. The authors thoroughly investigated the stress state of the notched region using strain gages, finite element analysis and moiré-fringe interference. They noted that the stress distribution deviated from ideal conditions and that the stress state was probably dependent upon the material properties. A modified specimen with a rounded notch eliminated the stress concentrations and possessed a wide region in which the shear stress was uniform. The authors also concluded that further refinement of the test method and specimen geometry was needed.

It is significant to note that Arcan and his colleagues [40,41] had introduced a test method in the late 1950's that was also similar to the Iosipescu Shear test. The specimen was of the same concept as the Iosipescu specimen; namely that the notched contours of the gage section were similar and that the loading fixtures had a similar S shape. The specimen configuration is shown on Fig. 2.22. The specimen is circular with axisymmetric cutouts and consists of the central region, or significant section, and exterior parts which transmit the load to the central region. The exterior sections function as grips and direct the isostatics into ±45-degree directions [26].

Initially the entire circular disk was both the specimen and the test fixture, but the difficulty of machining such a configuration from composite materials resulted in the cutting out of the central part and

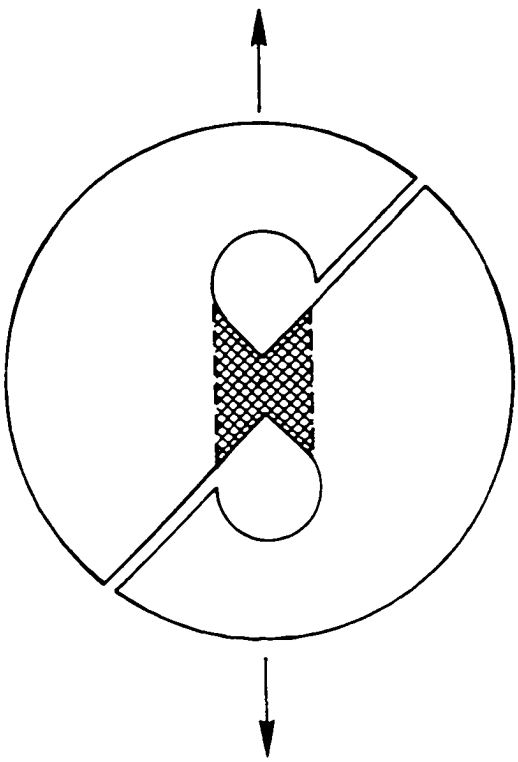

Fig. 2.22. The Arcan Shear test.

replacing it with a butterfly-shaped composite specimen as shown by the shaded region on Fig. 2.22. The specimen was glued to the aluminum disk, which now served solely as grips, with supporting tabs [26]. Supplementary experiments performed on this set-up showed the sandwiched specimen to have good plane stability. The results were not significantly affected by slight non-uniformity of the shear stress through the thickness [42].

There are some disadvantages to this test technique, however. For example, because of the circular shape of the apparatus, special intermediate grips between the specimen and the standard grips are needed to avoid out-of-plane bending or torsion. Also, Marloff [43] found that for the present configuration the transverse stresses at the notch were at least an order of magnitude larger than the other stress components and thus failure was due primarily to transverse tension rather than shear. Indeed, the same large transverse stresses can be found in the Iosipescu Shear test [15,39] and is due to the notched configuration used in both tests. Marloff suggested substituting a straight section for the radius at the gage section and utilizing loading tabs to force failure to occur in the central section.

Arcan's shear test does, however, provide a shear stress-strain curve, a shear modulus and a failure stress, though this value may be low due to the large transverse stresses. Also, because loading can be applied in different directions along the circumference of the disk, it is possible to determine the failure envelope and slip lines of a composite material by fatigue or mixed-mode loading [44].

2.19 Summary

This literature review has discussed many test methods used for determining the shear properties of composite materials. While there is an abundance of tests available for determining the in-plane shear properties, there is a dearth of interlaminar shear tests. The Short Beam Shear, Block Shear, Double-Notched Laminate Shear and Slant Shear tests attempt to determine an interlaminar shear strength, but the discussions presented in this review demonstrate the deficiencies of these test methods. Further, none of the techniques mentioned in this review completely satisfy the requirements for an ideal shear test. The most common hindrance is that none of the test methods produce an unambiguous state of pure shear, though this may be totally inescapable due to the nature of a composite material.

Perhaps the only test methods that compare to the ideal shear test are the Iosipescu Shear and Arcan Shear tests. Both are mechanically simple and use small specimens with simple geometry. Both do require their own fixtures, but then so do most other shear tests. Both have a simple data reduction procedure and have been shown to provide reproducible results. A state of uniform shear exists in the central region between the notches, but the presence of large, normal stresses at the notch tips prevents one from determining a "true" shear strength. Many authors have suggested rounding the notch, but only Walrath and Adams [39] have conducted parametric studies in qualifying notch angle, notch radius and notch depth.

Thus, there is a necessity for more analysis of the stress state in the notched region of the Iosipescu and Arcan shear specimens. For the purposes of this study, it was decided to examine the Iosipescu

Shear test. The ability of this test method to determine the in-plane and interlaminar shear moduli and strengths makes this technique particularly desirable for further investigation. The following chapter further discusses the research that has been conducted on applying the Iosipescu Shear test to composite materials. In particular, the work of Walrath and Adams and Slepetz, Zageski and Novello are highlighted. Discussions of the shear test fixtures utilized by the authors and their findings on which notch geometry was best suited for shear testing are presented.

Chapter 3

DISCUSSION OF THE IOSIPESCU SHEAR TEST

As previously mentioned, the Iosipescu Shear test induces a state of uniform shear stress at the specimen's mid-section by applying two counteracting moments which are produced by two force couples. A force diagram, together with shear and moment diagrams, is given on Fig. 3.1. Note that the maximum shear force is the applied load P and that the moment is zero at the center of the specimen. The load fixture which induces these forces is shown schematically on Fig. 3.2 and a photograph is given on Fig. 3.3. This particular fixture is similar to the one used by Walrath and Adams to conduct their experiments [37]. It closely resembles the fixture developed by Iosipescu [13].

Another Iosipescu Shear fixture is given on Fig. 3.4 and shown schematically on Fig. 3.5. This fixture was developed by Slepetz et al. [6] for their experiments and was termed by the authors as the Asymmetrical Four-Point Bend (AFPB) test. This fixture results in the loading depicted on Fig. 3.6. Note that the maximum shear force is now $P\,\frac{(a-b)}{(a+b)}$, which is a function of the loading-point locations. The moment at the centerline is, of course, zero.

There are several advantages and disadvantages to each of these fixtures. Both require a relatively long specimen, and the four-point loading of both fixtures can induce large bending deformations [44]. Walrath and Adams' fixture, herein referred to as the Wyoming fixture,

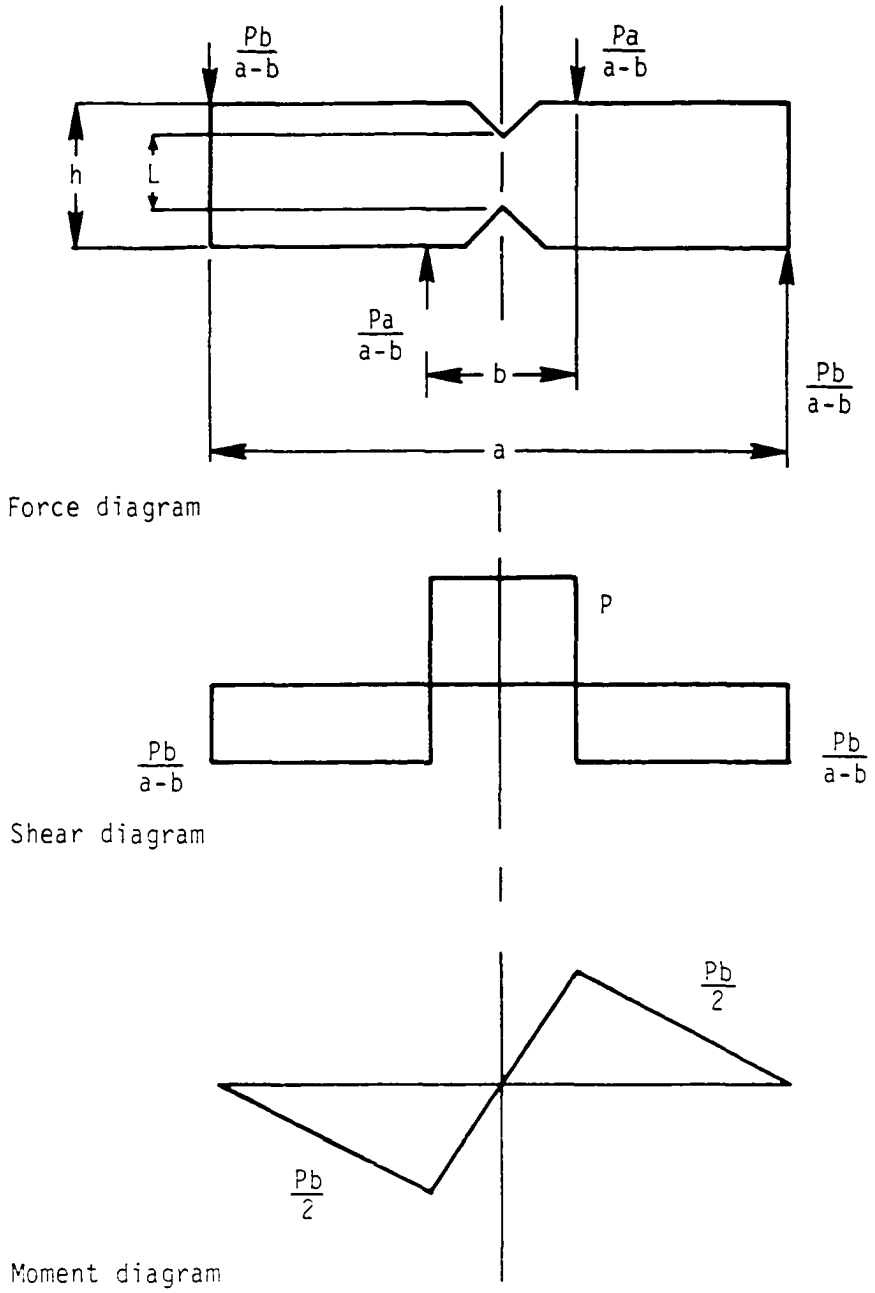

Fig. 3.1. Force, shear and moment diagrams of the Iosipescu Shear test.

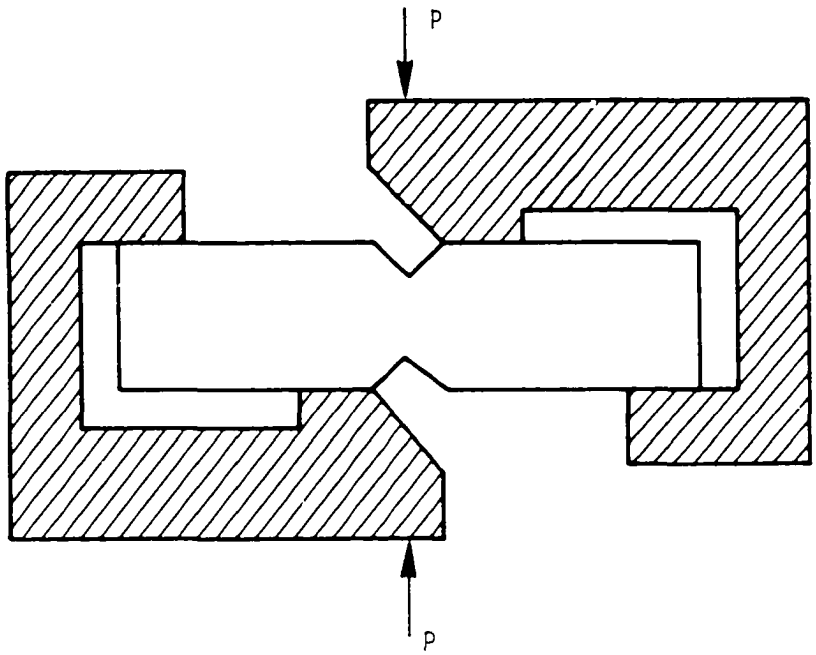

Fig. 3.2. Schematic of the Iospiescu Shear test fixture developed by Walrath and Adams.

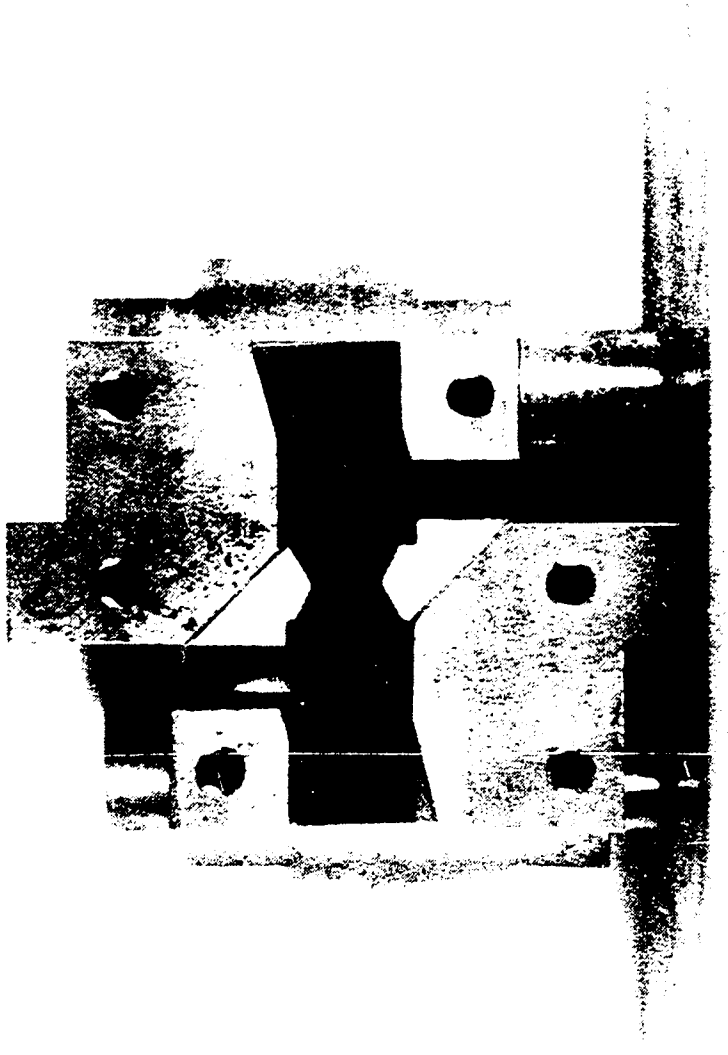

Fig. 3.3. Specimen set in the Iosipescu Shear test fixture.

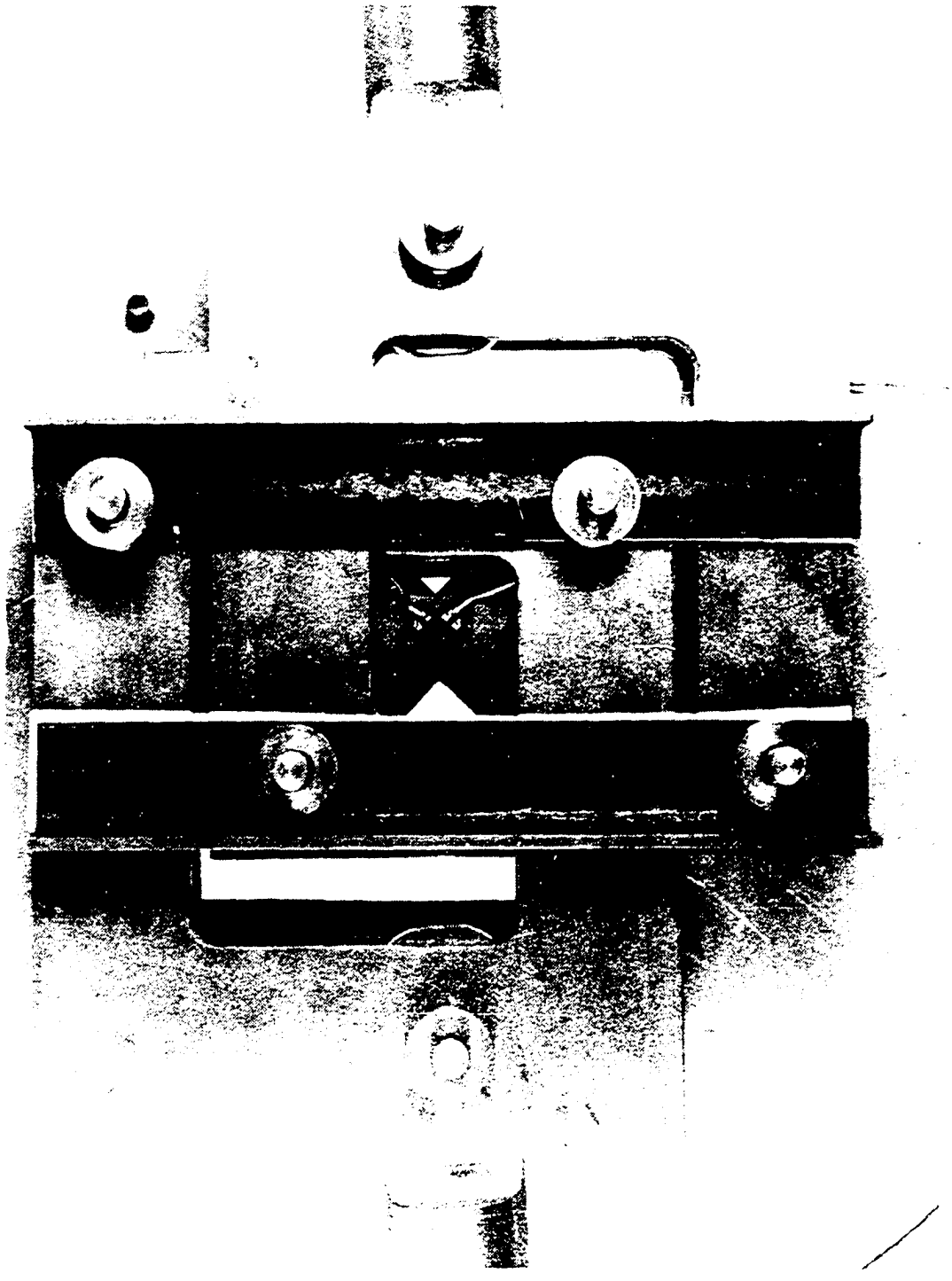

Fig. 3.4. Specimen set in the AFPB fixture.

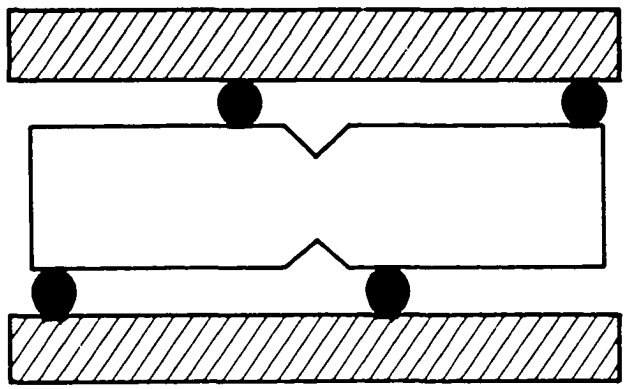

Fig. 3.5. Schematic of the AFPB Iosipescu Shear fixture.

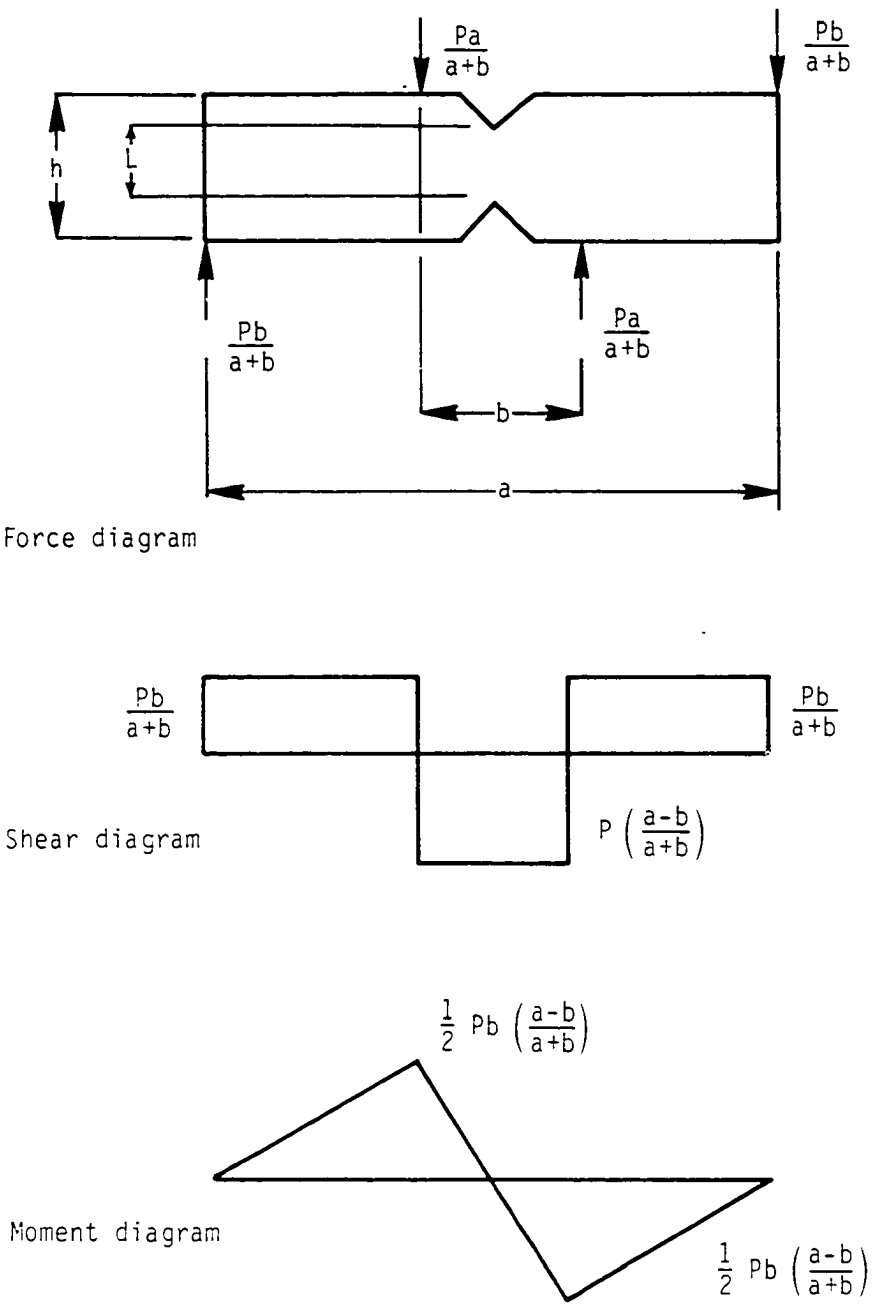

Fig. 3.6. Force, shear and moment diagrams of the AFPB Iosipescu Shear fixture

applies a distributed load on the specimen. The flat loading faces tend to avoid localized compressive stresses. The AFPB fixture, however, utilizes cylindrical loading rods which can cause local crushing on the edges of the specimens. Doublers must be glued onto the face of the specimen to alleviate the crushing forces.

The AFPB fixture does provide greater latitude in specimen width than the Wyoming fixture, and it is easier to set the specimen into the fixture. The Wyoming apparatus, because of the flat loading faces, requires exacting tolerances for specimen width so that the specimen sides and the loading faces are in contact at each point. Specimen sides that are not parallel and flush with the loading faces will result in the introduction of bending moments. Furthermore, because of the strict dimensional requirements, it is very difficult to set the specimen into the Wyoming fixture.

The fact that the shear force of the AFPB fixture is a function of the loading-point locations is more of a nuisance to the researcher than a disadvantage of the test method. It is important to remember this factor only when analyzing the shear data.

In addition to different load fixtures, there is some discussion as to what is the best specimen geometry. For an isotropic material, a 90-degree notch is the ideal geometry since the sides of the notch are isostatics of stress-free surfaces. However, this is not the case for an orthotropic material. Most researchers have agreed that it is necessary to round the notch tip and change the notch angle in order to eliminate the stress concentrations in an orthotropic material. Slepetz et al. analyzed a specimen with a 0.125-inch notch radius and found that the normal stresses were negligibly small at the notch tip and elsewhere

along the centerline. The authors conducted some experimental tests with unidirectional graphite/epoxy fillet-notched specimens but were unable to obtain a shear failure. The failure mode was tensile at the load points. However, the authors recommended additional testing on fillet-notched specimens of various material types and lay-ups because their finite element analysis showed the rounded notch to be the most useful specimen configuration.

Walrath and Adams conducted a rather extensive finite element analysis of the Iosipescu specimen notch geometry [39]. Nine different notch geometries were modeled involving variations in notch depth, notch angle and notch radius. Three degrees of orthotropy were also analyzed. The authors found that in an isotropic material, loading-induced compressive stresses extended into the test region. These unwanted stresses were due to the close proximity of the loading edges to the notch edges. This situation was aggravated further in orthotropic materials because the higher longitudinal modulus resulted in higher bending stresses and the lower shear modulus produced lower applied shear stresses. The authors recommended moving the loading points away from the notch, but they did not determine a new loading distance.

As for the notch geometry, Walrath and Adams found that a notch radius definitely reduced the stress concentrations in the notch area. They state that the shear stress gradients around the notch tips were reduced, though the shear stress still tended to rise near the notch tip. Higher notch angles also tended to reduce the shear stress concentrations at the notch, but there were few changes in either the bending stress or the transverse normal stress. The authors concluded that the stress concentrations at the notch tip were more a function of

notch radius rather than notch angle. The effect of notch depth on the stress concentrations was minimal compared to the effects of the other notch geometry factors.

The best orthotropic specimen, according to Walrath and Adams' results, would have a 120-degree notch angle, 0.05-inch notch radius and a notch depth of 20 percent of the width. It should be noted that Walrath and Adams did not carry their analysis any further beyond a 120-degree notch angle or a 0.05-inch notch radius.

Even though the research conducted by Walrath and Adams and by Slepetz, Zageski and Novello demonstrated the validity of employing the Iosipescu Shear test for composite materials, there are still questions that remain. A comprehensive experimental investigation has yet to be undertaken to determine how differences in notch geometry affect the shear properties measured for a composite material. Further, a comparison of the Wyoming and AFPB fixtures is necessary to determine how the differences in the load-introduction schemes affect the stress state in the gage section. It is the purpose of this work to examine both experimentally and analytically the Wyoming and AFPB shear fixtures in order to determine which technique is best suited for measuring the shear properties of composite materials. An experimental investigation is also undertaken which expands upon and complements the finite element analysis of Walrath and Adams in determining the most beneficial notch geometry for an Iosipescu Shear specimen.

Chapter 4

ANALYTICAL TECHNIQUE

A finite element analysis was initiated to determine the effects of loading variations on the Iosipescu Shear specimen. The finite element program EISI-EAL (Engineering Information Systems, Incorporated - Engineering Analysis Language) was utilized for this study. The baseline two-dimensional model is shown on Fig. 4.1. The model consists of 2159 nodes, 2010 quadrilateral membrane elements and 90 triangular membrane elements. The analysis was conducted assuming six degrees of freedom per node. Displacements in the X- and Y-directions and rotations about the Z-axis were permitted while displacements in the Z-direction and rotations about the X- and Y-axes were constrained. Because the Iosipescu specimen geometry was asymmetric, it was necessary to model the entire specimen.

Loading was applied to the specimen by designating displacement boundary conditions. This allowed the simulation of the rigid test fixture. The loading schemes for both the Wyoming and AFPB fixtures are given on Fig. 4.2. The major difference between the two techniques was that one applied an evenly distributed load and the other applied a concentrated load.

Table 4.1 presents a matrix of possible computer simulations. Two materials were modeled based upon the degree of orthotropy. The E_{11}/E_{22} ratios ranged from 1, for an isotropic material, to 12, for an

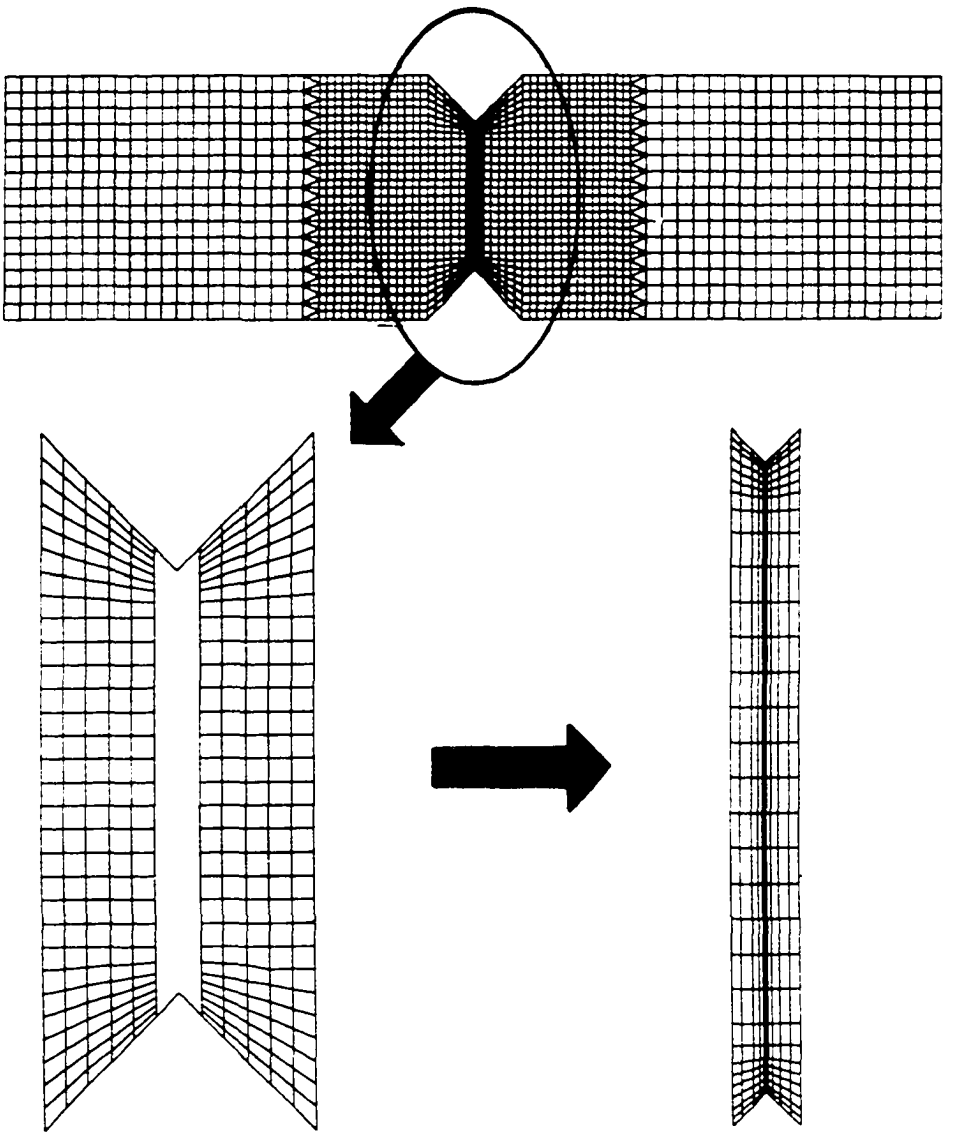

Fig. 4.1. Finite-element model of the iosipescu Shear specimen.

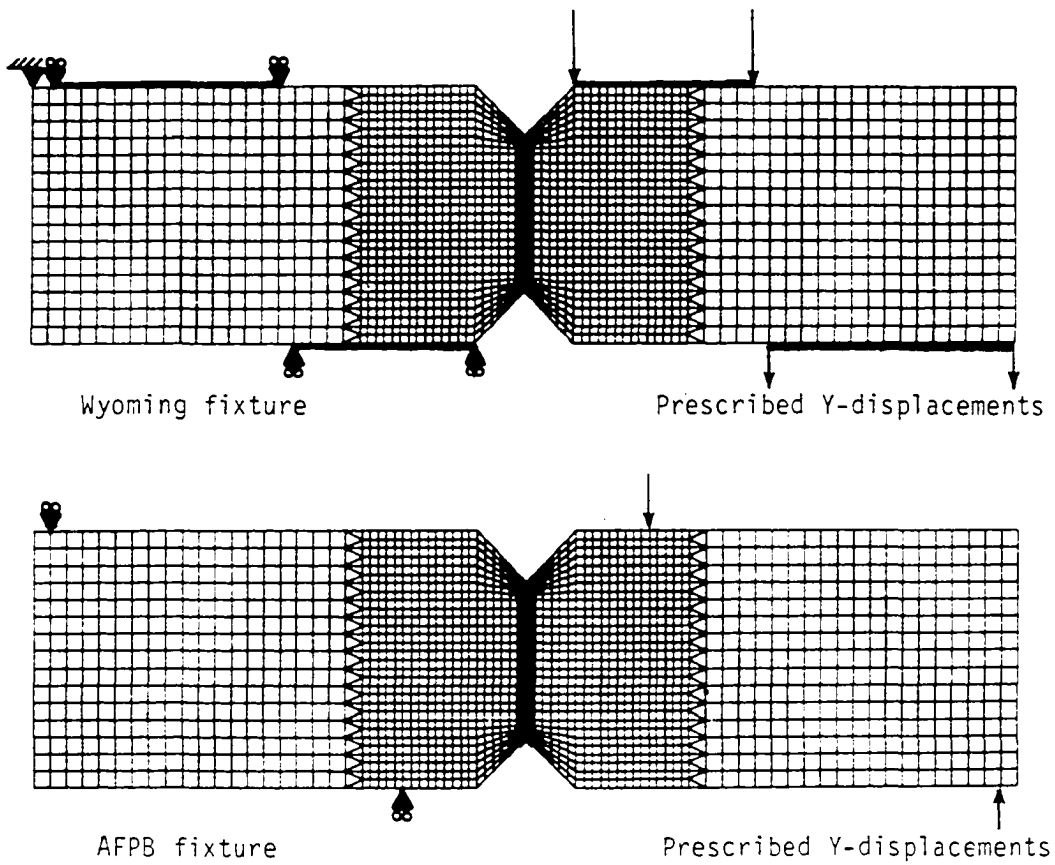

Fig. 4.2. Boundary conditions used for modeling the Iosipescu Shear fixtures.

Table 4.1 Iosipescu Shear test analysis variations

Property	Variations considered		
Material orthotropy ratio, E_{11}/E_{22}	1 (Steel)		12 (AS4/3502 Graphite/Epoxy)
Loading distance from notch edge (Wyoming fixture)*	0.0	0.1	0.2
Loading distance from notch edge (AFPB fixture)*	0.2	0.5	0.9
Off-symmetric loading	Selected analyses only		

*All variations run with baseline notch geometry of 90-degree angle, sharp notch. Selected variations run with notch geometry of 90-degree angle, 0.05-inch radius or 90-degree angle, 0.10-inch radius.

orthotropic material. The assumed material properties are given on Table 4.2. The baseline notch geometry was a 90-degree angle with no radius. The problem variations were related to the effects of load location. For both the Wyoming and AFPB fixtures, three load locations either at the notch edge or some distance away were chosen. Based upon the results of these analyses, programs were repeated for a specimen notch geometry with an angle of 90 degrees and a 0.05-inch radius or an angle of 90 degrees and a 0.10-inch radius. The finite element model for a notched radius is shown on Fig. 4.3. This modeling allowed direct comparison of the stress states due to sharp and radiused notches.

Examinations into the consequences of non-symmetric loading or bending on the stress state in the notch region were also conducted. From a practical viewpoint, non-symmetric loading would occur if the specimen was not aligned in the fixture properly or if the specimen was improperly machined. Analysis of a non-symmetric load case was conducted to determine the susceptibility of the Iosipescu Shear test to experimental error.

Table 4.2 Material properties used for finite element analysis

Steel (3.5% Ni, 0.4% C)[45]		$E_{11}/E_{22} = 1.0$
$E_{11} = E_{22} = E_{33}$	30.0 Msi	
$\nu_{12} = \nu_{13} = \nu_{23}$	0.30	
$G_{12} = G_{13} = G_{23}$	12.0 Msi	
AS4/3502 Graphite/Epoxy[46]		$E_{11}/E_{22} = 12$
E_{11}	20.5 Msi	
$E_{22} = E_{33}$	1.70 Msi	
$\nu_{12} = \nu_{13}$	0.30	
ν_{23}	0.36	
$G_{12} = G_{23}$	0.87 Msi	
G_{23}	0.26 Msi	

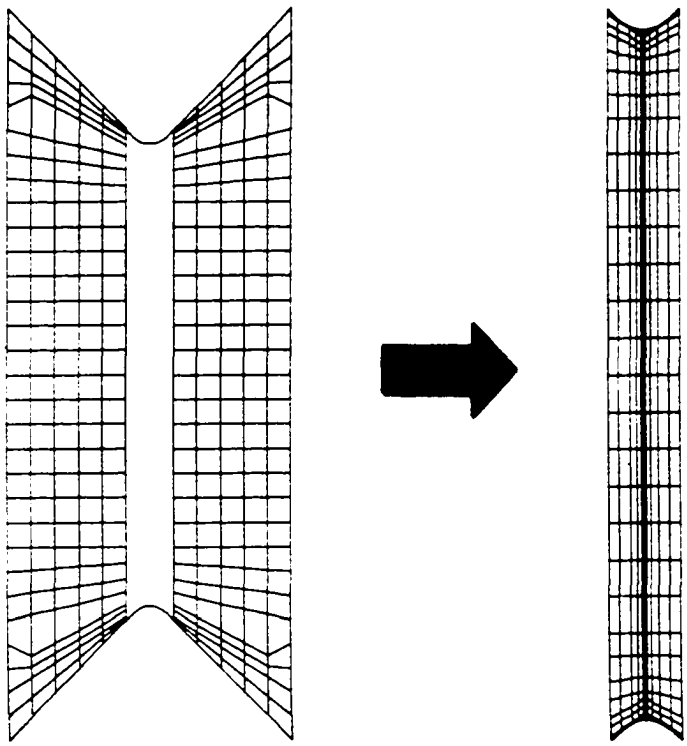

Fig. 4.3. Notch detail of the finite element model of an Iosipescu specimen with a notch radius.

Chapter 5

EXPERIMENTAL PROCEDURE

The Iosipescu Shear test specimens were prepared from AS4/3502 Graphite/Epoxy prepreg manufactured by Hercules, Inc. This material has an orthotropy ratio (E_{11}/E_{22}) of 12. Two 26- by 50-inch panels with 24 plies were fabricated by NASA/LRC. One panel had a unidirectional lay-up and the other panel had a quasi-isotropic configuration $[\pm 45,0,90,\mp 45,0,90,\pm 45,0,90]_S$ that is commonly found in aircraft structural components. A 12- by 12-inch plate was also manufactured. It had 96 plies and was used for determining interlaminar properties.

The specimen dimensions are given on Fig. 5.1. Note that the AFPB specimen was approximately three times larger than the Wyoming specimen. These drawings are of the final specimen configurations that resulted from reduction of the gage section and other modifications to insure shear failure in the notched region. The details of how these dimensions were obtained is fully explained in the comments on the test procedures.

The experimental test matrix is given on Table 5.1. At least three specimens for each variation were tested. A sharp notch geometry with a 90-degree angle was chosen as the standard configuration and most fixture modifications were conducted using this specimen geometry. A limited number of unidirectional specimens were tested once it was discovered that shear failure occurred at the fiber/matrix interface and

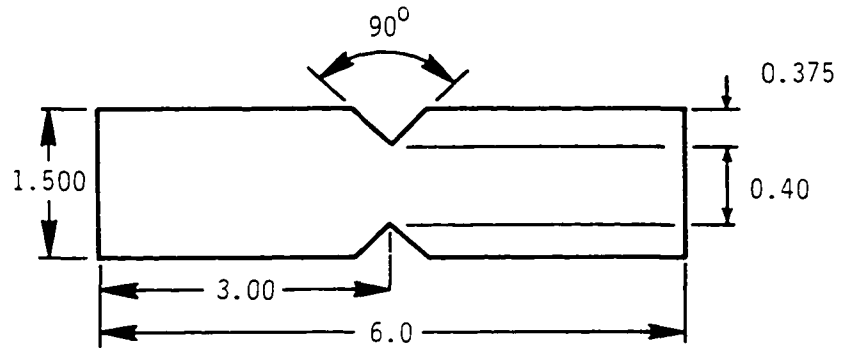

AFPB specimen

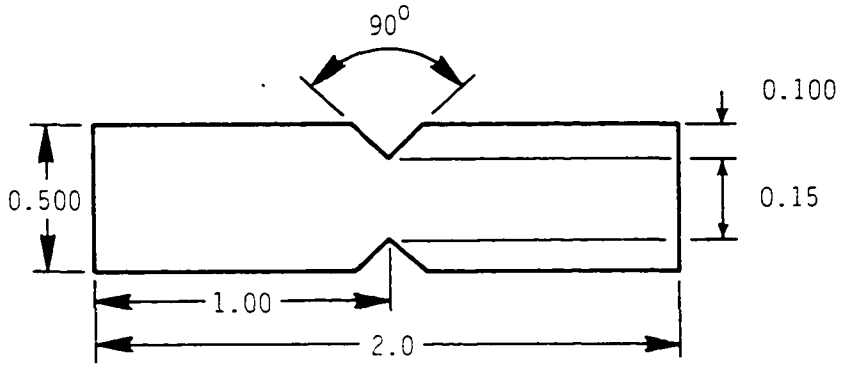

Wyoming specimen

Fig. 5.1. Iosipescu specimen dimensions.

Table 5.1 Experimental test program

Measured properties	Tensile test matrix: Unidirectional lay-up $[0]_s$	Tensile test matrix: Quasi-isotropic lay-up $[\pm45,0,90,\mp45,0,90,\pm45,0,90]_s$
Longitudinal shear modulus, E_{11} and Poisson's ratio, ν_{12}	3	3
Transverse shear modulus, E_{22}	3	

Shear test matrix

Specimen	Fixtures: Wyoming						AFPB			
				Modifications[1]					Modifications	
Angle/ radius	In-plane		Interlaminar	1	2	3	In-plane[2]		Without doublers	Distributed load
	U[3]	Q[3]	Q	Q	Q	Q	U	Q	Q	Q
90/0	3	3	3	3	3	3	3	3	3	3
90/0.05		3	3					3		
90/0.10		3	3					3		
105/0.05		3	3					3		
120/0		3	3					3		
120/0.05		3	3			3		3	3	3
120/0.10		3	3					3		
135/0.05		3	3					3		

Notes: 1. Modifications for Wyoming fixture involve locating the load edges away from the notch edge.

2. All AFPB specimens tested with doublers except for stated modifications.

3. U = Unidirectional lay-up $[0]_s$
Q = Quasi-isotropic lay-up $[\pm45,0,90,\mp45,0,90,\pm45,0,90]_s$.

not across the gage section. The shear failure of these specimens will be discussed in the following section.

Notch angles of 90, 105, 120 and 135 degrees were chosen to determine the effects of notch angle on the material's shear properties. For the Wyoming test technique, it was necessary to manufacture a separate fixture for each given notch angle in order to load a specimen with that angle exactly at the notch edge. A sharp notch and notch radii of 0.05 and 0.10 inches were selected to investigate the effects of notch radius on the results. The notation 90/0 indicates a specimen with a 90-degree notch angle and a sharp notch; 120/0.10 indicates a specimen with a 120-degree notch angle and a notch radius of 0.10 inches; etc. All tests were conducted to measure in-plane shear properties except as indicated on Table 5.1.

Testing of the Iosipescu specimens was performed in the Structures Research Laboratory at NASA/LRC. The experimental tests were conducted at a test speed of 0.05 inch/minute on hydraulic test machines. All test data were recorded on an X-Y recorder.

Modifications to the Wyoming fixture consisted of moving the loading edges away from the notch edge. To accomplish this, specimens with a 90-degree notch angle were placed in the fixtures designed for specimens with either a 105-, 120- or 135-degree notch angle. This moved the loading points to 0.03, 0.07 or 0.14 inches, respectively, from the notch edge of the specimen with a 90-degree angle. Also, specimens with a 120-degree angle and a 0.05-inch radius were tested in the 135-degree fixture to determine the effects of loading away from the notch edge. These series of tests should correlate with the results of the finite element analysis.

Modifications to the AFPB fixture consisted of finding ways to alleviate the crushing of the cylindrical load bars. Specimens were tested without doublers to give an indication of the severity of the crushing. Specimens with doublers were the standard test configuration. It was also decided to distribute the load by placing a rectangular bar between the cylindrical load rods and the specimen. The rectangular bars were placed parallel to the specimen edges and simulated the Wyoming fixture's load configuration.

Because of the large size of the AFPB specimen, it was not practical to run interlaminar shear tests using the AFPB fixture.

It should also be noted that improvements were made to the AFPB test fixture because of the possibility of frictional forces developing between the fixture halves as they slip past one another. The location is shown on Fig. 5.2. Small rollers were placed at the foot of the thinner leg of each part to prevent large frictional forces. This modification did increase the cost of the fixture and a simpler solution may have been found, but the placement of a roller at this location not only reduced the frictional forces but also helped to align the fixture halves. Another potential friction area was between the support rails of one fixture half and the other half as the parts slid by one another as shown on Fig. 5.2. Teflon strips were placed between the support rails and the fixture halves to lessen the frictional effects.

No alterations to the the Wyoming fixture were attempted.

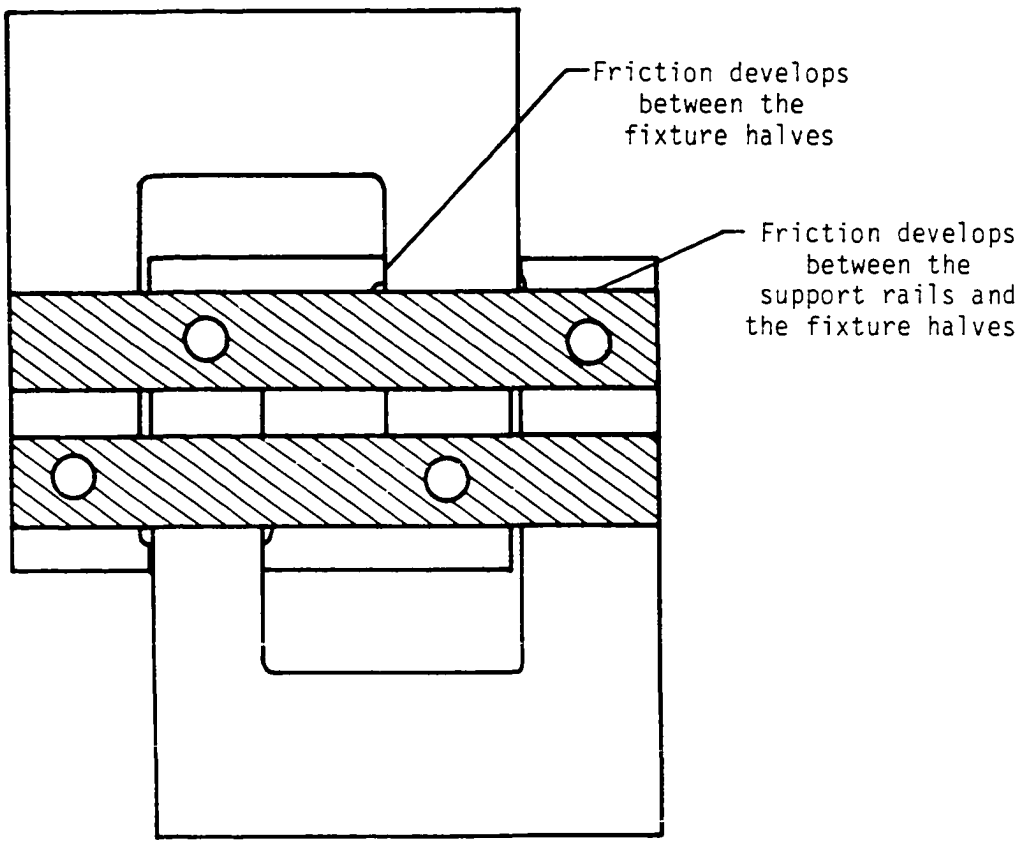

Fig. 5.2. Locations of potential friction forces developing in the AFPB Iosipescu Shear fixture.

Chapter 6

RESULTS AND DISCUSSION

6.1 Analytical Results

6.1.1 Specimen with a Sharp Notch/Wyoming Fixture

The results of the finite element analysis of the Wyoming loading conditions are given on Figs. 6.1 through 6.7. Figure 6.1 shows the variation of σ_x and Fig. 6.2 shows the variation of σ_y and T_{xy} in an isotropic material as the loading edges are moved away from the notch edge. Values have been normalized by the average shear stress, $\bar{T}$, as calculated from the reaction forces at the boundary. Though the σ_x stress concentration at the notch tip increases slightly as the loading distance increases, the stress value still tends toward zero elsewhere in the gage section. The σ_y stress curves, on the other hand, approach zero as the loading distance increases. The value of σ_y decreases from 50 percent of the average shear stress with loading at the notch edge to a low of 20 percent with loading 0.2 inches from the notch. The normalized shear stress approaches 1.0 in the gage section and the shear stress concentration at the notch tip decreases as the loading is moved away from the edge of the notch. Based on these results, a loading distance of 0.2 inches from the notch edge would be preferable. It may be assumed that the same trends will continue if the loading is further removed from the notch, but one must be aware of the danger of exceedingly high σ_x stresses at the notch tip.

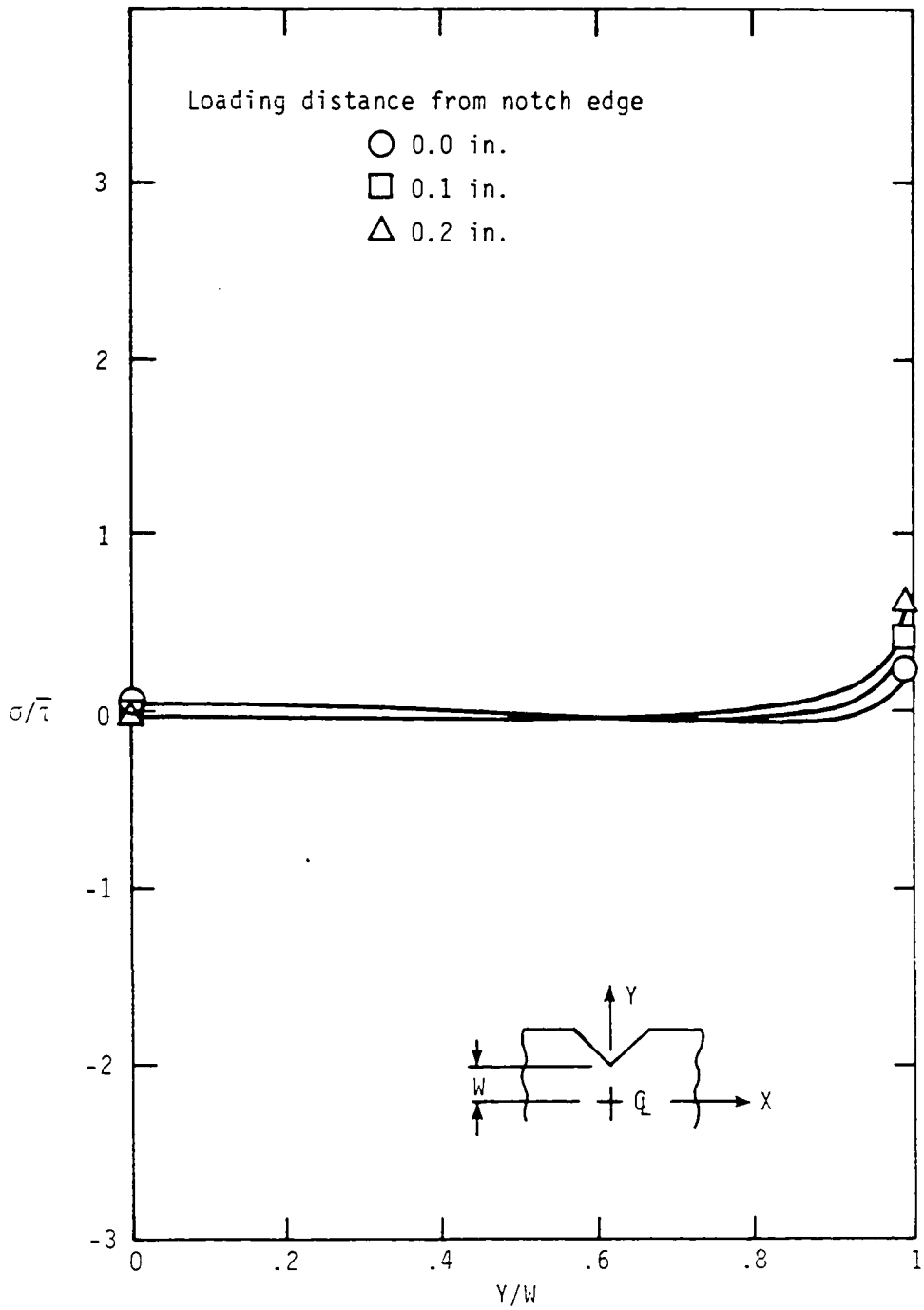

Fig. 6.1. Variation of σ_x in an isotropic material as the loading edges are removed from the notch edge in the Wyoming fixture.

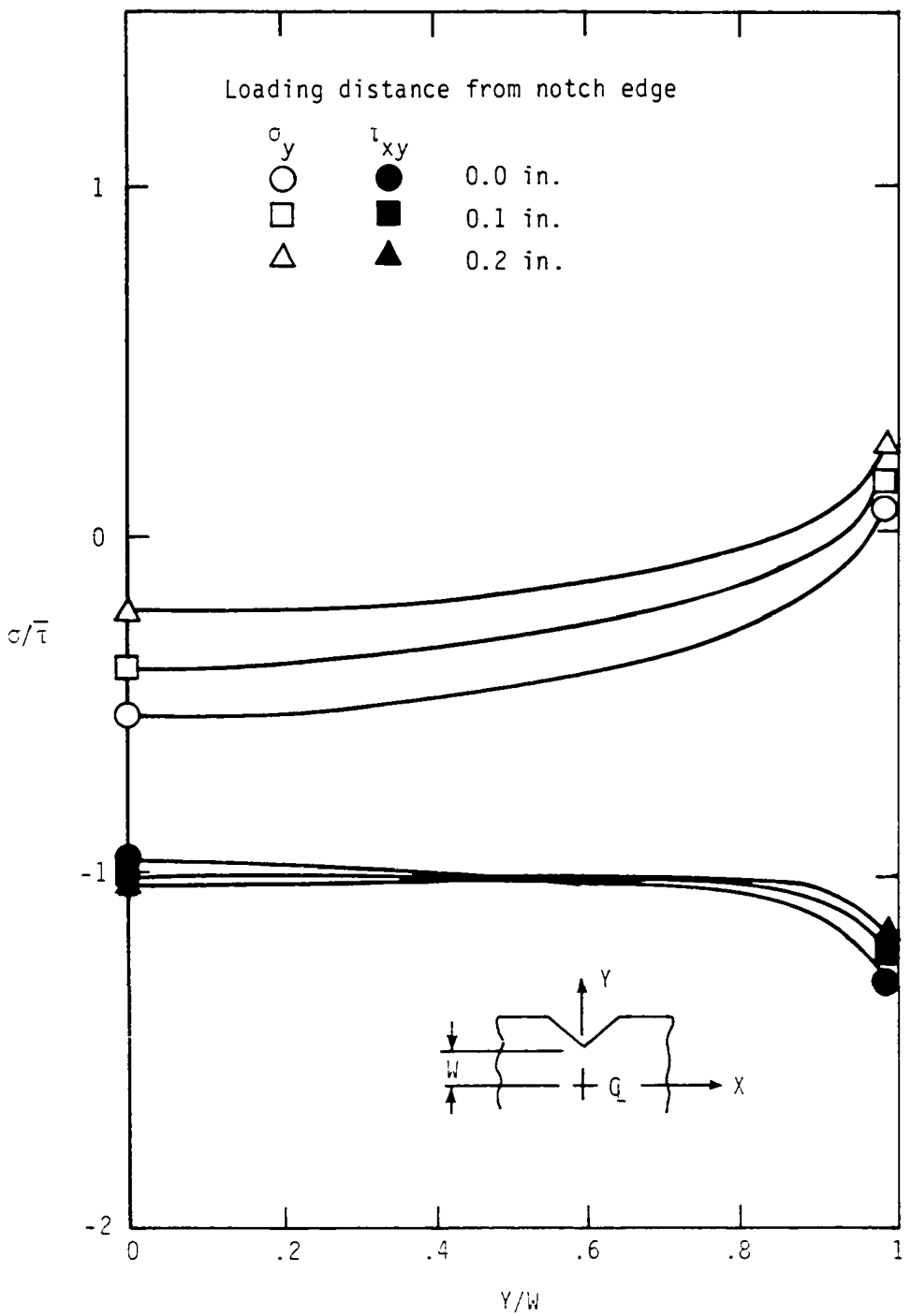

Fig. 6.2. Variation of σ_y and τ_{xy} in an isotropic material as the loading edges are removed from the notch edge in the Wyoming fixture.

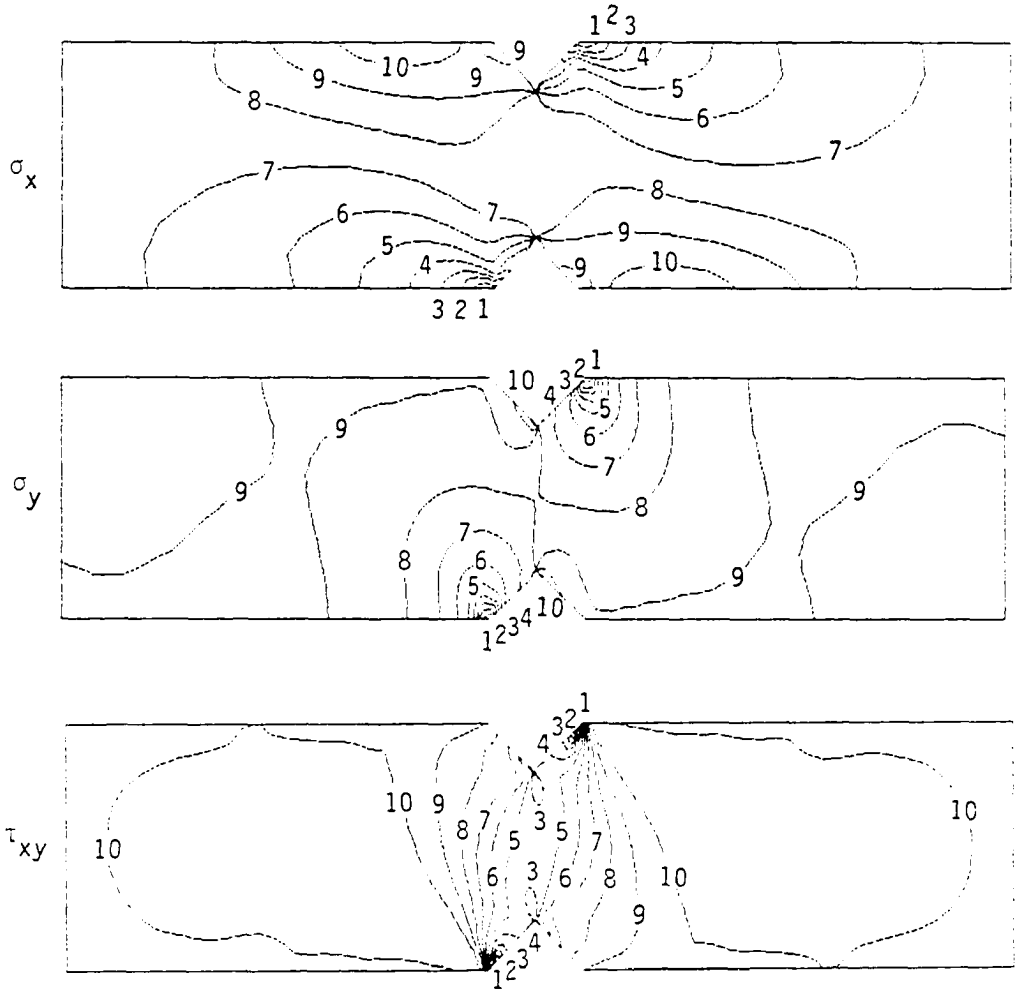

Contour number	Stress σ_x	σ_y	τ_{xy}
1	-1.7	-4.0	-1.5
2	-1.4	-3.5	-1.3
3	-1.1	-3.0	-1.2
4	-0.9	-2.5	-1.0
5	-0.6	-2.0	-0.8
6	-0.3	-1.5	-0.6
7	-0.1	-1.0	-0.5
8	0.2	-0.5	-0.3
9	0.5	0.0	-0.1
10	0.8	0.5	0.0

Fig. 6.3. Contour plots of an isotropic specimen loaded at the notch edge in the Wyoming fixture.

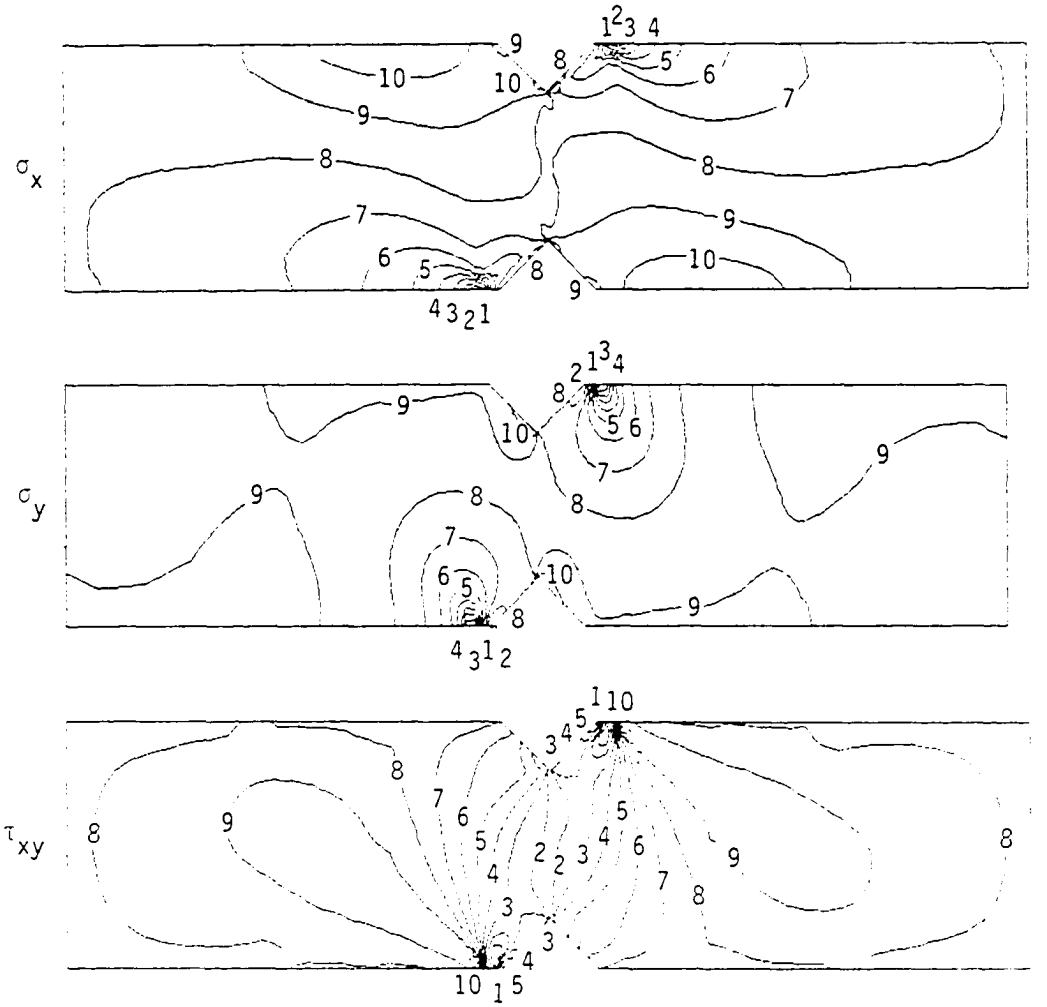

Contour number	Stress σ_x	σ_y	τ_{xy}
1	-2.6	-4.0	-1.1
2	-2.3	-3.4	-1.0
3	-1.9	-3.0	-0.8
4	-1.5	-2.5	-0.6
5	-1.1	-2.0	-0.5
6	-0.8	-1.5	-0.3
7	-0.4	-1.0	-0.1
8	-0.1	-0.5	0.0
9	0.4	0.0	0.2
10	0.7	0.5	0.4

Fig. 6.4. Contour plots of an isotropic specimen loaded 0.10 inches from the notch edge in the Wyoming fixture.

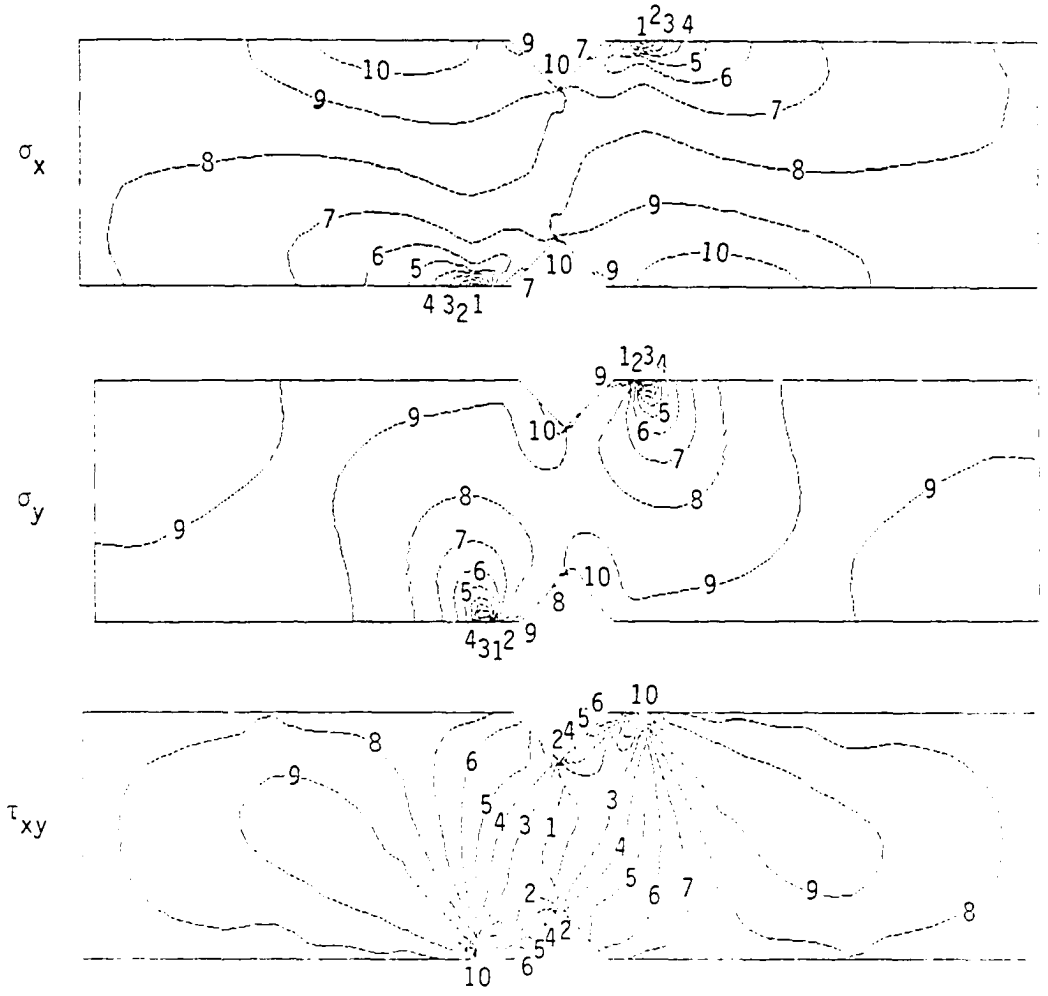

Contour number	Stress σ_x	σ_y	τ_{xy}
1	-3.1	-4.4	-1.2
2	-2.7	-3.8	-1.0
3	-2.2	-3.3	-0.8
4	-1.8	-2.8	-0.6
5	-1.3	-2.2	-0.4
6	-0.9	-1.7	-0.3
7	-0.5	-1.1	-0.1
8	0.0	-0.6	0.1
9	0.4	-0.1	0.3
10	0.9	0.5	0.5

Fig. 6.5. Contour plots of an isotropic specimen loaded 0.20 inches from the notch edge in the Wyoming fixture.

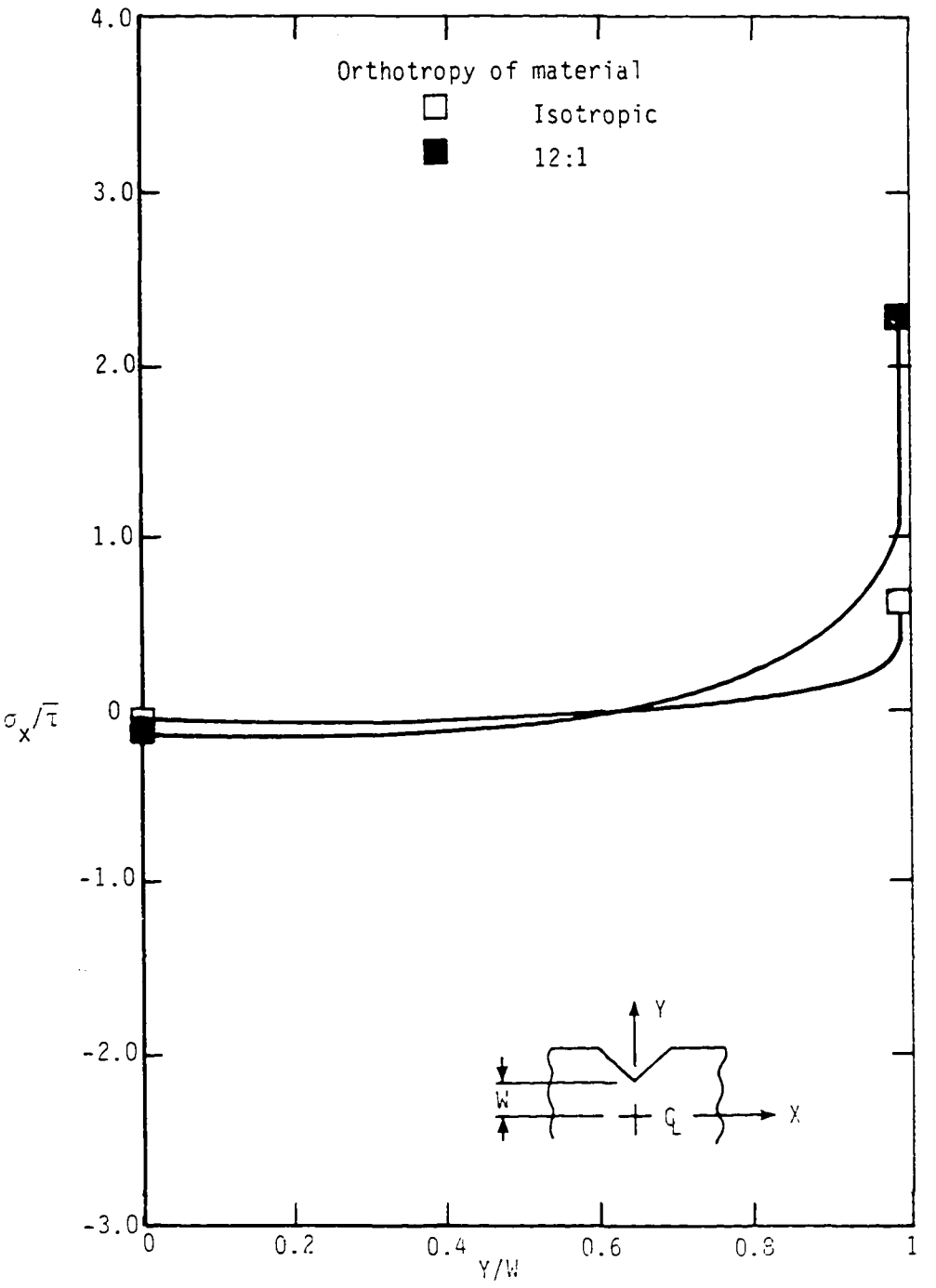

Fig. 6.6. Variation of σ_x in various materials when the loading edges are 0.20 inches from the notch edge in the Wyoming fixture.

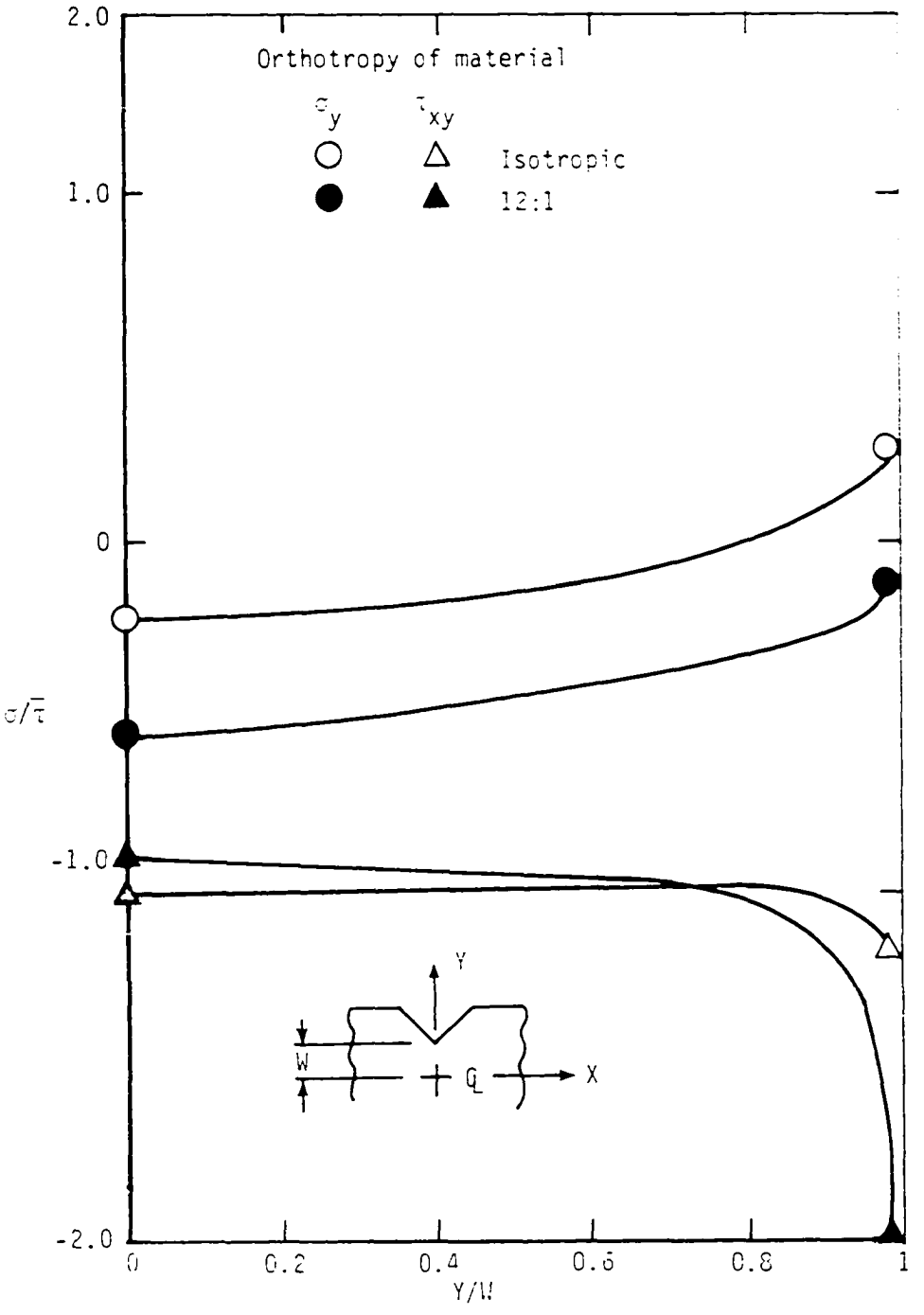

Fig. 6.7. Variation of σ_y and τ_{xy} in various materials when the loading edges Are 0.20 inches from the notch edge in the Wyoming fixture.

Figures 6.3, 6.4 and 6.5 show normalized contour plots of the stress states throughout an isotropic Iosipescu specimen as the loading points are removed from the notch edge. Note the decreasing nature of the τ_{xy} stresses and the growth of a region of relatively uniform shear stress in the gage section as the loading edges are removed from the notch region. Obviously, the influence of aberrant stresses is minimized by moving the loading points away from the notch edge.

The advantages of loading an isotropic specimen at 0.2 inches from the notch edge in the Wyoming fixture led to examining the behavior of orthotropic materials under this condition. Figures 6.6 and 6.7 show the variation of σ_x, σ_y and T_{xy} as a function of material orthotropy. As expected, the stress concentrations at the notch tip are aggravated by the increasing orthotropy, making the loading location of 0.2 inches unsuited for use with orthotropic materials.

Note that in the preceeding figures the values of the node right before the notch tip, and not on the notch tip, are shown. The limitations of finite element analysis at a discontinuity, such as a perfectly sharp notch, prevent an accurate determination of a nodal value at this point. The nodal values depicted on these figures are the average of the center values of the surrounding elements. The stress values are continuous throughout the interior of an element, but they are not continuous at the boundaries. Hence, even though the mesh used in this study is exceedingly fine at the notch tip, where the first elemental value is an average of zero and a high stress concentration, the mesh is sufficent only to observe trends in the results. A quantitative number cannot be determined at the notch tip. This applies to other figures also.

6.1.2 Specimen with a Sharp Notch/ AFPB Fixture

The results of the finite element analysis of the AFPB loading conditions are given on Figs. 6.8 through 6.17. Figure 6.8 shows the variation of σ_x and Fig. 6.9 shows the variation of σ_y and T_{xy} in an isotropic material as the loading edges are moved away from the notch edge. The same trends for σ_x that were evident under the Wyoming load conditions (Fig. 6.1) are continued with the point-loading of the AFPB fixture. The stress concentrations at the notch tip continue to rise as the load edges are shifted away from the notch, yet the stress quickly falls to zero elsewhere in the gage section.

The σ_y stresses also follow the same trends with loading distance from the notch edge as shown by the Wyoming fixture. Note however that for a loading point of 0.9 inches from the notch edge, the value of σ_y remains nearly constant at approximately ten percent of the average shear stress. On the other hand, at 0.5 inches from the notch edge, the transverse stresses are approximately zero near the centerline, though a stress concentration is apparent at the notch tip. The shear stress does not vary to any significant degree with loading distance.

The contour plots shown on Figs. 6.10 through 6.12 emphasize the effects of point loading on the specimen. Modeling of the extra stiffness provided by the doublers was not attempted, hence the stress contours shown are associated with specimen crushing. Since the concentrated load stresses have little or no influence on the stress state in the notch region, Figs. 6.13 through 6.15 depict the stress state in the notched areas. These contour plots substantiate the trends shown on Figs. 6.8 and 6.9. The bending stress concentrations at the

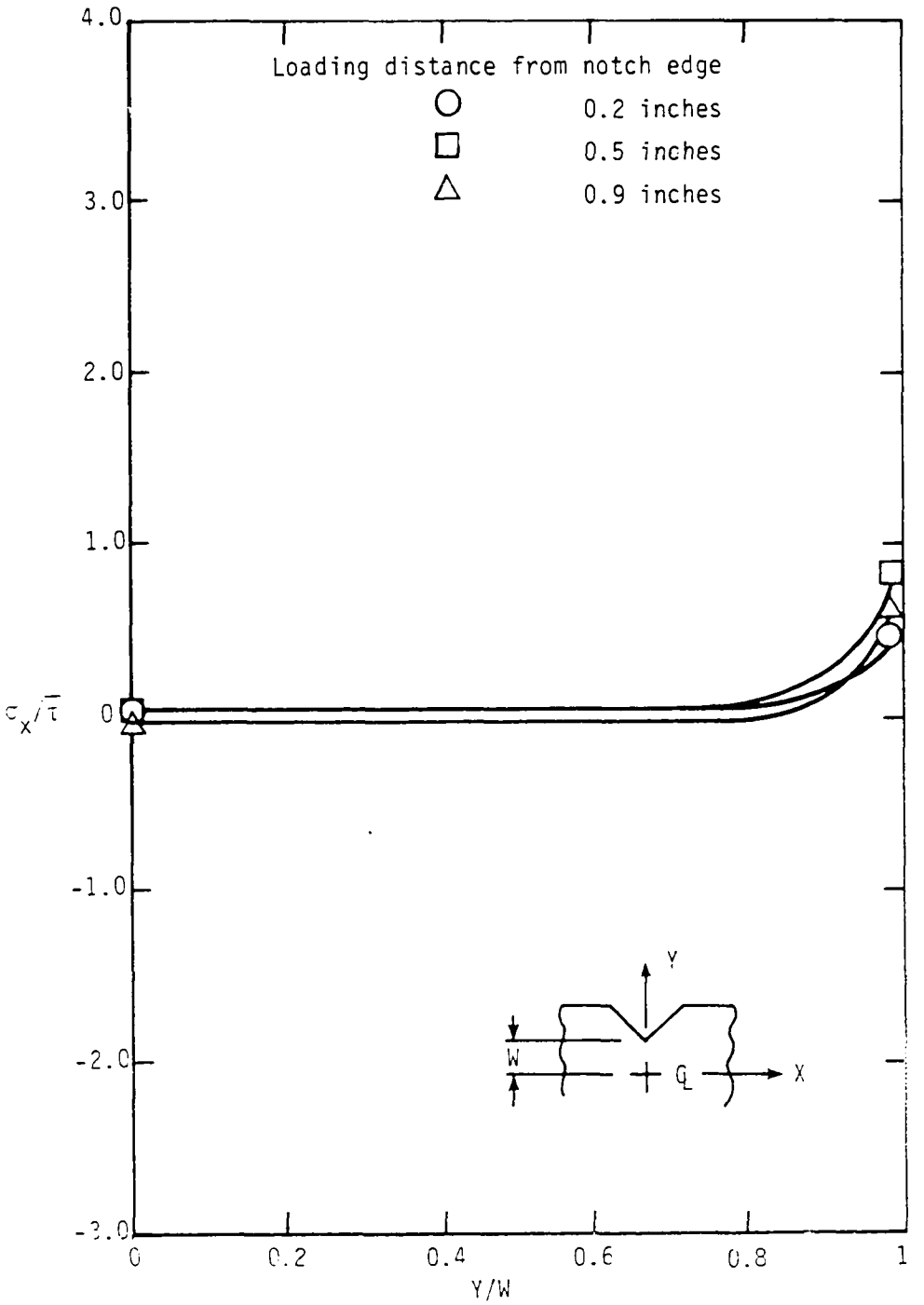

Fig. 6.8. Variation of σ_x in an isotropic material as the loading points are removed from the notch edge in the AFPB fixture.

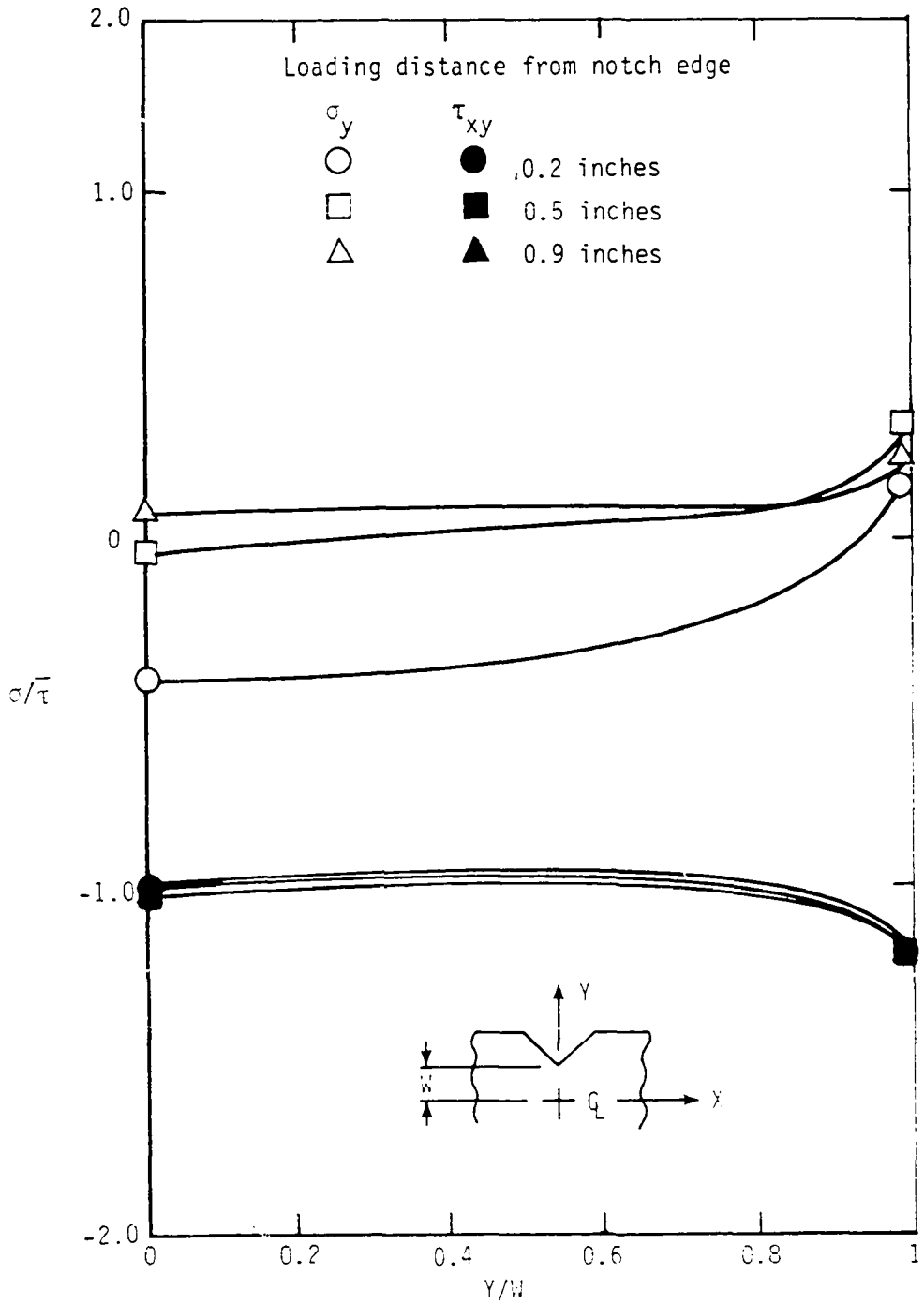

Fig. 6.9. Variation of σ_y and τ_{xy} in an isotropic material as the loading points are removed from the notch edge in the AFPB fixture.

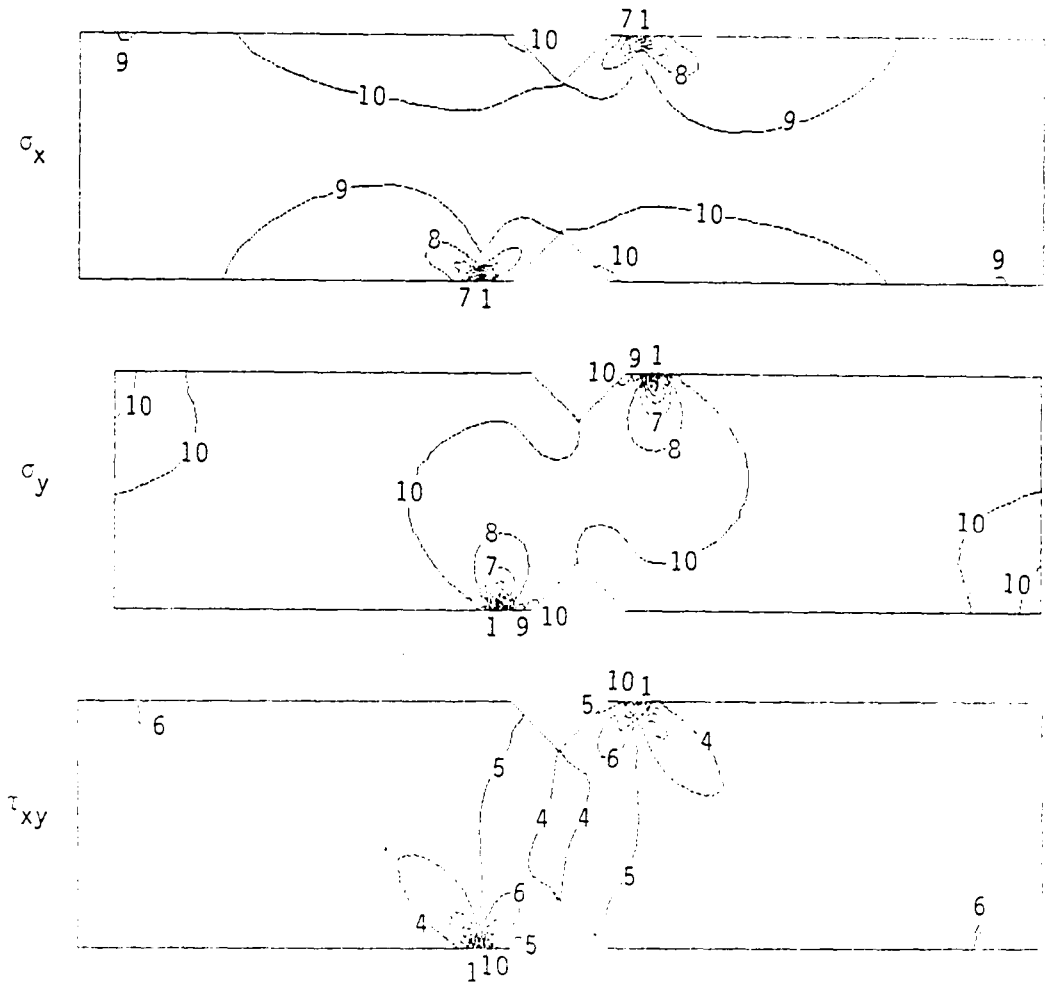

Contour number	Stress σ_x	σ_y	τ_{xy}
1	-5.6	-10.5	-2.7
2	-4.9	- 9.3	-2.1
3	-4.3	- 8.2	-1.5
4	-3.6	- 7.0	-0.9
5	-2.9	- 5.9	0.3
6	-2.3	- 4.8	0.3
7	-1.6	- 3.6	0.8
8	-0.9	- 2.5	1.4
9	-0.3	- 1.3	2.0
10	0.4	- 0.2	2.6

Fig. 6.10. Contour plots of an isotropic specimen loaded 0.20 inches from the notch edge in the AFPB fixture.

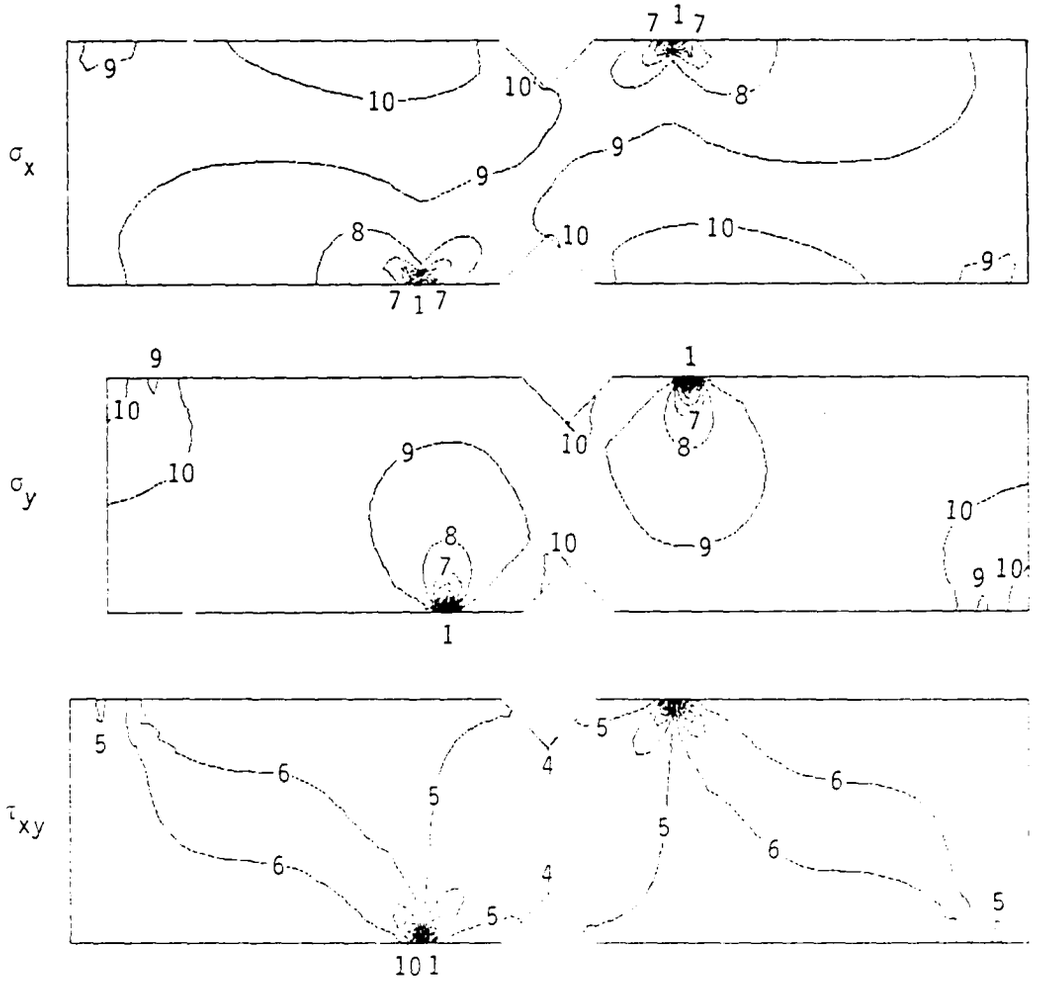

Contour number	Stress σ_x	σ_y	τ_{xy}
1	-7.0	-12.1	-3.1
2	-6.1	-10.2	-2.4
3	-5.3	- 9.5	-1.7
4	-4.4	- 8.1	-1.0
5	-3.5	- 6.9	-0.4
6	-2.7	- 5.6	0.3
7	-1.8	- 4.2	1.0
8	-0.9	- 2.9	1.7
9	-0.1	- 1.6	2.4
10	0.8	- 0.3	3.1

Fig. 6.11. Contour plots of an isotropic specimen loaded 0.50 inches from the notch edge in the AFPB fixture.

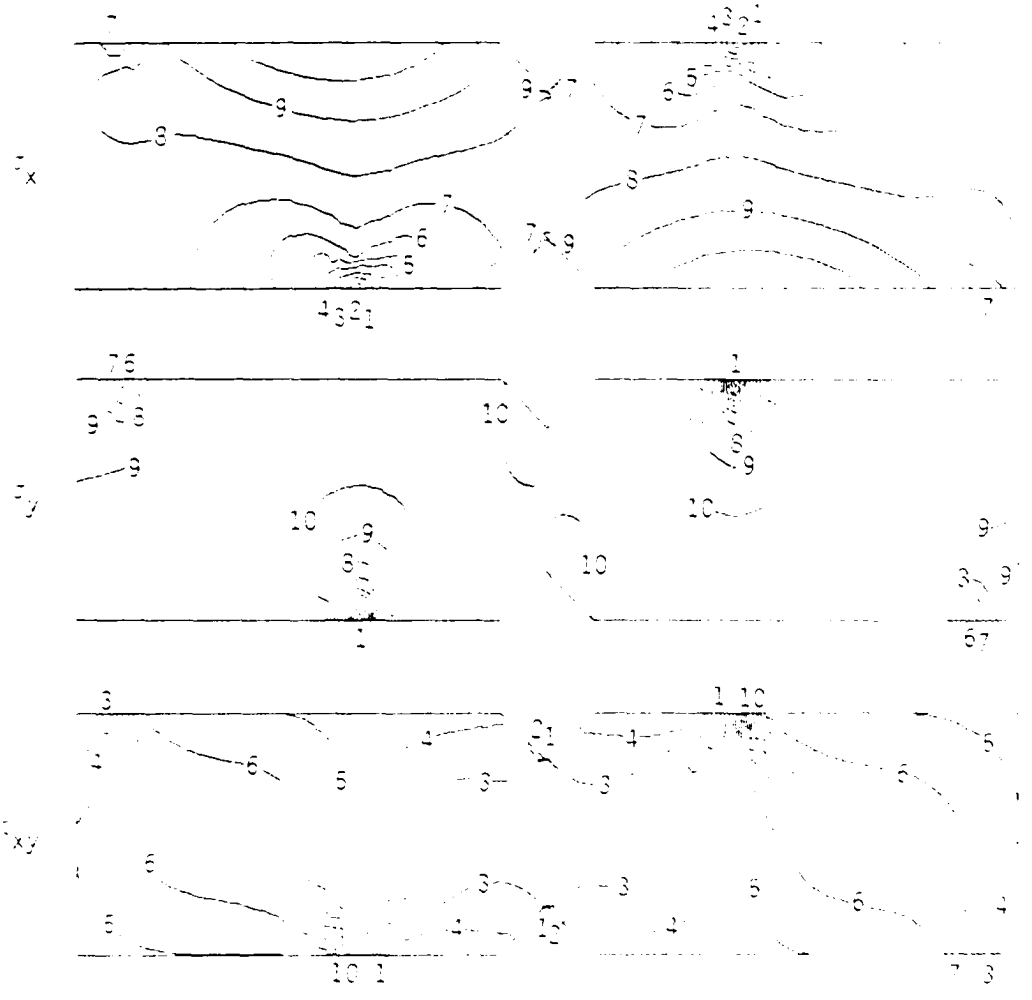

Contour number	Stress σ_x	σ_y	τ_{xy}
1	-5.1	-7.7	-1.4
2	-4.3	-6.9	-1.0
3	-3.6	-6.0	-0.7
4	-2.8	-5.1	-0.3
5	-2.1	-4.2	0.1
6	-1.3	-3.3	0.5
7	-0.6	-2.5	0.8
8	0.1	-1.6	1.2
9	0.9	-0.8	1.6
10	1.6	0.1	2.0

Fig. 6.12. Contour plots of an isotropic specimen loaded 0.90 inches from the notch edge in the AFPB fixture.

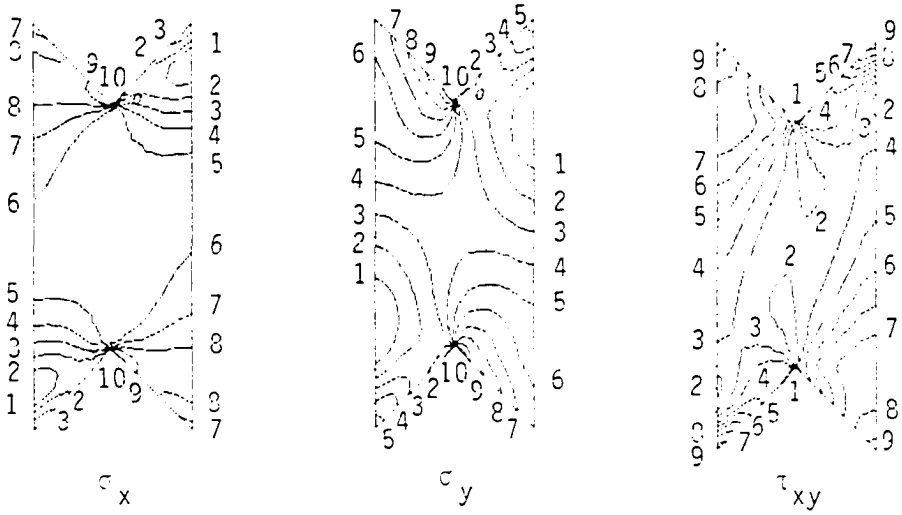

Contour number	Stress σ_x	σ_y	τ_{xy}
1	-0.8	-0.9	-1.1
2	-0.6	-0.7	-1.0
3	-0.4	-0.5	-0.9
4	-0.3	-0.3	-0.8
5	-0.1	-0.1	-0.7
6	0.1	0.0	-0.5
7	0.3	0.2	-0.4
8	0.5	0.4	-0.3
9	0.7	0.6	-0.2
10	0.9	0.8	-0.1

Fig. 6.13. Notch detail of an isotropic specimen loaded 0.20 inches from the notch edge in the AFPB fixture.

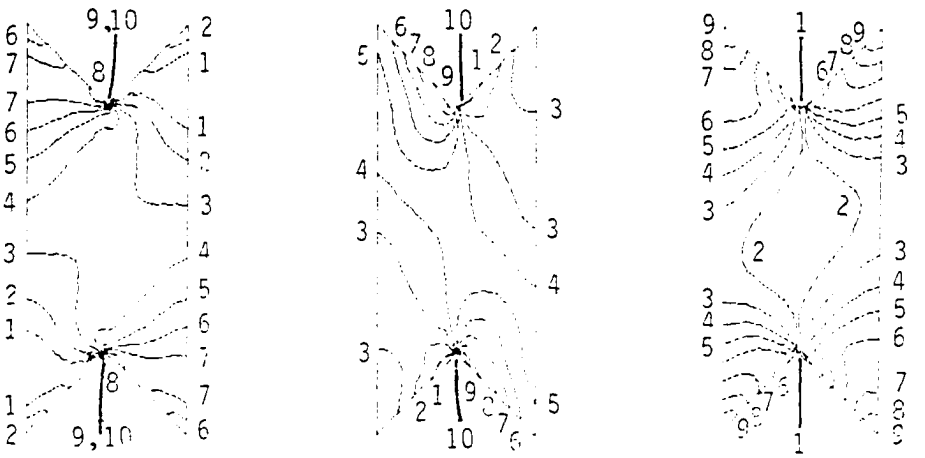

Contour number	Stress σ_x	σ_y	τ_{xy}
1	-0.5	-0.5	-1.1
2	-0.3	-0.4	-1.0
3	-0.1	-0.2	-0.9
4	0.1	-0.1	-0.7
5	0.3	0.1	-0.6
6	0.4	0.3	-0.5
7	0.6	0.4	-0.4
8	0.8	0.6	-0.3
9	1.0	0.7	-0.2
10	1.2	0.9	-0.1

Fig. 6.14. Notch detail of an isotropic specimen loaded 0.50 inches from the notch edge in the AFPB fixture.

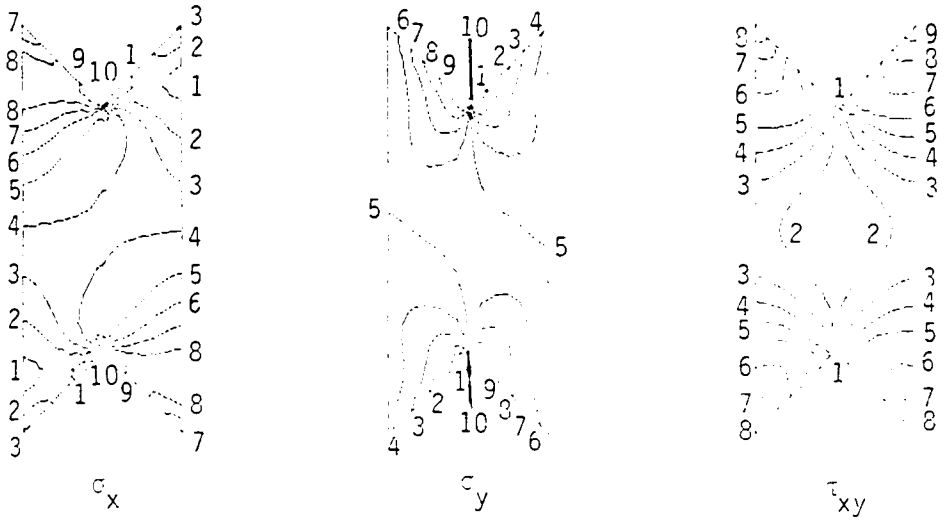

Contour number	Stress σ_x	σ_y	τ_{xy}
1	-0.6	-0.6	-1.1
2	-0.4	-0.4	-1.0
3	-0.2	-0.3	-0.8
4	-0.1	-0.1	-0.7
5	0.1	0.0	-0.6
6	0.3	0.2	-0.5
7	0.4	0.4	-0.4
8	0.6	0.5	-0.3
9	0.8	0.7	-0.2
10	0.9	0.8	-0.1

Fig. 6.15. Notch detail of an isotropic specimen loaded 0.90 inches from the notch edge in the AFPB fixture.

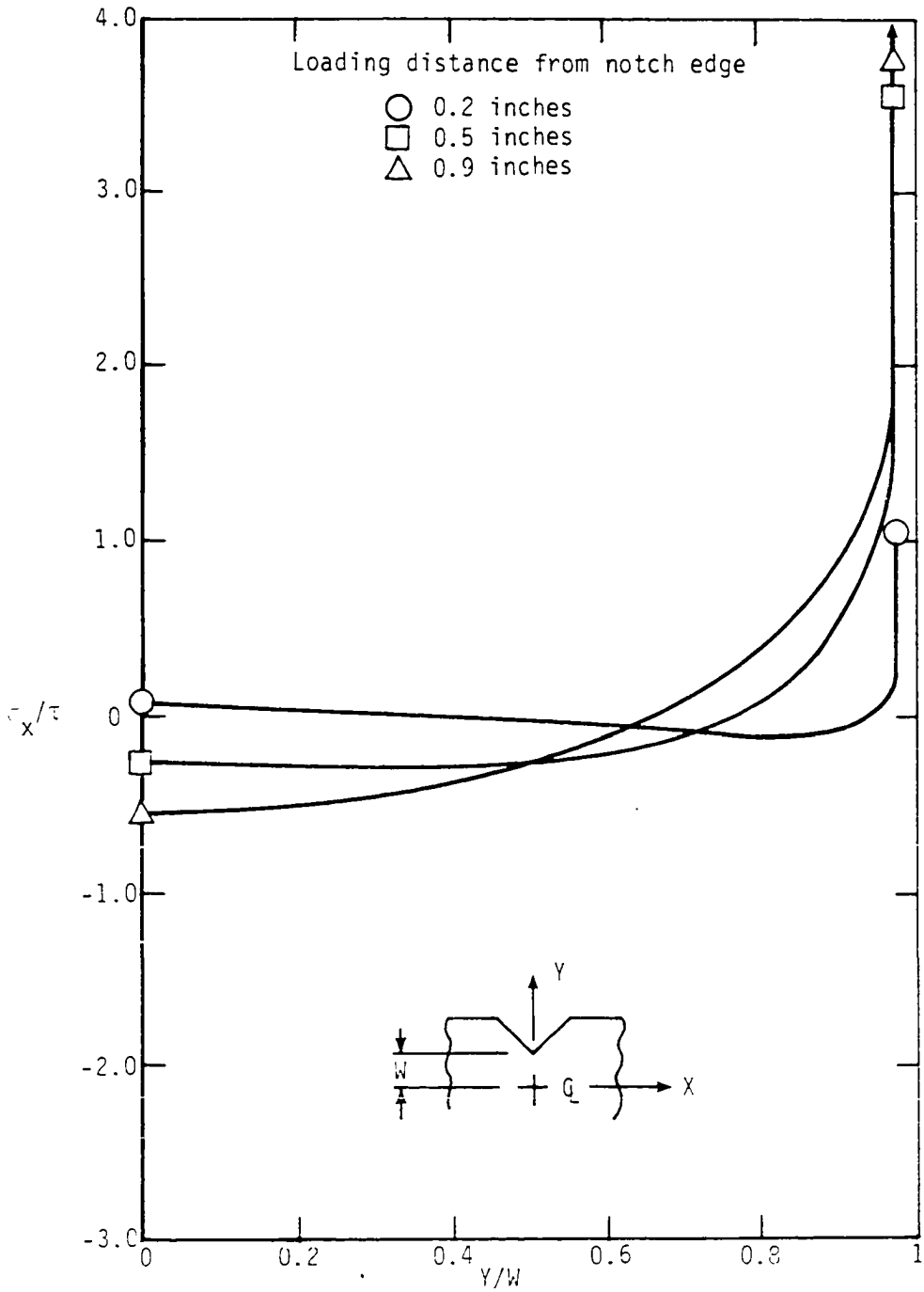

Fig. 6.16. Variation of σ_x in a 12:1 orthotropic material as the loading points are removed from the notch edge in the AFPB fixture.

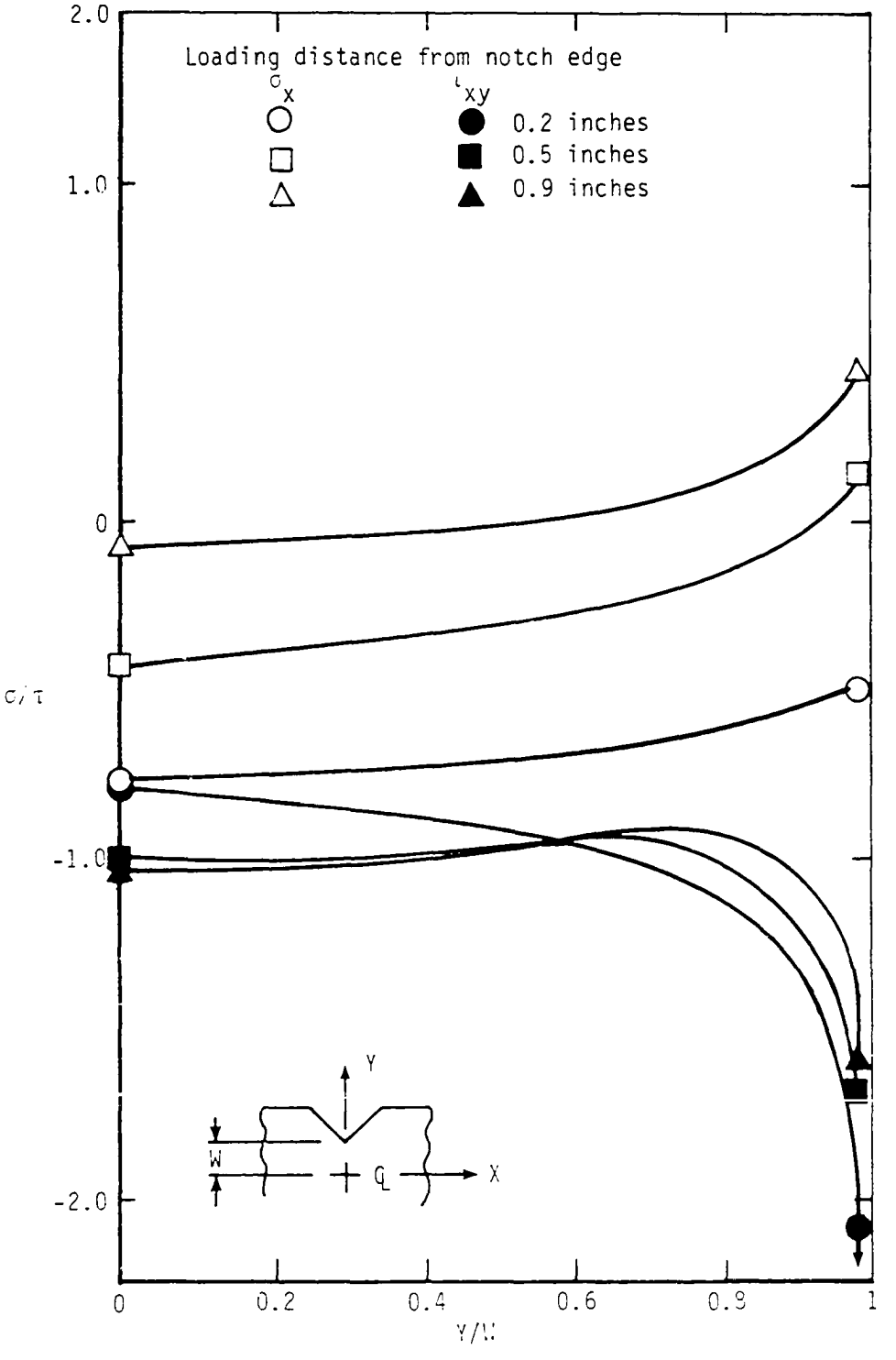

Fig. 6.17. Variation of σ_y and τ_{xy} in a 12:1 orthotropic material as the loading points are removed from the notch edge in the AFPB fixture.

notch tip increase with increasing load distance from the notch. The central region of relatively low transverse stresses enlarges as the load edges are moved from the notch and a definite expansion of a uniform shear stress region where the value approaches 1.0 is apparent.

Figures 6.16 and 6.17 show the trends of σ_x, σ_y and T_{xy} as a function of loading distance for an orthotropic ratio of 12:1. As was the case for an isotropic material, the increasing loading distance aggravates the bending stress concentrations at the notch tip. Similarly, the transverse stresses approach zero and the shear stresses approach 1.0 as the loading distance is increased. A 0.2-inch loading distance for the AFPB fixture gives questionable results since the transverse and shear stresses are of the same magnitude for an orthotropic material.

It appears that a loading distance of 0.9 inches will produce nearly ideal transverse and shear stress states, though the presence of large bending stresses make this loading distance somewhat undesirable. A loading distance of 0.5 inches minimizes the bending stresses, but the transverse stresses are of significant magnitude to raise questions about the desirability of this loading distance. Yet because an orthotropic material is stronger in the 1-direction than in the 2-direction, it is better adapted to handling large bending stresses. Hence, a distance of 0.9 inches from the notch edge would appear to be a reasonable loading position for the AFPB fixture.

6.1.3 Specimen with a Notch Radius/Wyoming and AFPB Fixtures

The conclusion stated above is based upon the finite element analyses of an Iosipescu specimen with a sharp notch tip. It is advantageous to also determine the effects of loading distance on the stress states of an Iosipescu Shear specimen with a rounded notch.

The analysis of an orthotropic Wyoming specimen with a sharp notch showed that a loading distance of 0.2 inches from the notch edge resulted in unfavorable conditions for determining the shear properties of a composite material. For comparison, a Wyoming specimen with a 0.05-inch notch radius was examined at this particular load location for an isotropic and orthotropic material. The results of the analyses are given on Figs. 6.18 and 6.19 and provide a remarkable contrast to the sharp-notched results of Figs. 6.6 and 6.7. The bending stress concentrations found in isotropic and orthotropic materials with a notch radius remain relatively unchanged. There is, however, a considerable improvement in the transverse and shear stress states. At the notch tip there is a tendency for the stress concentrations to be alleviated when a notch radius is used. But the stress values at the centerline remain relatively unchanged.

Calculations were also made for an isotropic Wyoming specimen with a 0.10-inch notch radius. The results were the same as for a 0.05-inch notch radius, indicating that a larger notch had little effect on the stress states in the material.

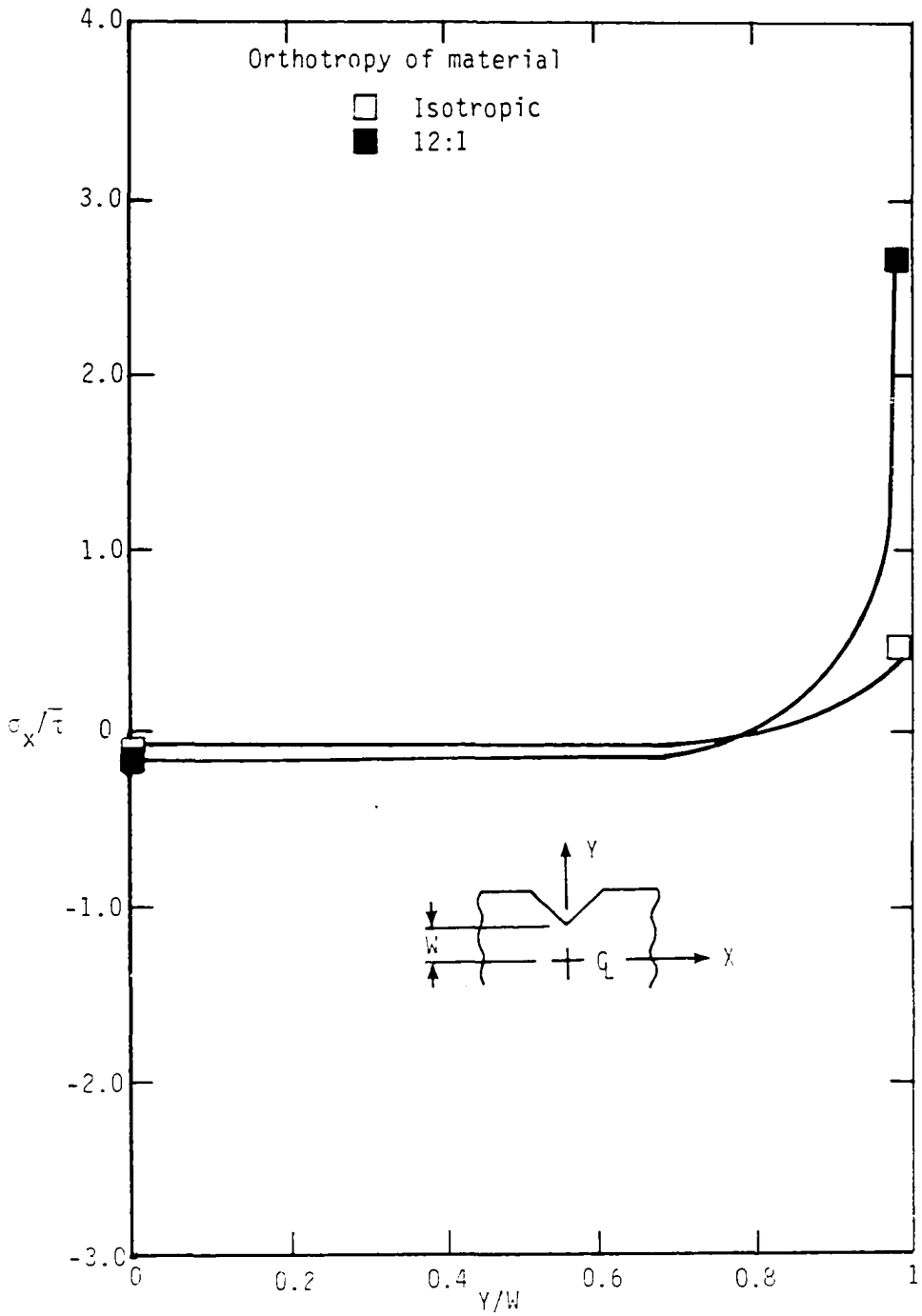

Fig. 6.18. Variation of σ_x in various materials with a notch radius of 0.05 inches when the loading edges are 0.20 inches from the notch edge in the Wyoming fixture.

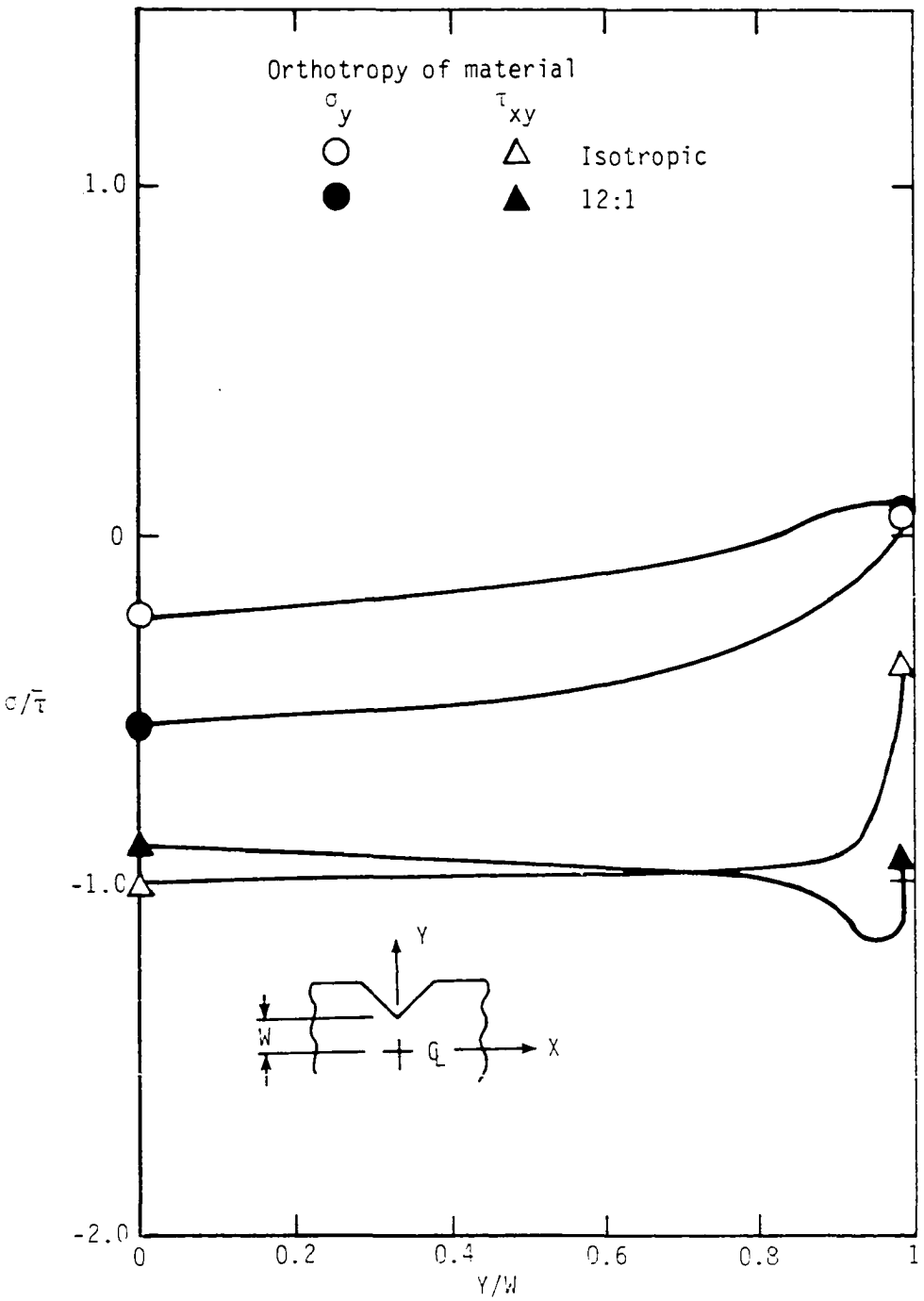

Fig. 6.19. Variation of σ_y and τ_{xy} in various materials with a notch radius of 0.05 inches when the loading edges are 0.20 inches from the notch edge in the Wyoming fixture.

Figures 6.20 through 6.23 give the results of the AFPB loading technique on a specimen with a rounded notch. Figure 6.20 depicts the variation of the bending stress in an isotropic material as a function of loading distance from the notch edge. In comparison to Fig. 6.8, it can be seen that the radius alleviates the stress concentrations. The same result occurs with the transverse and shear stresses as shown on Fig. 6.21. Results for an isotropic AFPB specimen with a 0.10-inch notch radius were also identical to the results for a specimen with a 0.05-inch notch radius.

For an orthotropic material, a radius makes little difference in the bending stress state as a comparison between Fig. 6.22 and Fig. 6.16 reveals. As in the case of an isotropic material, the most significant reductions in stress concentrations occur with the transverse and shear stress states. Figures 6.23 and 6.17 relate the differences in the stress states due to a rounding of the notch tip. Note that the advantages of loading a specimen 0.9 inches from the notch edge are again substantiated as evidenced by the low transverse stresses and the near uniformity of the shear stress around 1.0 on Fig. 6.23.

In summary, the results of the finite element analyses indicate the desirability of loading an orthotropic Iosipescu Shear specimen at least 0.9 inches from the notch edge and machining a radius into the notch tip. These conditions will result in a more uniform shear stress in the notch region and will minimize the transverse stresses. One must be aware, however, of the magnitude of the bending stresses along the centerline which may be as great as 50 percent of the average applied

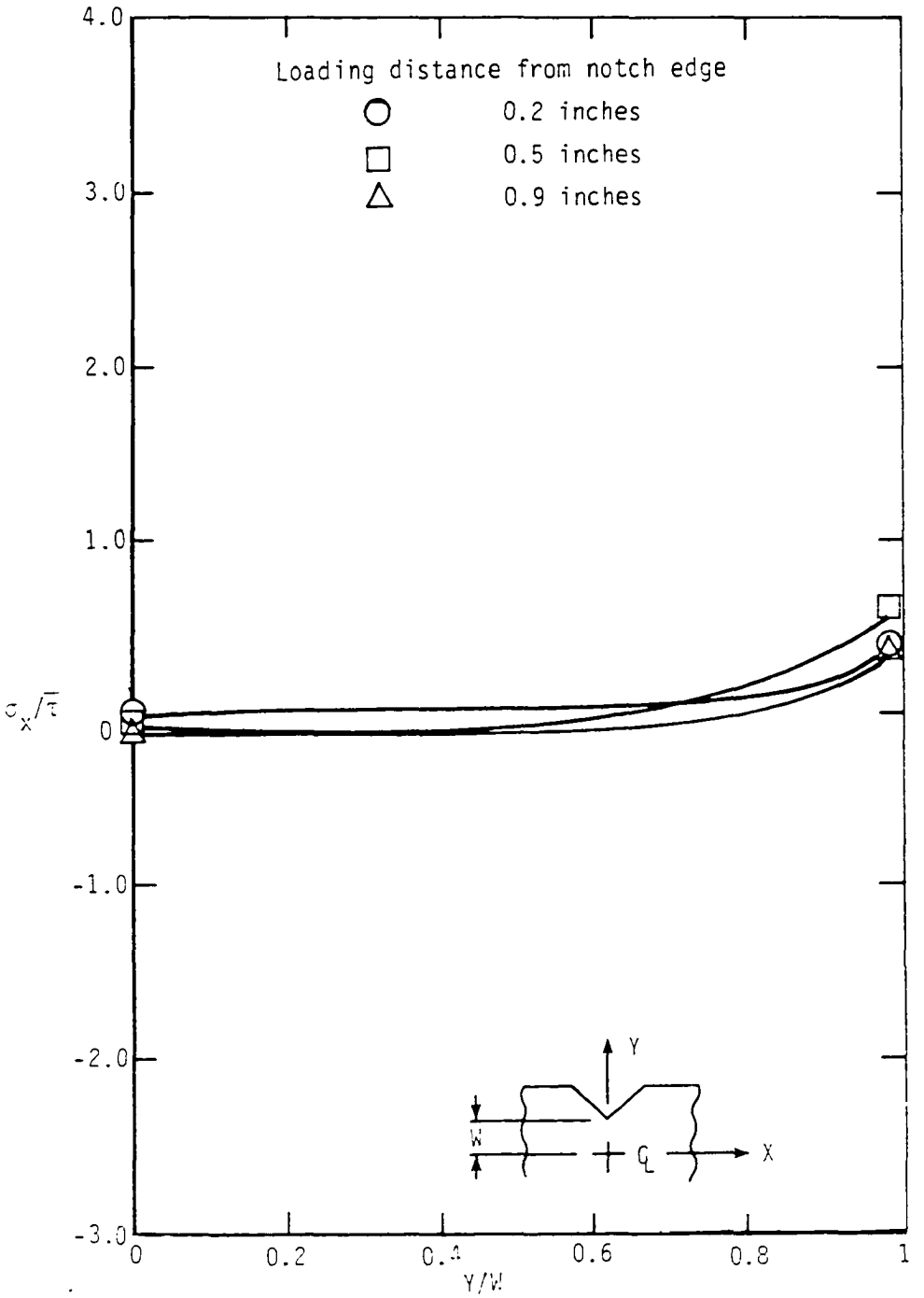

Fig. 6.20. Variation of σ_x in an isotropic material with a notch radius of 0.05 inches as the loading points are removed from the notch edge in the AFPB fixture.

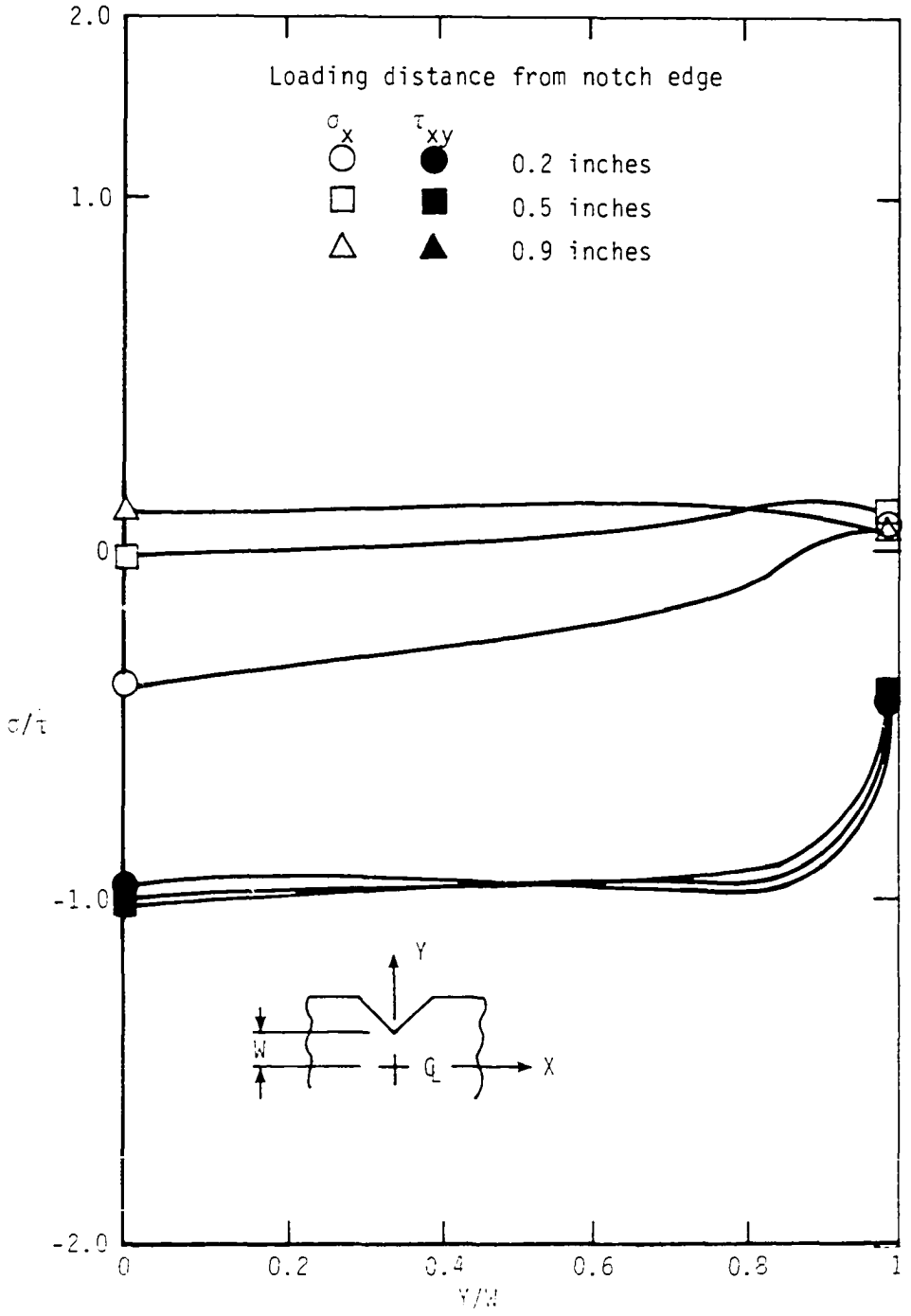

Fig. 6.21. Variation of σ_y and τ_{xy} in an isotropic material with a notch radius of 0.05 inches as the loading points are removed from the notch edge in the AFPB fixture.

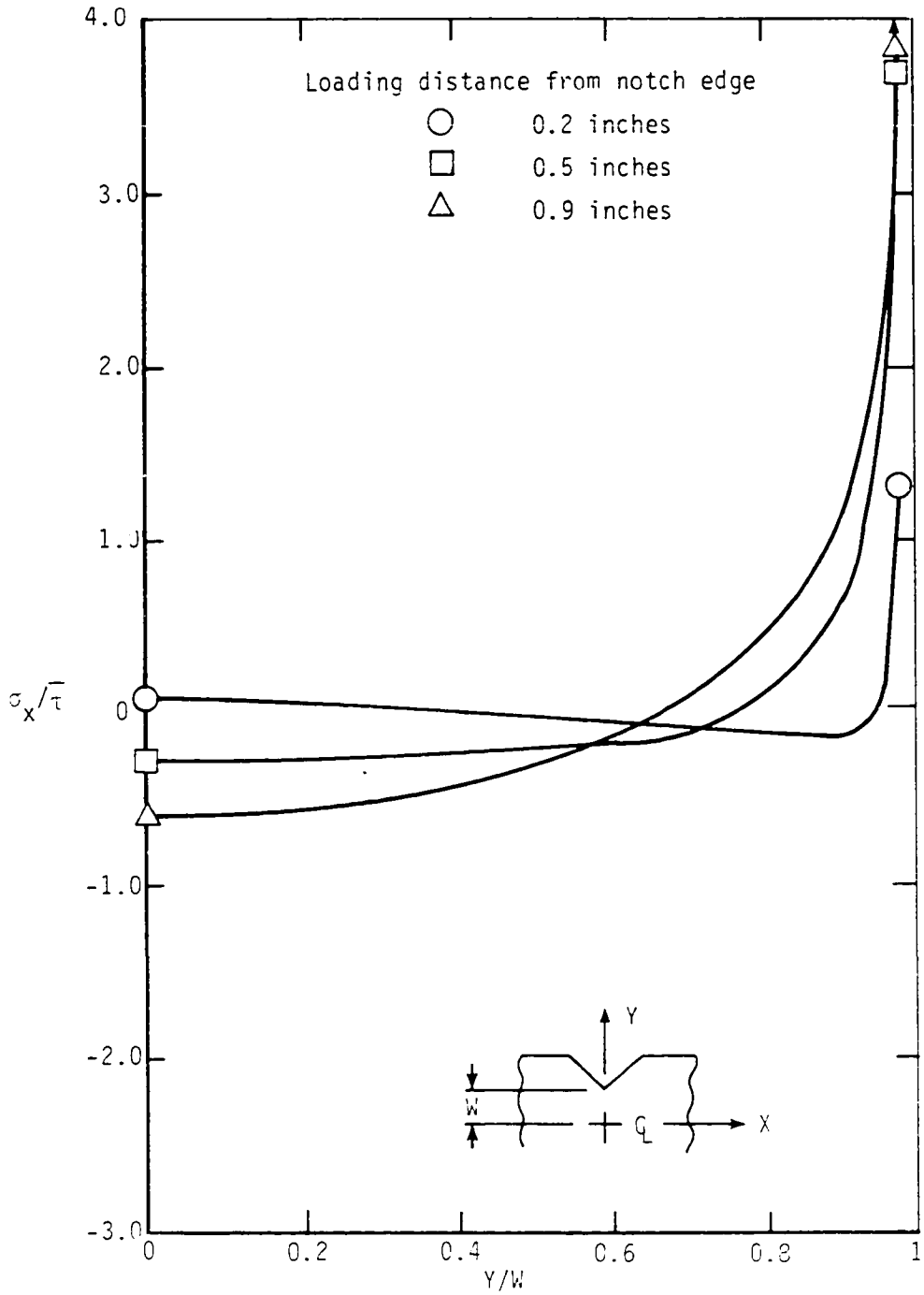

Fig. 6.22. Variation of σ_x in a 12:1 orthotropic material with a notch radius of 0.05 inches as the loading points are removed from the notch edge in the AFPB fixture.

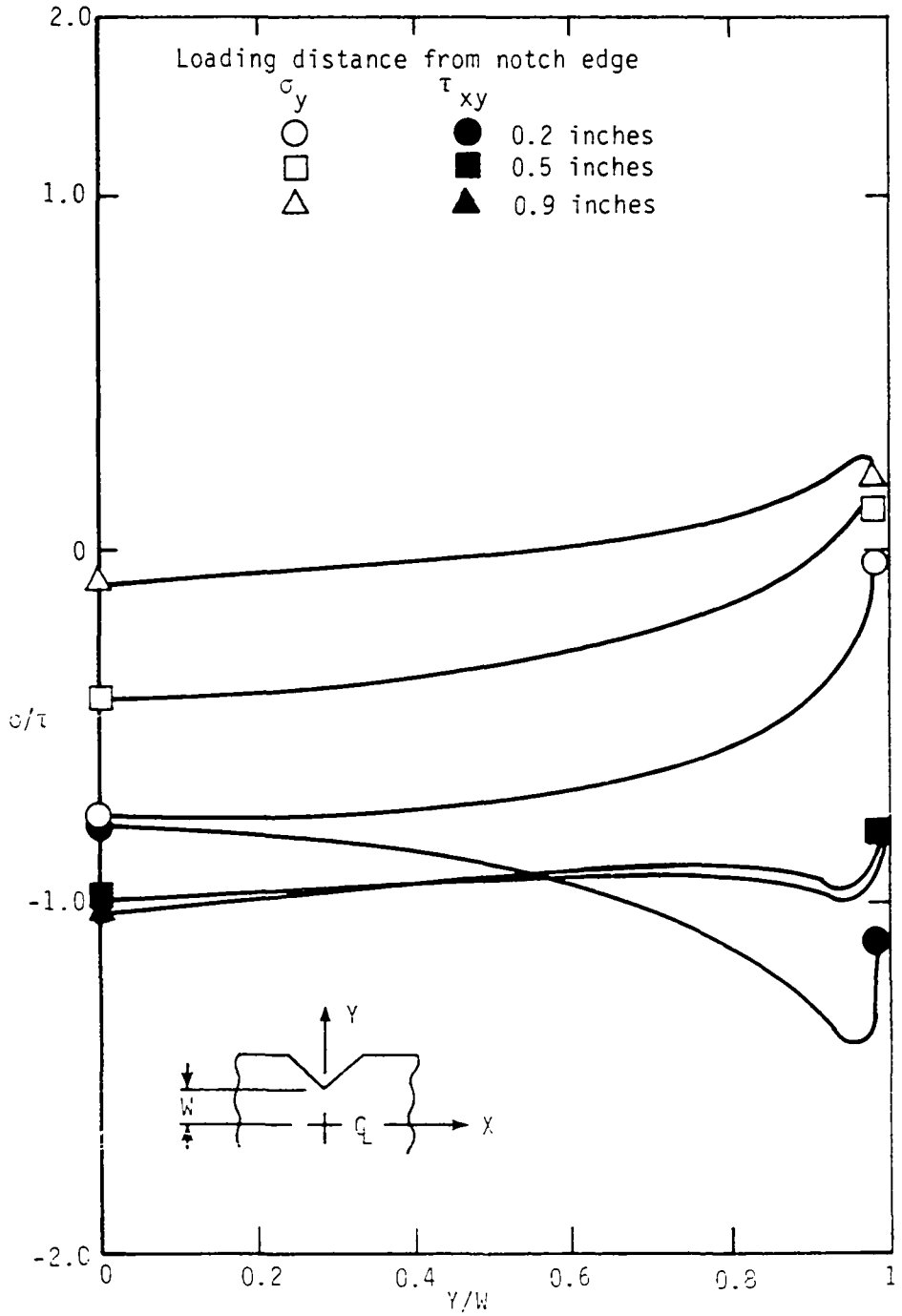

Fig. 6.23. Variation of σ_y and τ_{xy} in a 12:1 orthotropic material with a notch radius of 0.05 inches as the loading points are removed from the notch edge in the AFPB fixture.

shear stress. Yet because of the inherent strength of a composite material with fibers aligned in this direction, the bending stresses may have negligible influence on the failure mode of the specimen.

6.2 Experimental Results

The experimental investigations conducted for this study were intended to evaluate the effects of notch geometry modifications on the stress state and to examine the consequences of fixture modifications on the measured shear properties of a composite material. The failure modes were to be examined to determine the influences of normal stresses and to experimentally justify or refute the results of the finite element analysis. It should be noted that since the ratios of tensile modulus to shear modulus for steel and quasi-isotropic graphite/epoxy were similar, it was assumed that the finite element results for steel would approximate the responses for quasi-isotropic graphite/epoxy.

Table 6.1 lists the mechanical properties for AS4/3502 Graphite/Epoxy. The design data were determined by Lockheed-Georgia and the experimental data were the results of tensile tests performed on the plates of material fabricated at NASA/LRC. The excellent correlation of the unidirectional tensile data indicates that the fabricated plates were representative of typical material. Note that the design shear modulus was obtained by a Rail Shear test using [0/90] material.

Table 6.2 gives the shear properties as determined by the Iosipescu shear test for 90/0 unidirectional specimens. For both the Wyoming specimens which were loaded at the notch edge, and the AFPB specimens which were loaded at 0.9 inches from the notch edge,

Table 6.1 Properties of AS4/3502 Graphite/Epoxy

Design data for		Experimental results for	
Unidirectional material[1]	Quasi-isotropic material	Unidirectional material	Quasi-isotropic material
E_{11} = 20.50 Msi	--	20.80	7.80
E_{22} = 1.67 Msi	--	1.66	--
ν_{12} = 0.39	--	0.30	0.35
G_{12} = 0.87 Msi[2]	2.85[3]	Note 4	Note 4
T_{max} = --	--	Note 4	Note 4

Notes: 1. Design data obtained from Lockheed-Georgia by NASA/LRC, February 8, 1982. Data shown are tensile properties at room temperature, dry material.

2. Shear data obtained from Rail Shear test of [0/90] configuration.

3. Shear modulus obtained fom computer analysis using laminated plate theory.

4. Shear data to be obtained for this study using the Iosipescu Shear test.

Table 6.2 Iosipescu Shear properties for unidirectional material 90/0 notch geometry

Test fixture	T_{max} [1] (psi)	G_{12} (Msi)
Wyoming	10273	0.96
AFPB	7731	1.18

Note: 1. Shear failure occurred at fiber/matrix interface in the notch region.

failure occurred at the notch tip at the fiber/matrix interface. Cracks, originating from the notch tips, propagated parallel to the fibers. The cracks were probably due to shear failures since the shear stresses predicted by the finite element analysis are high at the notch tip and because the shear strength of the material is lower than the longitudinal tensile strength. Furthermore, the transverse tensile stresses are predicted to be low near the notch tip.

The experimental shear modulus for the unidirectional specimens was slightly higher than the given design data, but this was to be expected due to the conservative nature of the design data. The strength data listed on Table 6.2 is the value of the shear strength at the fiber/matrix interface. It was impossible to obtain a shear failure across the fibers because the fiber shear strength was so much greater than the fiber/matrix bond strength.

Because of this failure mode, it was felt that further testing of unidirectional specimens would not be beneficial in determining the effects of notch geometry and fixture modifications on the stress state in the gage section. Attention was then focused on the quasi-isotropic specimens, where a shear failure across the fibers was anticipated. All remaining tests were conducted on quasi-isotropic specimens.

The shear properties for quasi-isotropic specimens tested in the Wyoming fixture are given on Table 6.3. All data listed on this table are from specimens with the load edges placed at the notch edge. Table 6.4 gives the results for quasi-isotropic specimens tested in the AFPB fixture. Loading of the specimens occurred at 0.9 inches from the notch edge.

Table 6.3 Average in-plane shear properties of Wyoming Iosipescu specimens[1]

Specimen geometry (angle/radius)	T_{max} (psi)	G_{12} (Msi)
90/0	63237	3.23
90/0.05	56239	2.77
90/0.10	51624	2.53
105/0.05	51944	2.65
120/0	47521	2.55
120/0.05	40538	2.43
120/0.10	39367	2.40
135/0.05	<36111[2]	2.38

Notes: 1. All specimens tested with load edges placed at notch edge.

2. Unable to obtain 135/0.05 shear strength. Specimen failed at loading points.

Table 6.4 Average in-plane shear properties of AFPB Iosipescu specimens

Specimen geometry (angle/radius)	T_{max} (psi)	G_{12} (Msi)
90/0	65249	3.55
90/0.05	44087	3.44
90/0.10	48582	2.72
105/0.05	47452	3.15
120/0	47164	3.12
120/0.05	47524	2.63
120/0.10	48564	2.79
135/0.05	36202	2.48

Note: 1. All specimens tested with load points placed 0.9 inches from the notch edge.

Figures 6.24 and 6.25 depict the variation of the shear modulus and shear strength, respectively, as a function of the notch angle for the Wyoming fixture. Figures 6.26 and 6.27 show the trends of the shear modulus and shear strength as a function of notch angle for the AFPB fixture. Similarly, for the Wyoming fixture, Figs. 6.28 and 6.29 show the shear modulus and shear strength variations as a function of notch radius, and Figs. 6.30 and 6.31 show the trends of shear modulus and shear strength as a function of notch radius for the AFPB fixture. The range of measured values are indicated on each figure and the curves are drawn through the average values.

The trends of the data presented in these eight figures possess some interesting and unusual qualities. For example, Figure 6.24 depicts the variations in shear modulus due to a change in notch angle for the Wyoming fixture. A decrease in the shear modulus occurs with an increase in the notch angle. Although there is some overlapping data points due to scatter, there is a definite trend of decreasing modulus with increasing notch angle. Also, a decrease in the shear strength was obtained as shown on Fig. 6.25. One explanatory note is required: the ultimate shear strengths for specimens with a 135-degree angle were not obtained since the failure modes were crushing of the specimen occurred under the load points.

These data contradicted the results determined by the finite element analysis of Walrath and Adam's publication [39]. Their finite element analysis stated that higher notch angles tend to reduce the shear stress concentrations at the notch. Also, they noted that there were very few changes in the contours of the bending stress or the transverse stress with changing notch angle. Thus the reductions in the

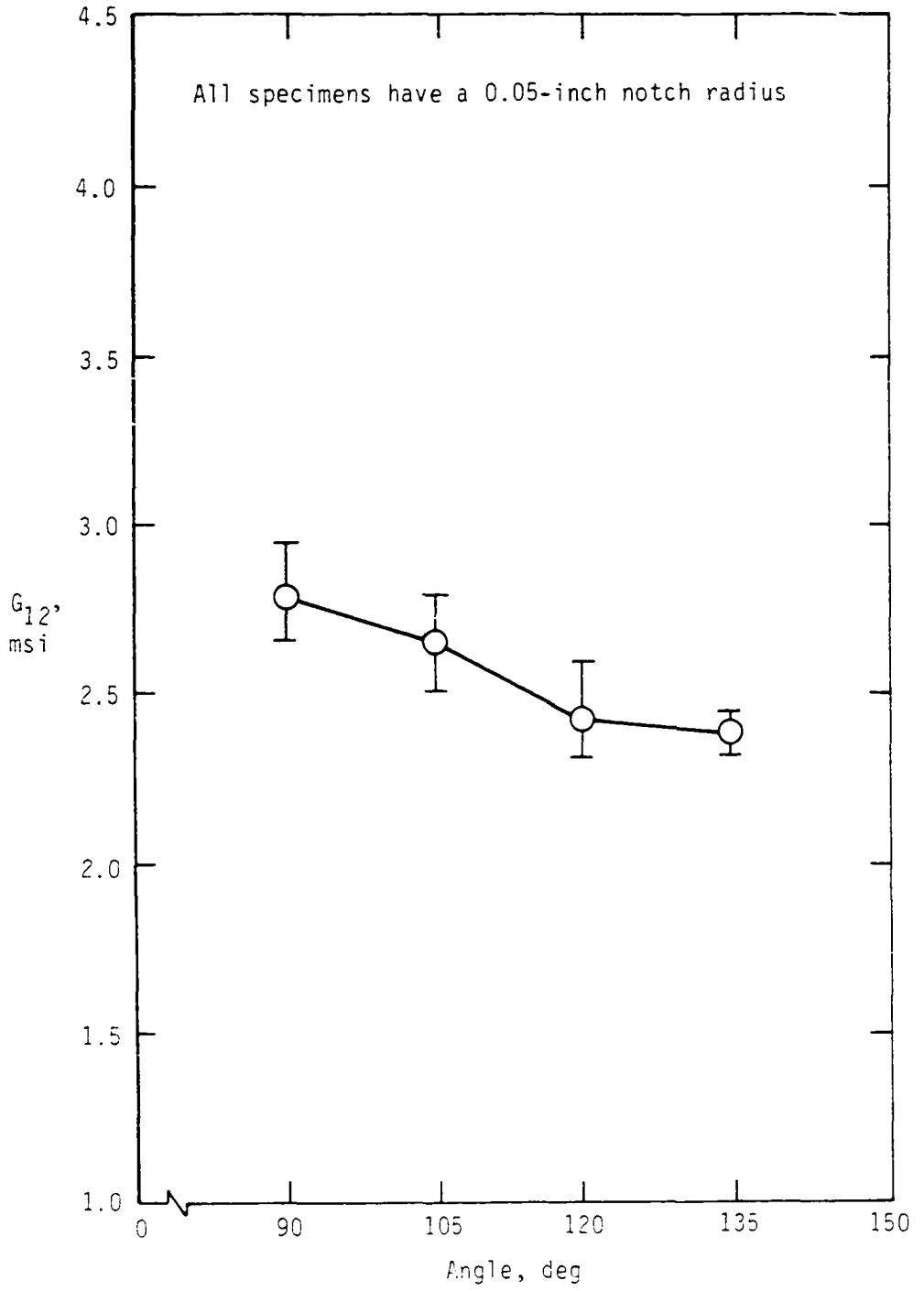

Fig. 6.24. Variation of the shear modulus G_{12} with notch angle as tested in the Wyoming fixture.

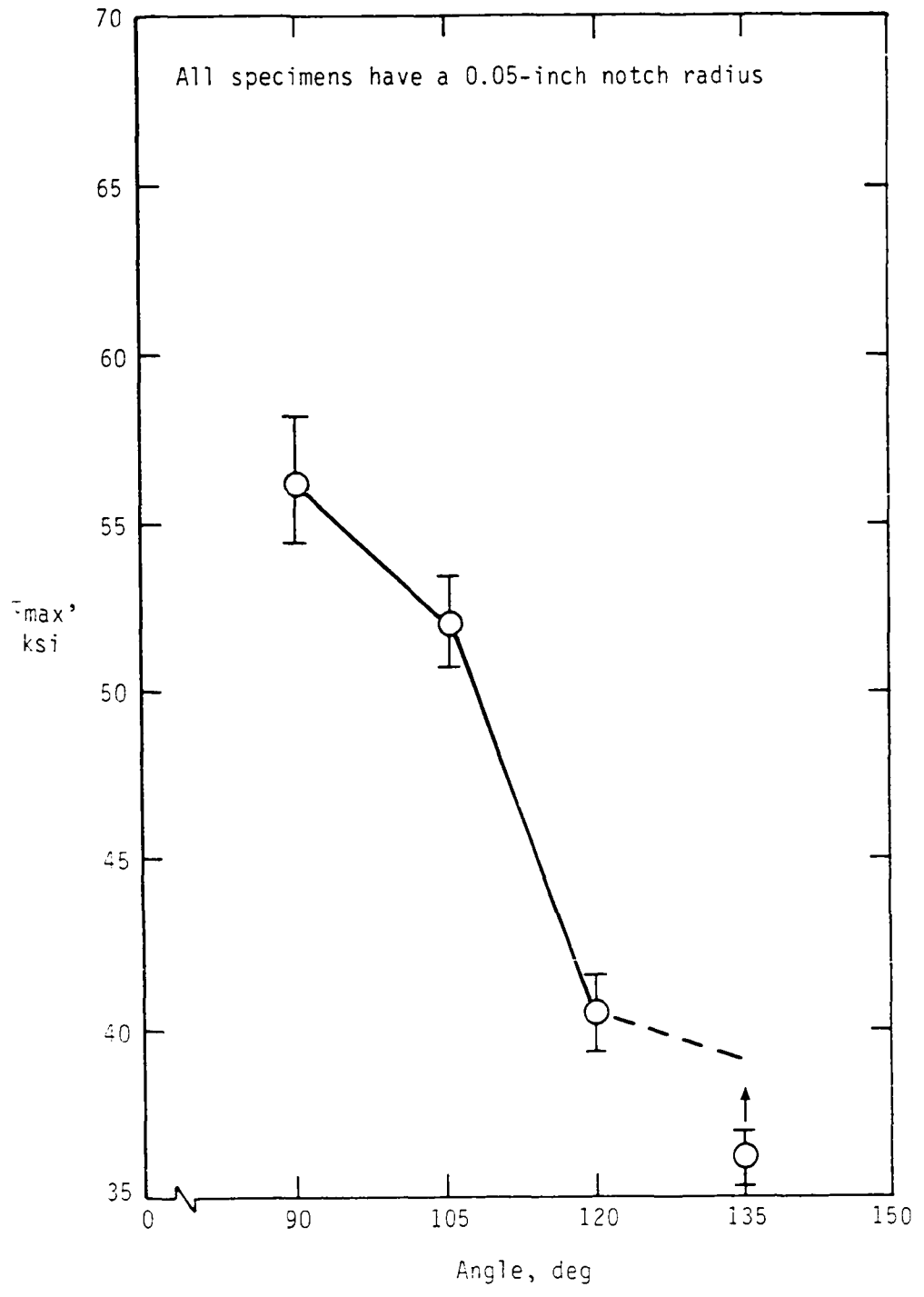

Fig. 6.25. Variation of the ultimate shear strength τ_{max} with notch angle as tested in the Wyoming fixture.

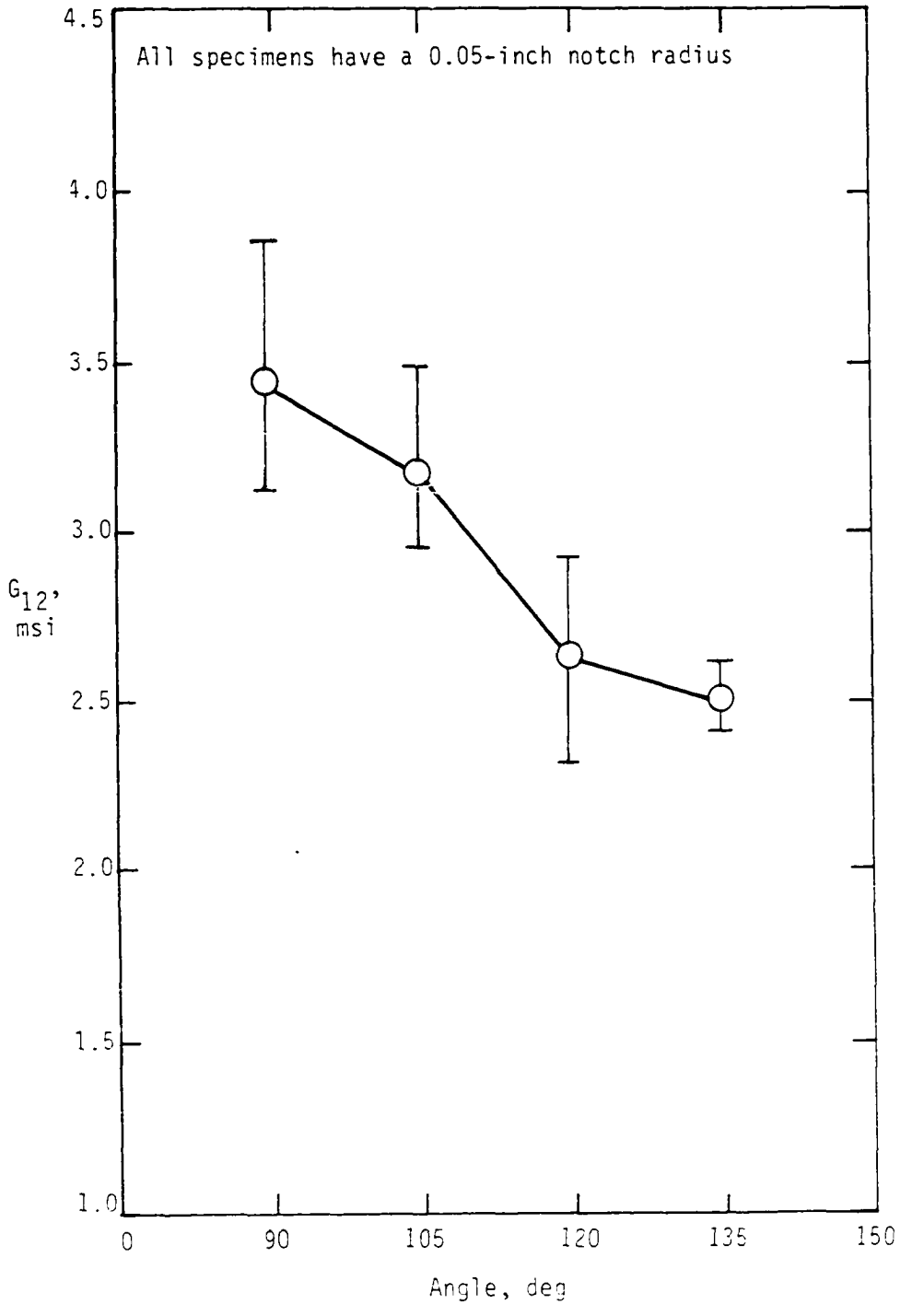

Fig. 6.26. Variation of the shear modulus G_{12} with notch angle as tested in the AFPB fixture.

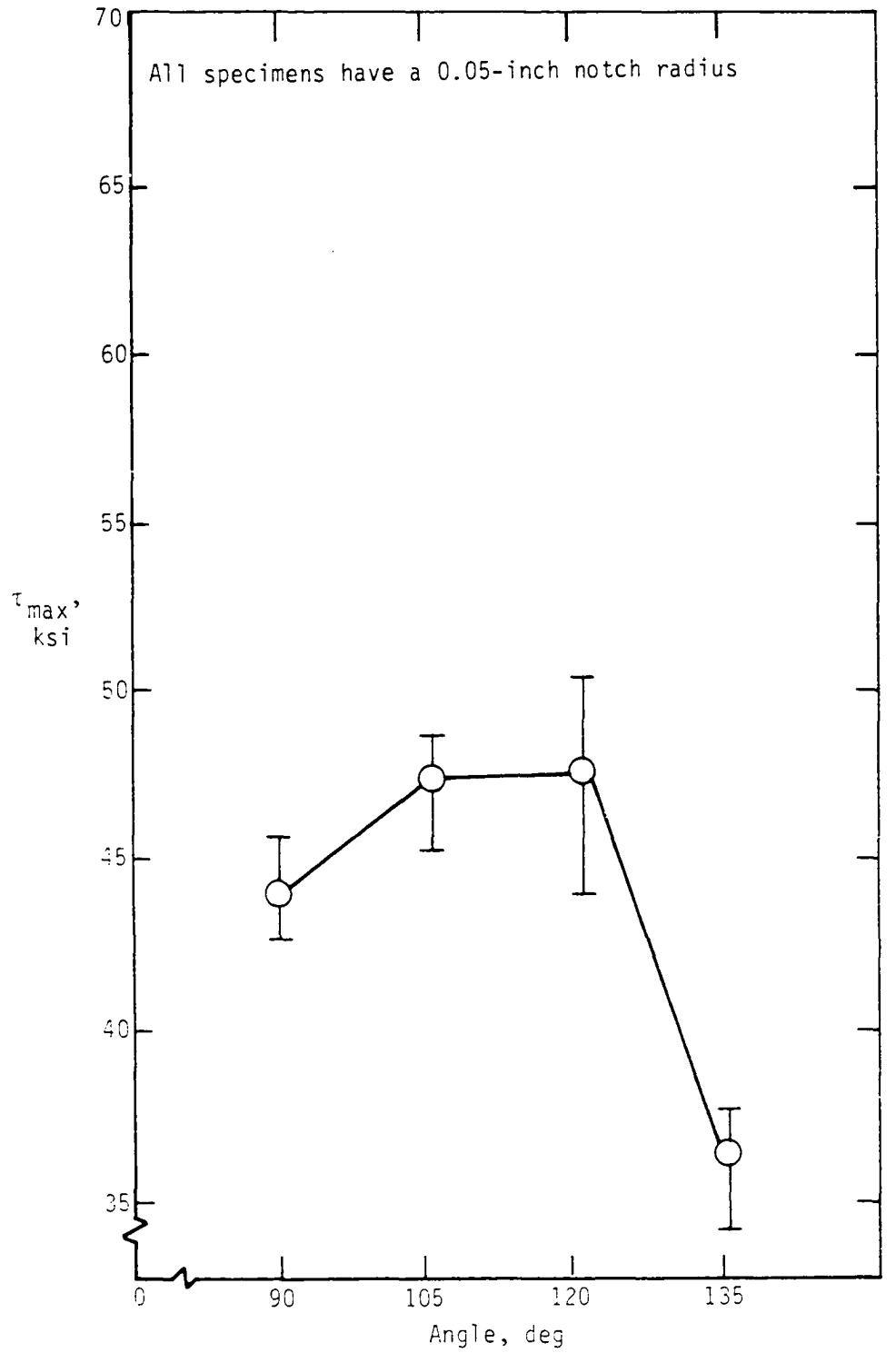

Fig. 6.27. Variation of the ultimate shear strength τ_{max} with notch angle as tested in the AFPB fixture.

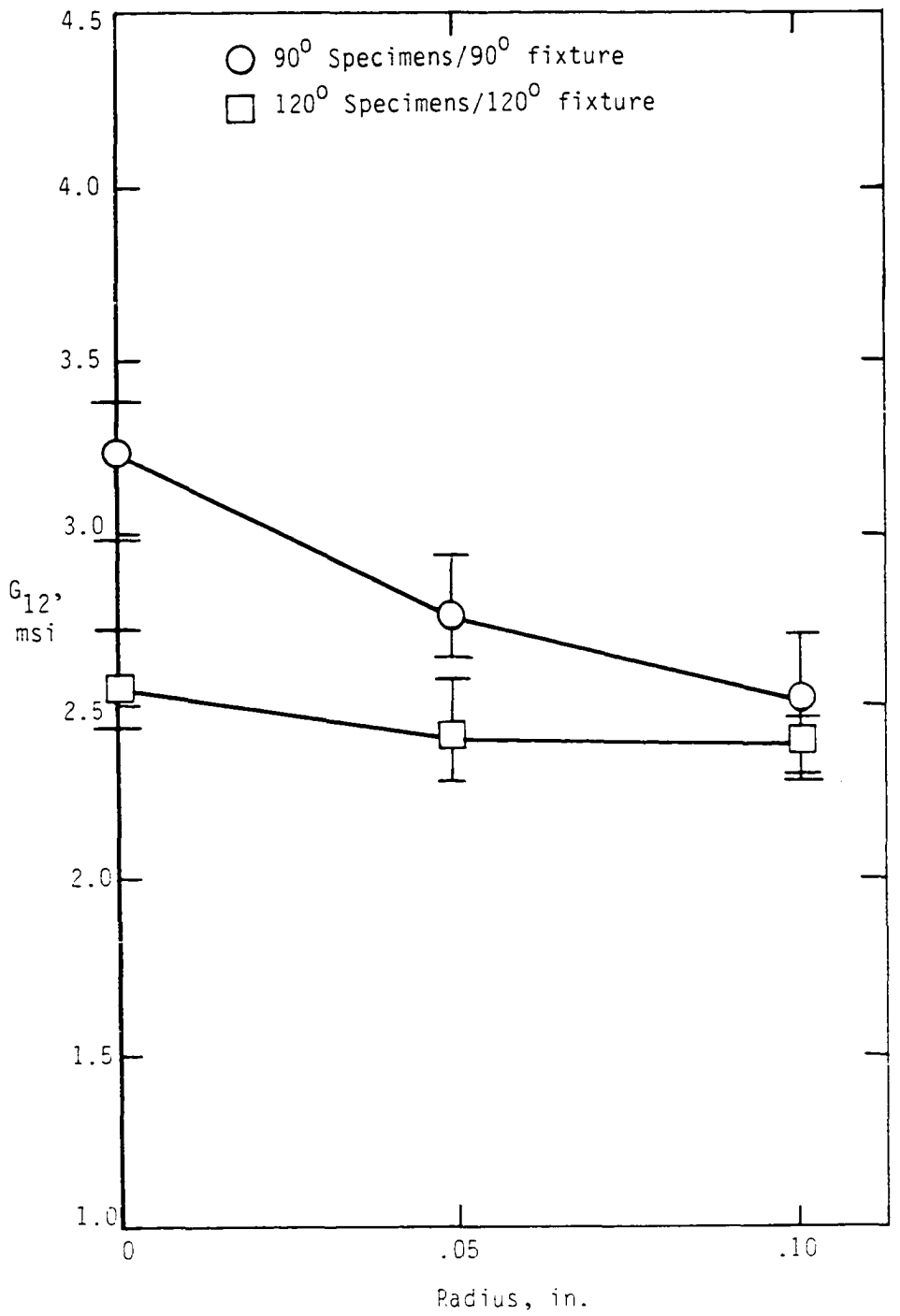

Fig. 6.28. Variation of the shear modulus G_{12} with notch radius as tested in the Wyoming fixture.

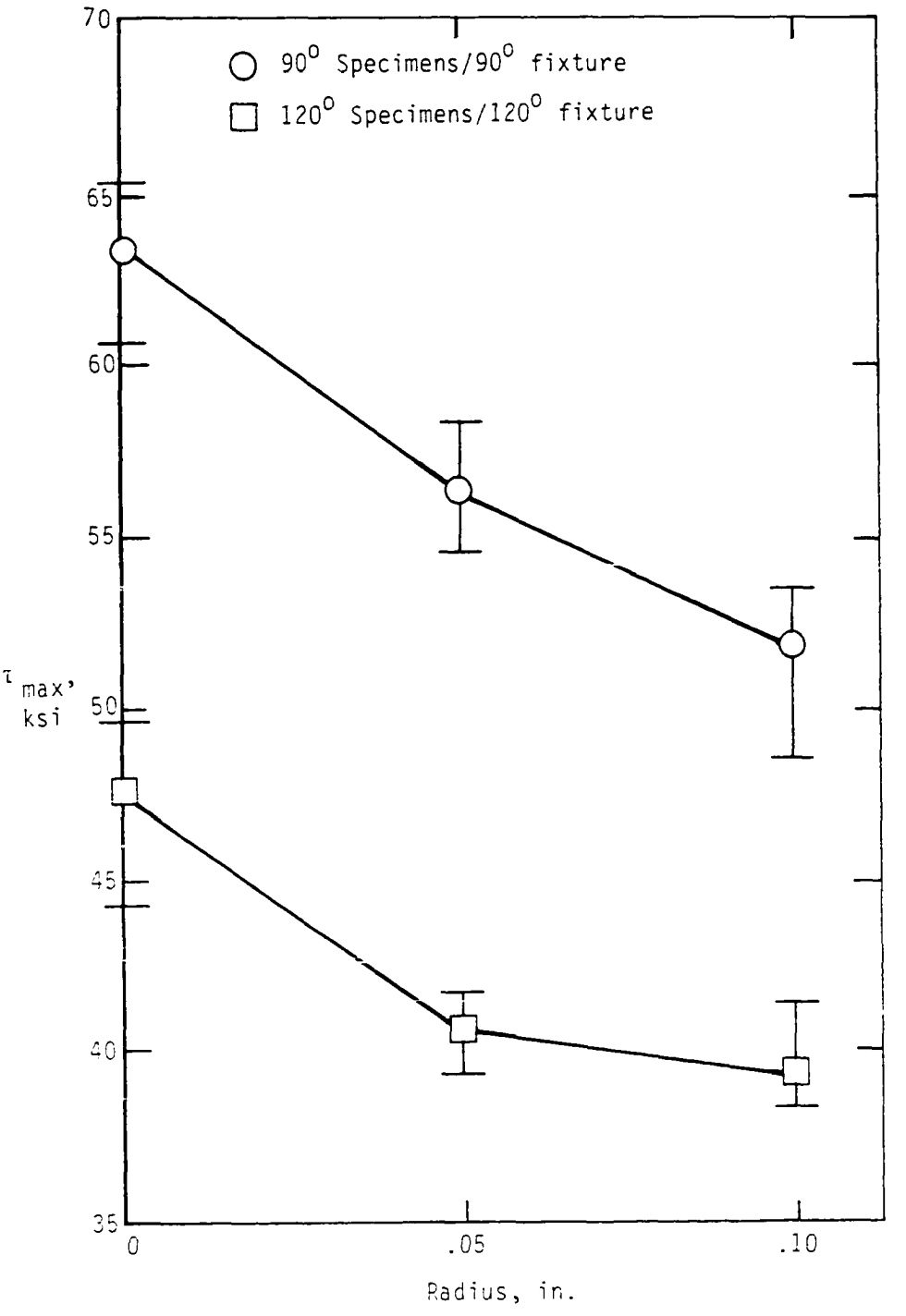

Fig. 6.29. Variation of the ultimate shear strength τ_{max} with notch radius as tested in the Wyoming fixture.

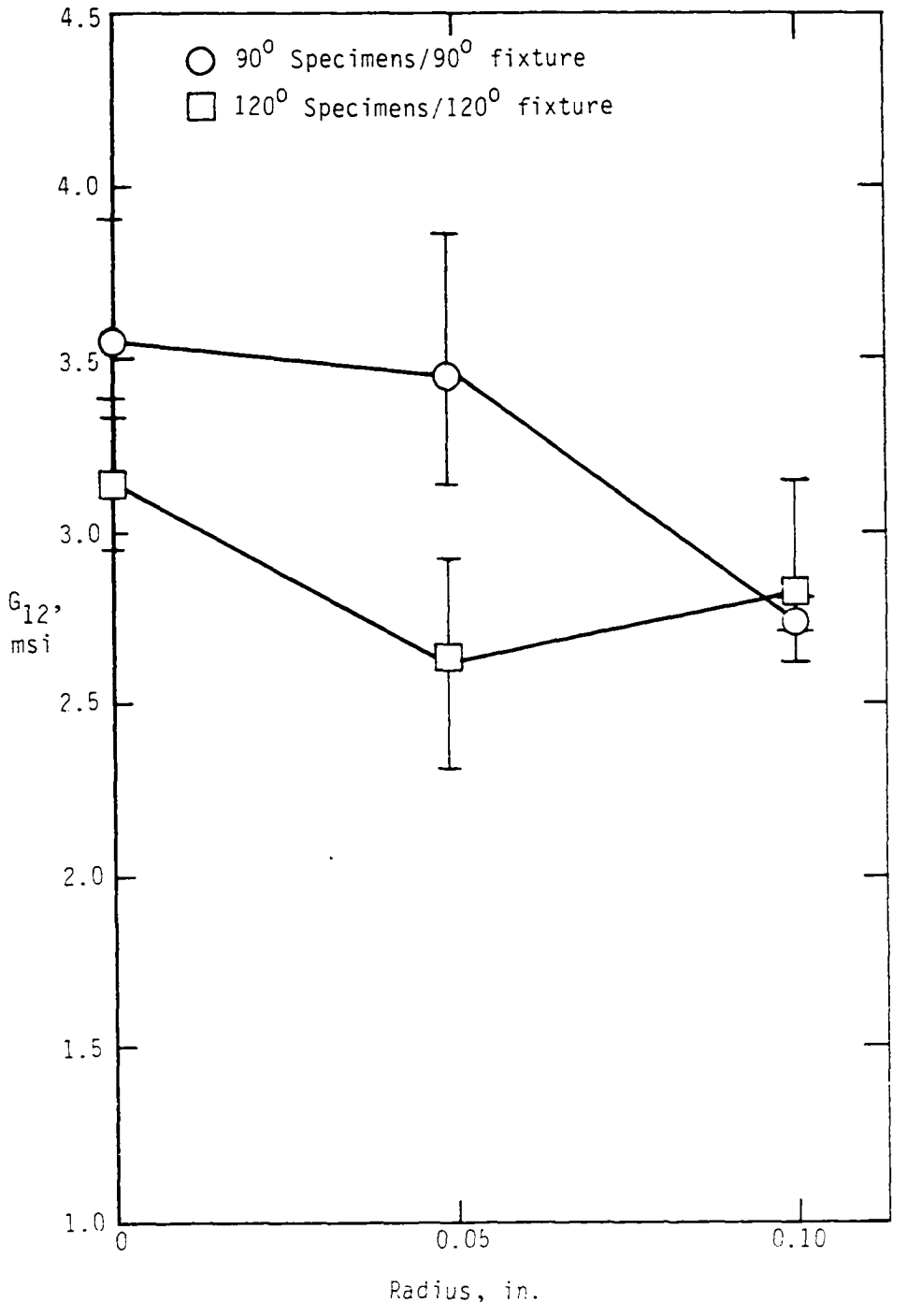

Fig. 6.30. Variation of the shear modulus G_{12} with notch radius as tested in the AFPB fixture.

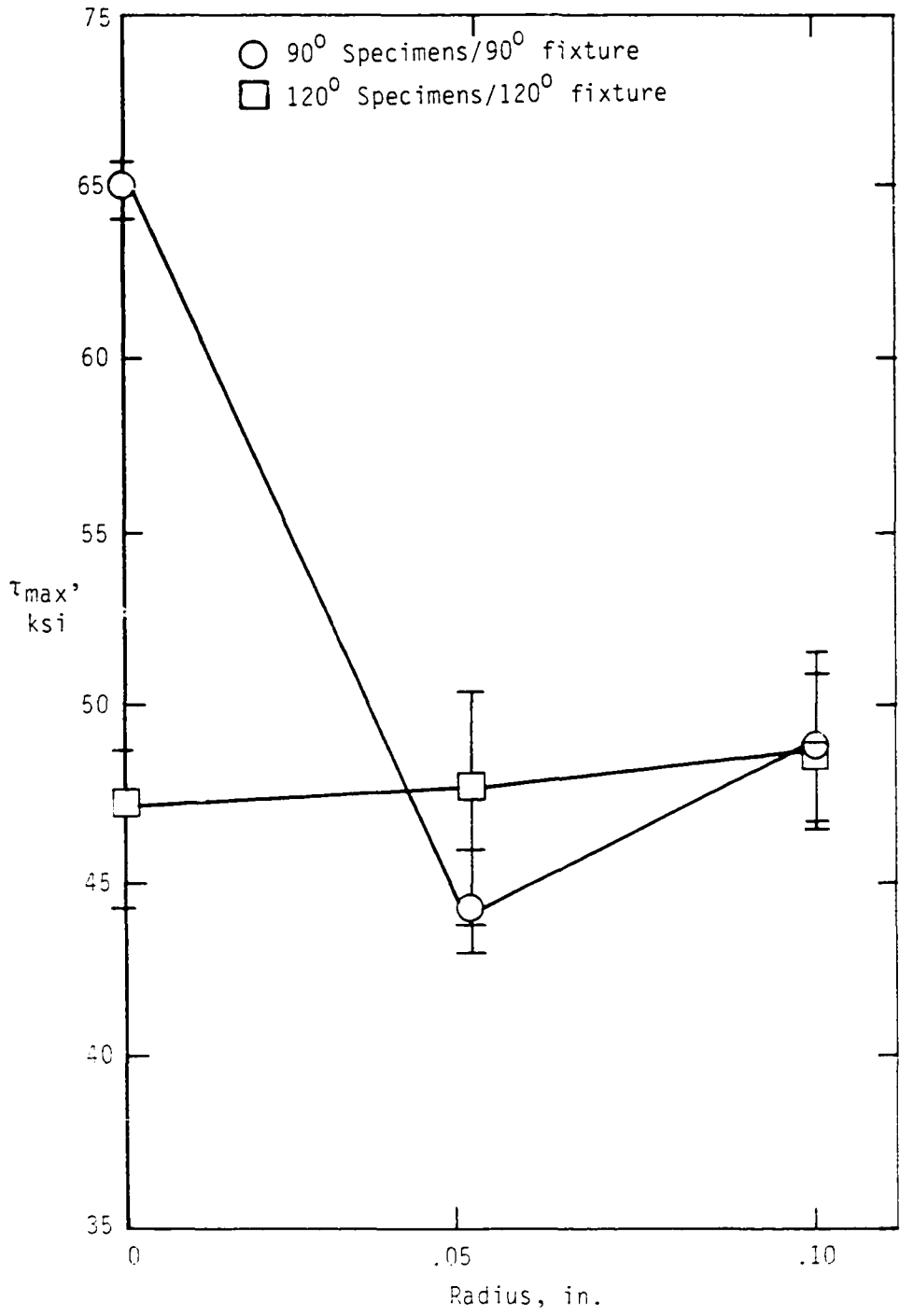

Fig. 6.31. Variation of the ultimate shear strength τ_{max} with notch radius as tested in the AFPB fixture.

stress concentrations indicated by the analysis should have resulted in higher measured shear strengths for the larger notch angles. The experimental results show an opposite trend.

This data trend was not an isolated occurrence. Figures 6.26 and 6.27 demonstrate similar decreasing trends for the shear modulus and shear strength as a function of increasing notch angle when specimens were tested in the AFPB fixture. Decreasing trends for the shear modulus and shear strength as a function of increasing notch radius are also exhibited by specimens tested in both the Wyoming and AFPB fixtures as shown on Figs. 6.28 through 6.31. Again, overlapping of the data does occur, but the trends are consistent. Also, some data points for the shear strengths of Figs. 6.29 and 6.30 do appear out of line, but this may be attributed to data scatter that is inherent in shear strength testing.

The results of the finite element analyses of this report and of Walrath and Adam's publication demonstrate a relaxation of the transverse normal and shear stress concentrations as the notch radius increases. The bending stresses tended to remain the same with only minor differences. This should result in an increasing trend in shear strength, but the experimental data show otherwise.

Even allowing for data scatter, examination of Figs. 6.24 through 6.31 reveals an undeniable decreasing trend in both the shear modulus and shear strength as functions of notch angle and notch radius. In general, there is a 20 percent decrease for both the shear modulus and strength. This trend cannot be attributed to variations in either the bending stress, the transverse normal stress or the shear

stress, nor can it be attributed to differences in the stress state as a result of using two shear fixtures.

The decreasing trend in the shear modulus is again exhibited by the experimental data for loading that is progressively removed from the notch edge. Table 6.5 lists the results for these modifications to the Wyoming loading technique and Fig. 6.32 shows the variation of the shear modulus with the distance from the center of the notch. The decreasing trend is obvious for a 90/0 quasi-isotropic specimen. However, for a 120/0.05 specimen, the modulus remains virtually constant. The data for the 90/0 specimens are contradictory to the results of the finite element analysis which indicated that the stress state approached nearly-ideal conditions as the loading edges were removed from the notch edge. Note that the shear strength data on Table 6.5 is incomplete and that no trends could be obtained since the gage sections of some specimens were not reduced in order to obtain the shear strength.

A clue to these puzzling data may possibly be found upon re-examination of Figs. 6.24, 6.26, 6.28, 6.30 and 6.32. The shear modulus on each figure converges to a range of 2.4-2.7 Msi. On Figs. 6.24 and 6.26, the shear modulus decreases between notch angles of 90 and 120 degrees and levels off between 120 and 135 degrees. On Figs. 6.28 and 6.30, the shear modulus for a 90-degree notch angle decreases with increasing radius while the modulus for a 120-degree notch angle remains almost constant. Figure 6.32 shows a definite decreasing trend to 2.5 Msi for a 90/0 specimen whereas a 120/0.05 specimen's shear modulus remains constant at 2.5 Msi. Similarly, the shear strength tends to converge to a range of 35-45 Ksi as shown on

Table 6.5 Average in-plane shear properties of quasi-isotropic Wyoming specimens with loading removed from the notch edge

Specimen geometry (angle/radius)	Fixture design	Distance from notch center (inches)	T_{max} (psi)	G_{12} (Msi)
	90	0.10	63230	3.23
90/0	105	0.13	>42177[1]	2.80
	120	0.17	>39338[1]	2.68
	135	0.24	61154	2.44
120/0.05	120	0.17	40538	2.43
	135	0.24	43173	2.47

Note: 1. Gage section of these specimens not reduced in order to obtain a shear strength.

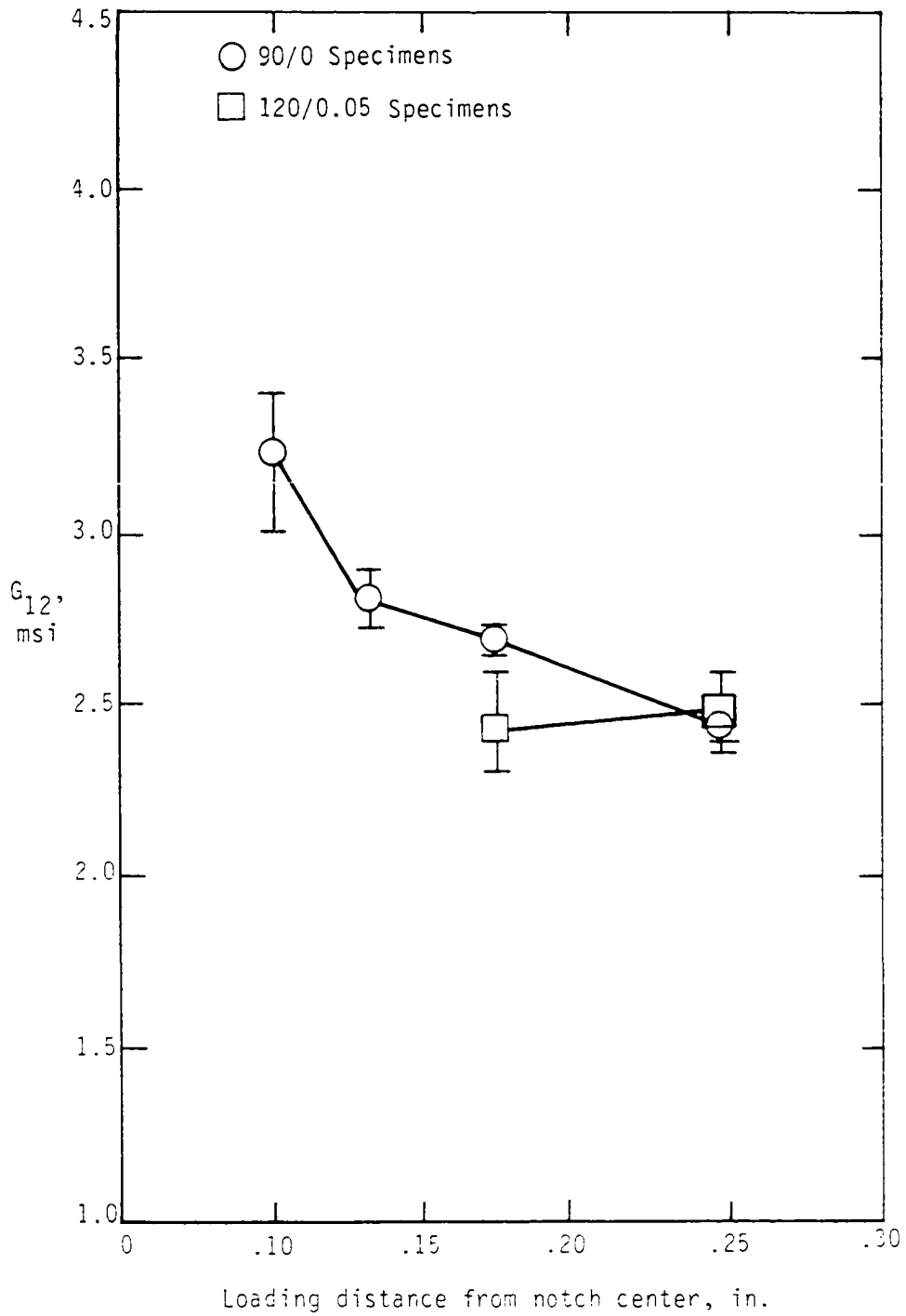

Fig. 6.32. Variation of the shear modulus G_{12} with loading distance from the notch center as tested in the Wyoming fixture.

Figs. 6.25, 6.27, 6.29 and 6.31, though this range may be expanded due to data scatter.

The convergence of the shear modulus and shear strength leads to the conclusion that for a quasi-isotropic material, a large notch angle influences the stress state behavior in the gage section in the same manner as a notch radius.

Though this conclusion explains the similarities of the results between a large notch angle and a radius, it does not resolve the decreasing trend of the data. One possible explanation can be found upon examination of the test specimen failure modes. Figure 6.33 shows the failure of a 90/0 Wyoming specimen and Fig. 6.34 shows the failure of a 90/0 AFPB specimen. The failures in both specimens are ones of shear and the failure surfaces are identical. Note that the ±45-degree plies run parallel to the notch sides and that a sharp angle is formed where the plies meet in failure.

Examination of the failures of specimens with different notch geometries reveals a markedly different failure surface. Figures 6.35 and 6.36 are photographs of the failures of 90/0.05 and 90/0.10 AFPB specimens, respectively. In both cases, the outer 45-degree fibers have delaminated from the notch region to the edge of the specimen. The outline of the notch can still be seen. The interior laminae, however, appear to have failed in shear. Similar failure surfaces are seen on 105/0.05 Wyoming and AFPB specimens, as shown on Figs. 6.37 and 6.38, respectively.

Fig. 6.33. Typical failure of a 90/0 Wyoming specimen.

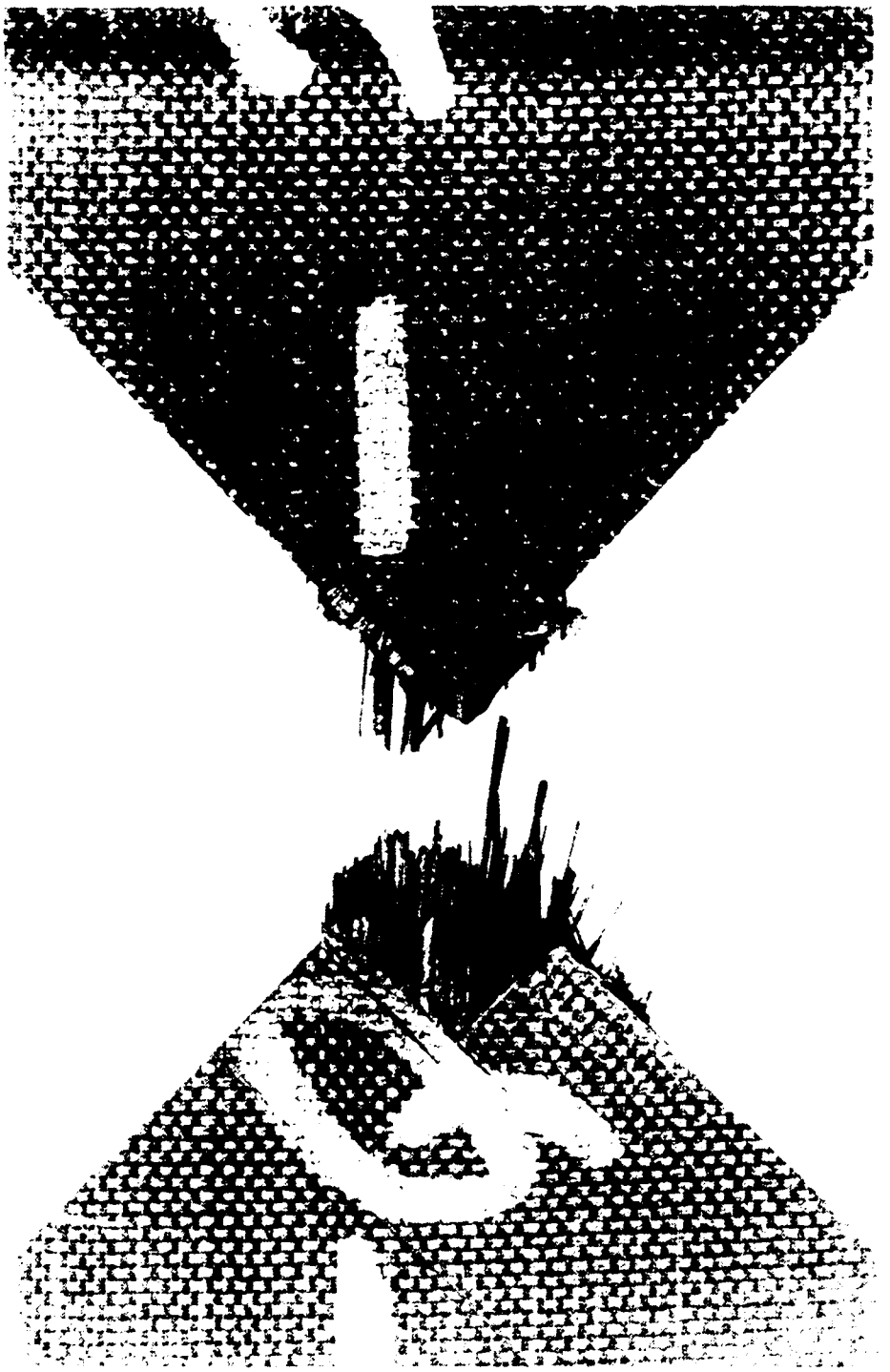

Fig. 6.34. Typical failure of a 90/0 AFPB specimen.

Fig. 6.35. Typical failure of a 90/0.05 AFPB specimen.

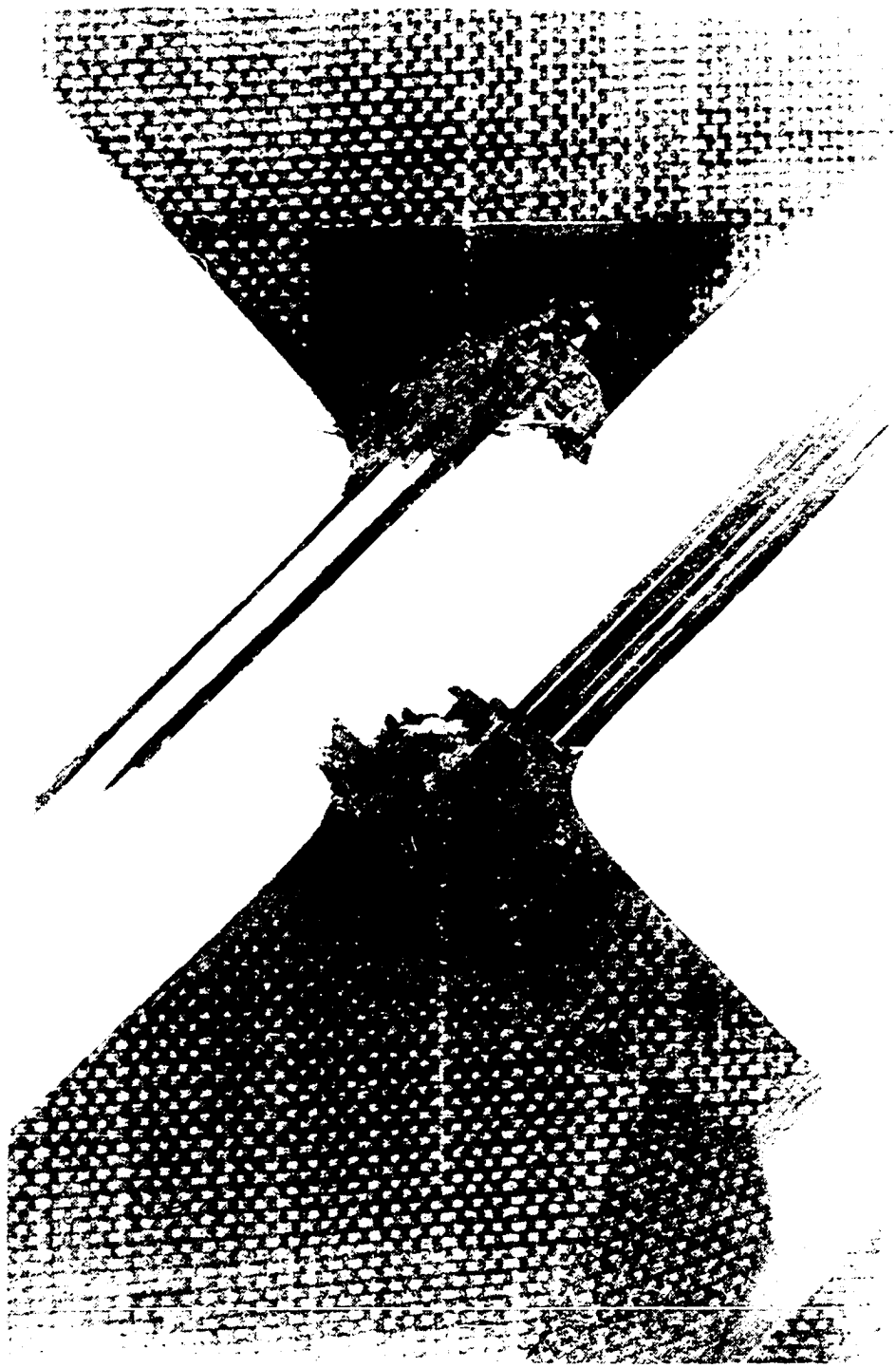

Fig. 6.36. Typical failure of a 90/0.10 AFPB specimen.

Fig. 6.37. Typical failure of a 105/0.05 Wyoming specimen.

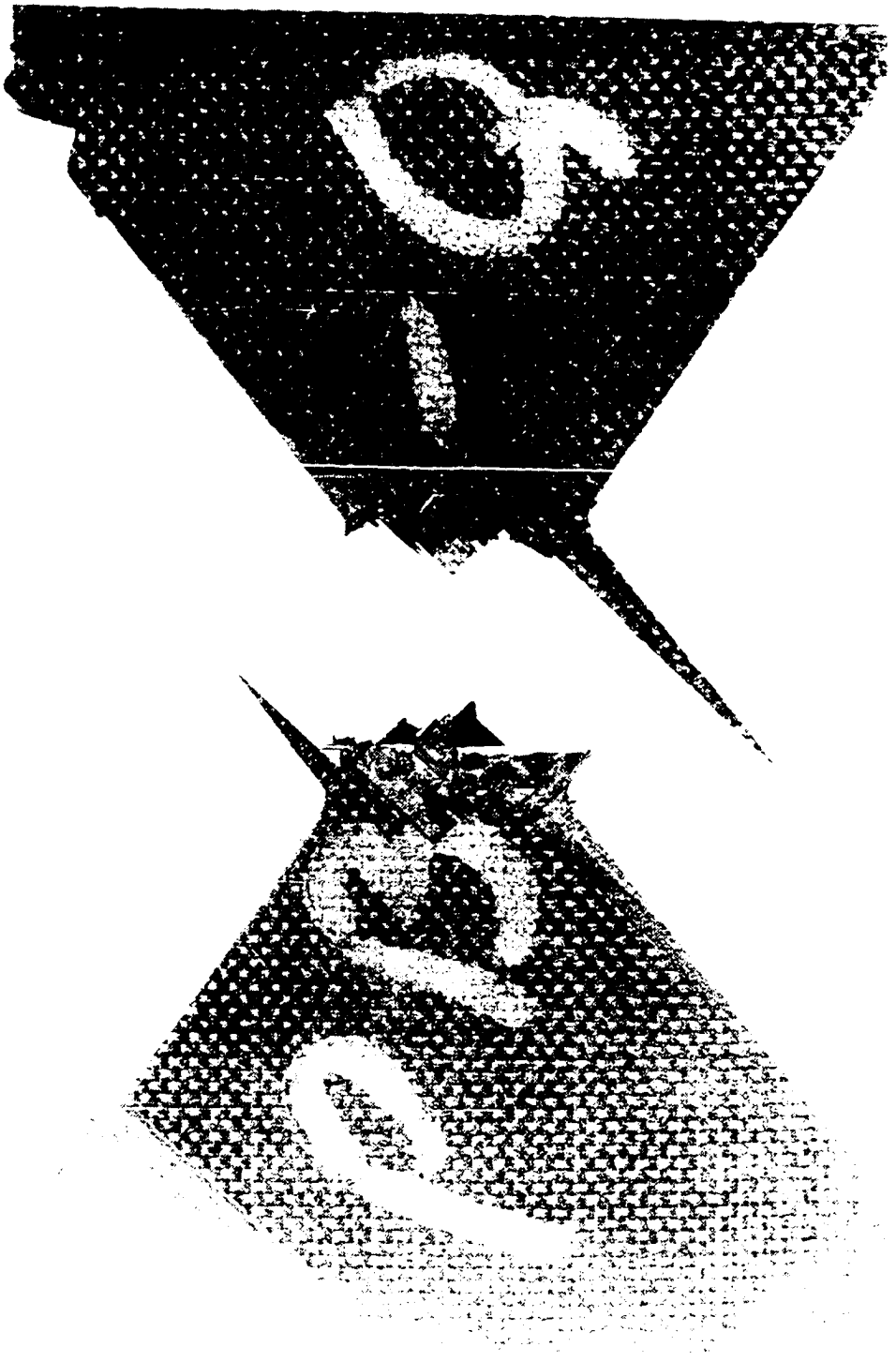

Fig. 6.38. Typical failure of a 105/0.05 AFPB specimen.

Identical failures occurred on all of the remaining specimens. Figs. 6.39, 6.40 and 6.41 are photographs of the failures of 120/0, 120/0.05 and 120/0.10 AFPB specimens and Fig. 6.42 shows the failure of a 135/0.05 AFPB specimen. In each picture the 45-degree fibers have delaminated at the notch and the interior laminae showed indications of having failed in shear. Similar failures were also apparent in the Wyoming specimens.

The differences between the failure surfaces of a 90/0 specimen and all other specimens may be attributed to free edge effects. It is well known that stress free edges of a composite laminate can induce localized stress concentrations or a fully three-dimensional stress field in the vicinity of the free edge [47,48]. Further, the free edge effects on the interlaminar stresses can be important in determining the strength of a laminated composite [49]. Pipes, Kaminski and Pagano [48] note that significant interlaminar shear stresses are necessary to allow shear transfer between the laminae. The authors cite analyses that show the interlaminar shear stresses are confined to a narrow region in the vicinity of the free edge, and that the distribution of the interlaminar shear stresses through the thickness is at a maximum at the interface between laminae of +8 and -8 fiber orientations. This could account for the observed delaminations of the outer +45-degree fibers from the specimens as a -45-degree lamina is directly underneath. It also appears that at the interfaces between the ±45-degree fibers in the interior of the specimen delaminations also occurred, but this is difficult to determine in all of the test specimens due to the extensive damage in the notch region.

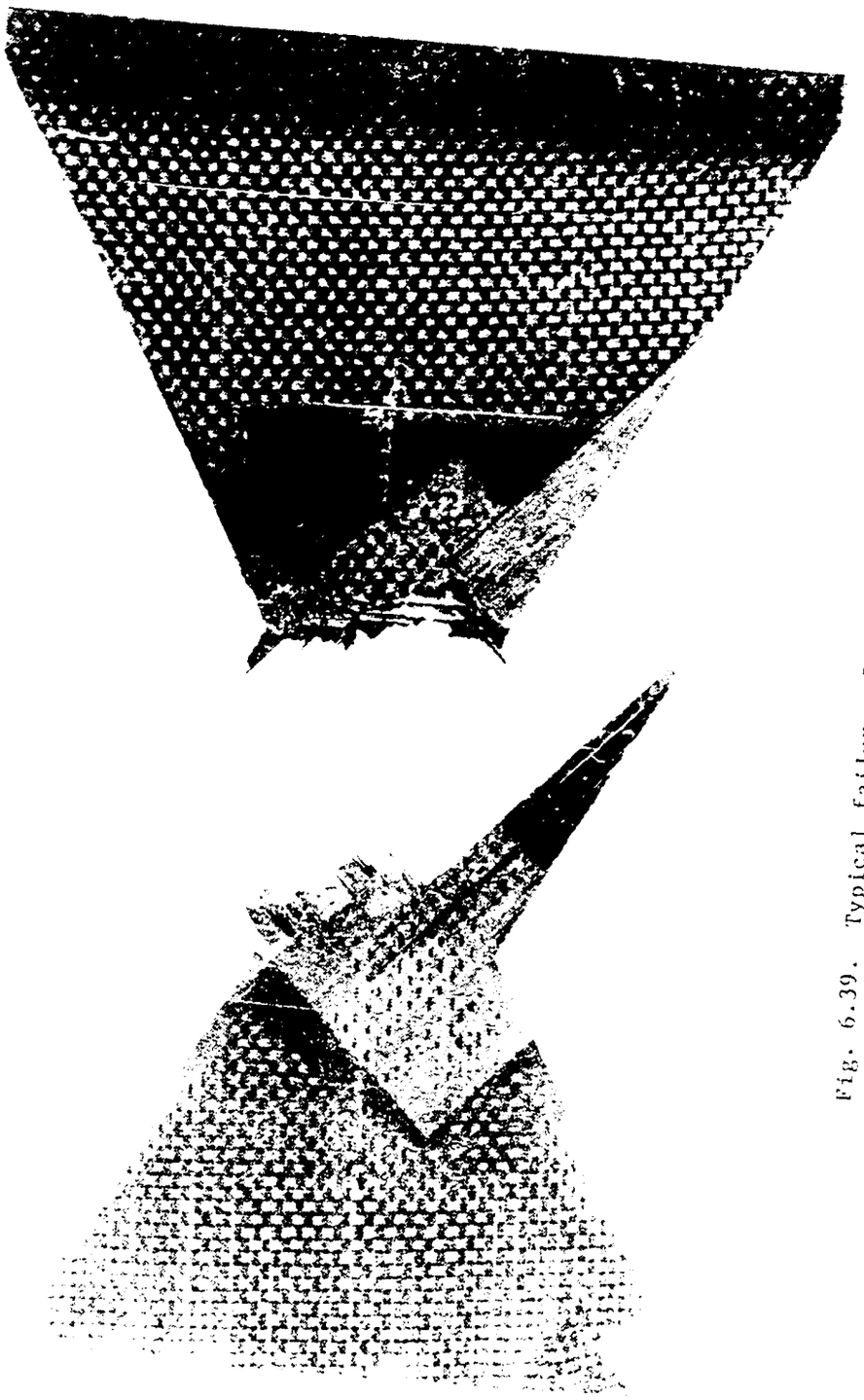

Fig. 6.39. Typical failure of a 120/0 AFPB specimen.

Fig. 6.40. Typical failure of a 120/0.05 AFPB specimen.

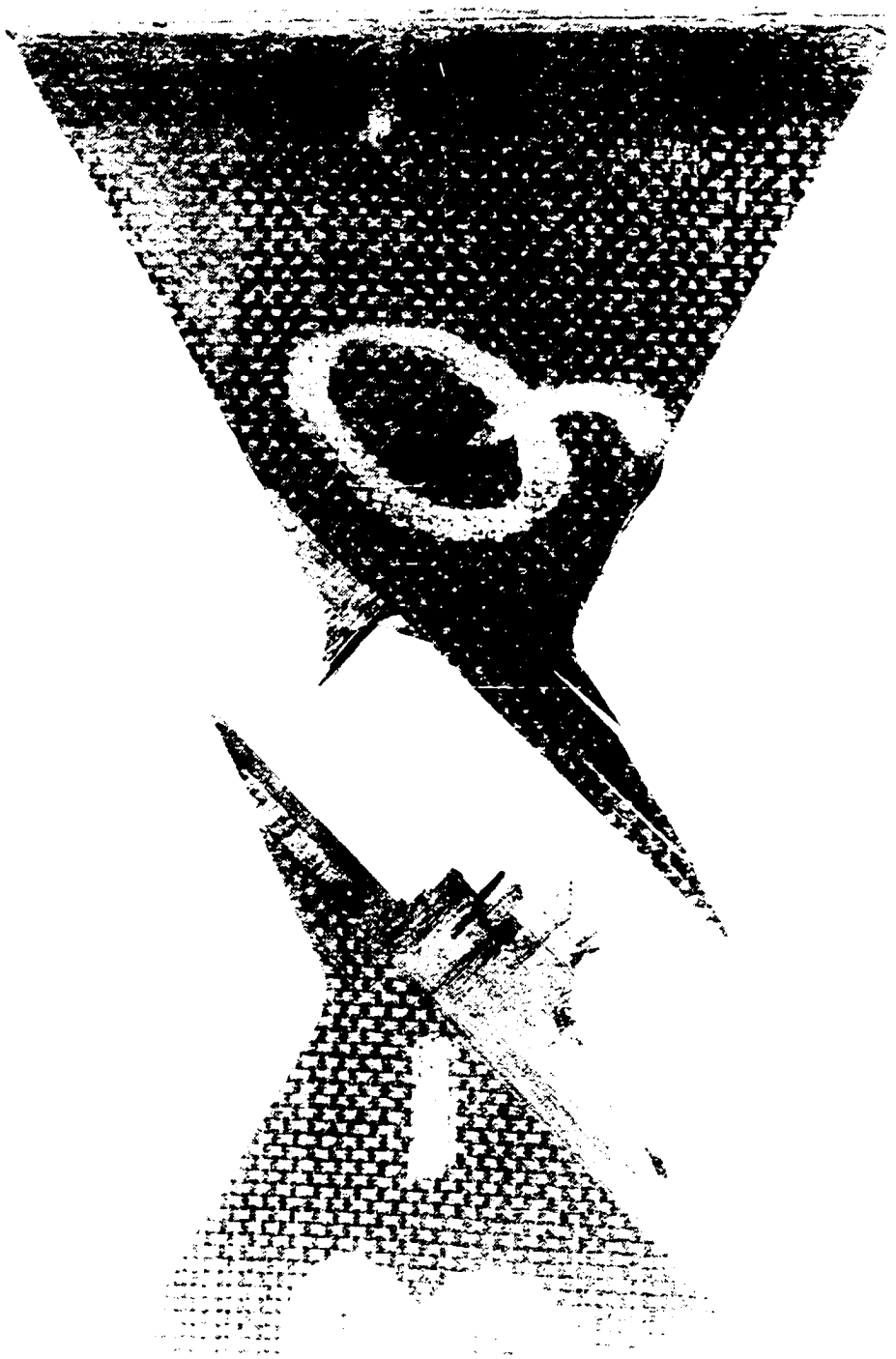

Fig. 6.41. Typical failure of a 120/0.10 AFPB specimen.

Fig. 6.42. Typical failure of a 135/0.05 AFPB specimen.

From their evaluations, Pipes, Kaminski and Pagano also note that the interlaminar shear strains result in interlaminar shear delaminations at the free edge. The delaminations produce matrix cracks which propagate from the free edge into the interior of the specimen, traveling parallel to the fiber directions. The matrix cracks are held responsible for the subsequent failure of the specimen.

Whitney [47] notes that for the case of a standard tensile specimen with a thin gage section, the fibers are not continuous through the length of the specimen. For such a specimen, the strength is controlled by matrix failure as a result of free edge effects and not by fiber failure. Because of this, Whitney advocates the use of wide tensile specimens which would have more continuous fibers in the gage section.

Though their work was with tensile specimens, the observations by Pipes et al. [48] and Whitney may be applicable to the Iosipescu Shear test results. The notch geometries examined in this study result in discontinuous fibers along the notch sides. A sketch of the fiber orientations and notch modifications is given on Fig. 6.43. In the case of a specimen with a 90-degree angle and a sharp notch tip, the region of discontinuous fibers is localized at the notch tip. Indeed, it is the 0 and 90-degree plies that are discontinuous since ideally the ±45-degree fibers run parallel to the notch sides. For this specimen, the failure may have been more a result of fiber failure than matrix failure.

However, once a radius is placed at the notch tip of a specimen with a 90-degree notch angle, the number of discontinuous fibers increases. In particular, the 45-degree fibers in the notch tip area

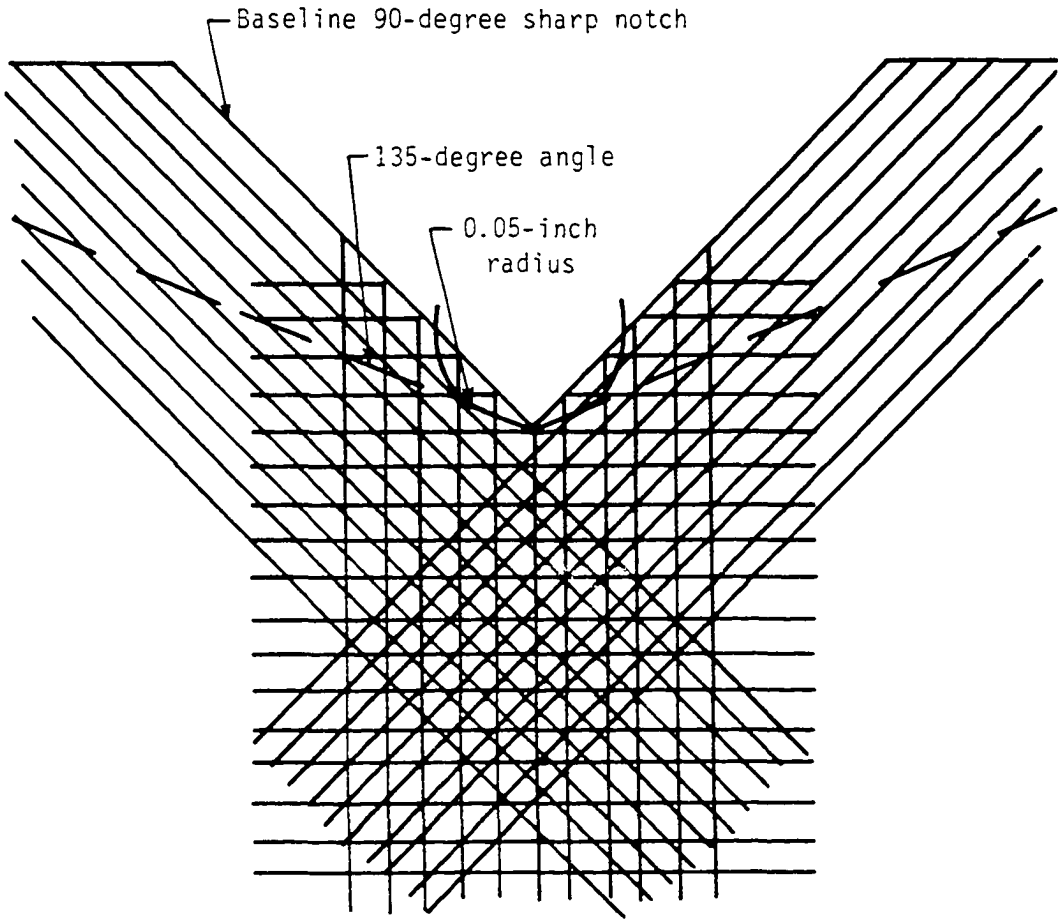

Fig. 6.43. Comparison of a 90-degree sharp notch with a 135-degree angle and a 0.05-inch radius.

are now discontinuous. Subsequently, the failure of the specimen may have been governed by matrix cracks and delaminations. The interlaminar shear stresses may have been at a maximum at the interface between the +45 and -45 fiber orientations, resulting in the delaminations of the outer 45-degree lamina. The reduction in the shear strength due to the possible matrix failures of 90-degree specimens with notch radii can be seen on Figs. 6.29 and 6.31.

A larger notch angle also produces a considerable number of discontinuous fibers. Now, however, the free edge area has increased dramatically and more 45-degree fibers are exposed to the free surface. As in the case of a notch radius, the high interlaminar stresses at the ±45 laminae interface may result in lower failure strengths. This may explain the trends seen on Figs. 6.25 and 6.27. The data for a specimen with a 90-degree notch on Fig. 6.27 can be assumed to be low as a result of data scatter or laboratory error. It tends to defy the reasoning mentioned above, but examination of Fig. 6.31 shows this same data point to follow the trend of decreasing strength due to fiber discontinuities at a notch radius. Note that the strength data for a Wyoming specimen follows the established trends as shown on Figs. 6.25 and 6.29.

The failure strength of a specimen with a 120-degree notch angle remains fairly constant with increasing notch radius, as shown on Figs. 6.29 and 6.31. It is believed that a radius placed in a specimen with this large notch angle does not significantly modify the number of discontinuous fibers and does not alter the failure mechanisms to a notable extent.

Free edge effects are thus seen to be a viable explanation for the shear strength data presented in this report. Free edge effects may also be the catalyst for the observed degradation of the shear modulus. Wang and Crossman [49] conducted a finite element analysis of the free edge effects in a $[\pm 45/0/90]_s$ tensile specimen with properties similar to that of AS4/3502 graphite/epoxy. Though not exactly the same configuration used for the experimental specimens of this study, the authors' analysis qualified the effects of a free edge on interlaminar stresses in a quasi-isotropic laminate. At the midplane, σ_o was found to rise 25 percent as one approached the free edge. They noted that this fact must be considered in determining the strength of the laminate as it may contribute to an early failure. Also, at the interface between the ±45-degree laminae, the distribution of T_{xy} indicated that the edge effect extended far inside the laminate. The T_{xz} distribution at this interface displayed a "singularity" or an infinitely large value at the free edge, indicating that the strength of this shear stress is significant. The T_{yz} distribution, however, was found to have a relatively small magnitude. The authors also noted that large tensile σ_z singularities developed in the midplane at the free edge.

Wang and Crossman concluded that proof of the existence of the interlaminar normal and shear stress singularities remains to be determined. But whether or not the singularities do exist, in reality the stresses would probably dissipate into the laminate, resulting in a stress redistribution or stress relaxation. The resulting effect would be that the material properties would be degraded in the region of the stress redistribution or relaxation. The authors further concluded that

delaminations induced at the free edge may also reduce the material stiffness in addition to the material strength.

Assuming that Wang and Crossman's conclusion is correct, that is, abnormally high free edge stresses dissipate into the laminate and degrade the material properties in the region of the stress redistribution/relaxation, the free edge stress field may also affect the shear modulus. The delaminations at the free edge may also contribute to the degradation of the shear stiffness. The data presented on Figs. 6.24, 6.26, 6.28 and 6.30 clearly show a deterioration of the shear modulus as the number of discontinuous fibers increases. The small gage sections may also have exasperated the shear modulus data by contributing to the effects of the matrix failures and edge delaminations. Furthermore, the strain gages were placed on the outer 45-degree lamina and may have been affected by the high interlaminar shear stresses present in the laminae.

The shear modulus was also seen to degrade as the loading edges were removed from the notch edge as shown on Fig. 6.32. The data for both the 90/0 and 120/0.05 specimens behave as if subjected to free edge effects. In this case, however, the notch angle and notch radius have remained constant. Yet, it is obvious that a stress discontinuity exists between loaded and unloaded points of the specimen. Examination of the edges of the specimen revealed that the loading surface produced localized delaminations at the points between the loaded and unloaded areas. Since there are no previous studies in the literature on this effect, it can only be speculated that the matrix cracks caused by the delaminations at the loaded edge propagated into the interior of the specimen and degraded the shear modulus data. It is important to note

that with these specimens the outer 45-degree fibers did not delaminate from the remainder of the specimen.

In summary, it can be concluded that the experimental data presented on Figs. 6.24 through 6.32 do not correlate with the finite element results due to free edge effects and a transition in failure modes. Though not valid data for examining the consequences of fixture modifications, the experimental results are significant in evaluating the effects of notch geometry modifications on the stress state of a composite material. The degrading effects of the free edge on the in-plane shear properties of composite material have been clearly demonstrated.

The last experimental tests were conducted on interlaminar Wyoming specimens. The results are given on Table 6.6 and the variation of the interlaminar shear modulus with notch angle and radius are given on Figs. 6.44 and 6.45, respectively. The variation of shear modulus with notch angle would at first appear to decrease then increase, but this may be a result of data scatter and not of an experimental trend. There is no apparent trend due to increasing notch radius because of the large data scatter. The shear strength results given on Table 6.6 show no variations due to either notch angle or notch radius. Free edge effects on the interlaminar shear properties were not discernible. These test results indicate that the Iosipescu Shear test may be a valid test method for determining the interlaminar shear properties of a composite material.

Table 6.6 Average interlaminar shear properties of Wyoming Iosipescu specimen

Specimen geometry (angle/radius)	T_{max} (psi)	G_{12} (Msi)
90/0	12867	0.84
90/0.05	13044	0.73
90/0.10	12005	0.76
105/0.05	11311	0.60
120/0	10972	0.57
120/0.05	11356	0.53
120/0.10	10272	0.54
135/0.05	10306	0.60

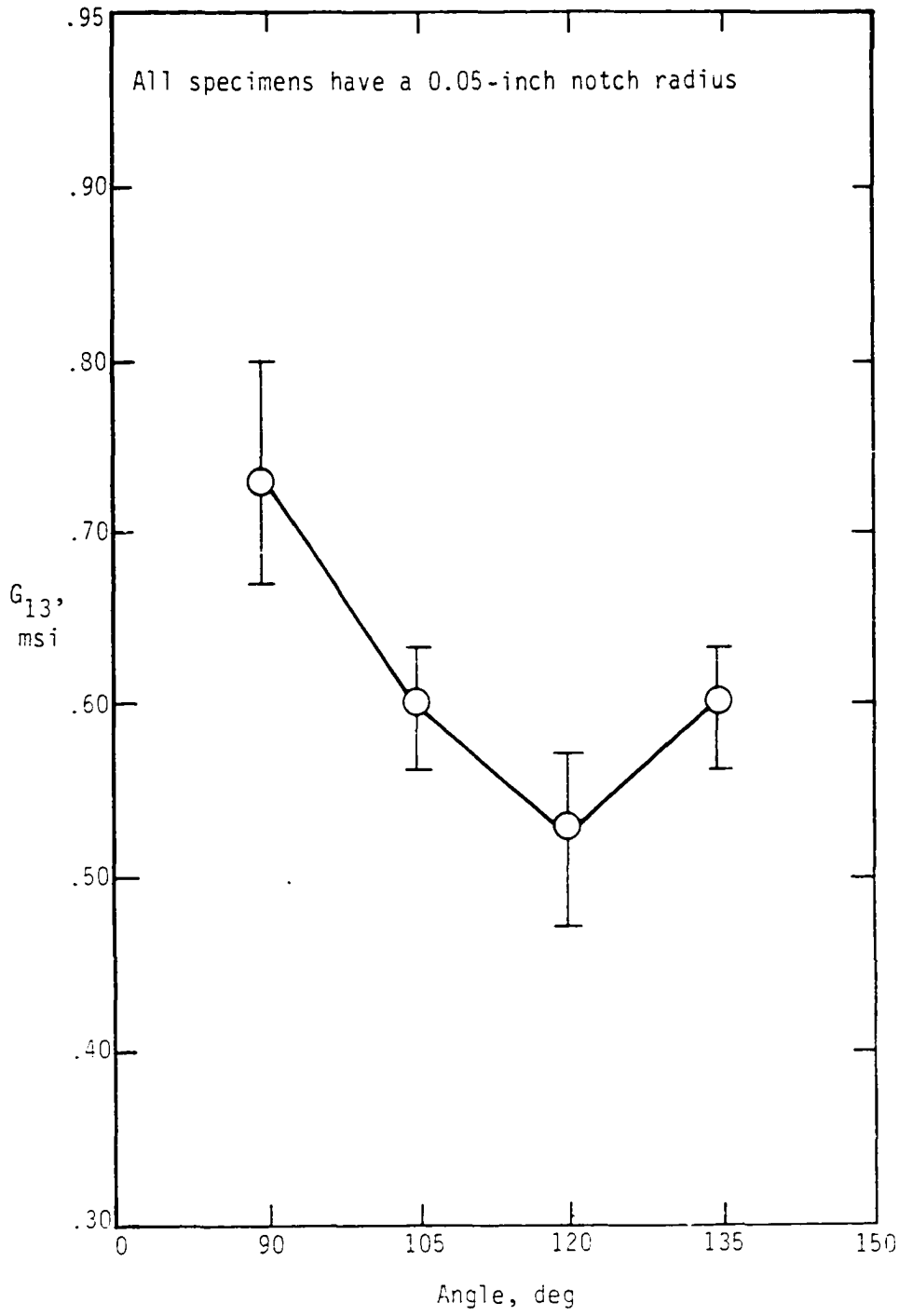

Fig. 6.44. Variation of the interlaminar shear modulus G_{13} with notch angle as tested in the Wyoming fixture.

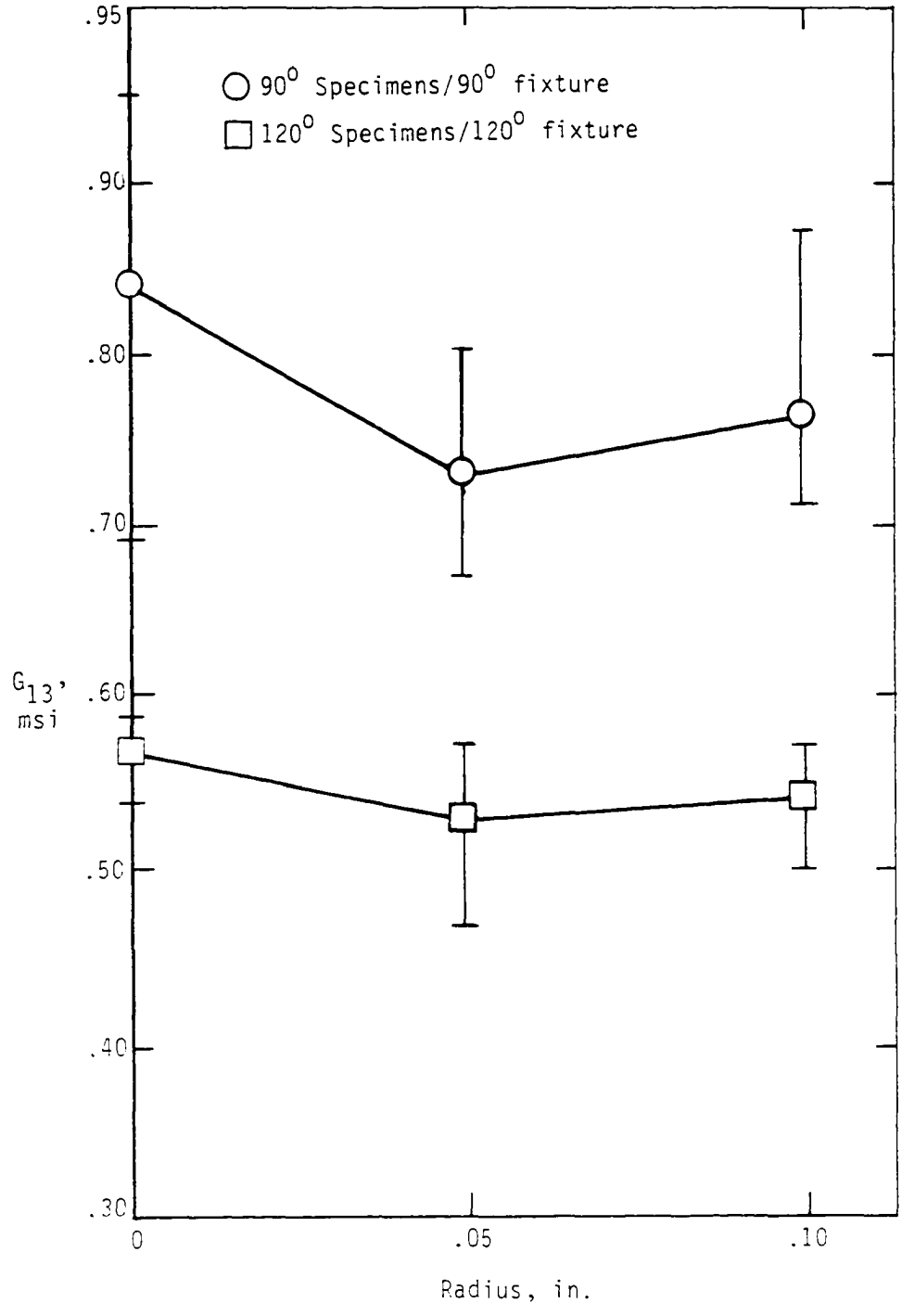

Fig. 6.45. Variation of the interlaminar shear modulus G_{13} with notch radius as tested in the Wyoming fixture.

Chapter 7

COMMENTS ON TEST PROCEDURES

Besides investigating the Iosipescu Shear test to determine if a specific notch geometry and fixture loading can produce an unambiguous state of shear, another purpose of this study was to determine the practicality of this test technique. Many times a researcher will report a new test method, but it is only after other investigators examine the technique will it be determined that the specimen is difficult to machine, the cost of manufacturing the fixture is exorbitant or the cost of running a series of tests is excessive in terms of man- and machine-hours. The Iosipescu Shear test was not unreasonable with time or money, but there were some annoying problems.

The machining of the Wyoming specimen was made difficult due to the strict dimensional tolerances of the Wyoming test fixture. It was necessary to hold the width of the specimen to the nearest thousandths of an inch so that the specimen would set in the fixture easily and not be subjected to bending moments. Even so, one had to develop an elaborate ritual in order to place the specimen in the fixture. The required strict tolerances made it necessary to cram the specimen into the fixture and the close fit made it difficult to align the specimen with the fixture and the load train. Indeed, even when using an alignment tool, one could never be sure if the specimen was cocked in

the fixture. It became necessary to preload the specimen in order to prevent the introduction of bending moments. Still, the stress-strain curves indicated that bending occurred during the initial phases of the test.

The AFPB fixture, on the other hand, was not as troublesome to handle in the laboratory. The specimen was easy to set and align in the fixture. It was only necessary to slide the bottom half of the fixture up and slip the specimen inbetween the fixture halves on each side. Sometimes it was necessary to pry the sides apart with a screwdriver, but this was a minor inconvenience compared to the Wyoming procedure. No preloading of the specimen was required and the stress-strain curves showed little or no initial bending.

The AFPB specimen took longer to machine than the Wyoming specimen. Because of its size, it was necessary to make two passes with a grinding wheel in order to cut the notch, versus only one pass for the smaller Wyoming specimen. Also, it took time to bond the doublers to the specimen and then to grind the specimen and doublers flush with one another. More time was used when it became necessary to pin the doublers to the specimens. Initially, a 0.75-inch gage section was utilized, but it was impossible to obtain a proper shear failure in the gage section with this width. After much trial and error experimentation, a 0.4-inch gage section with doublers pinned to the specimen was found to be the best test configuration for a quasi-isotropic lay-up.

In order to cut down on the machining costs of the AFPB specimen, different fixture modifications were attempted. Table 7.1 presents the data for specimens tested without doublers or with a rectangular bar placed along the edges to simulate a distributed loading. Without

Table 7.1 Results of AFPB fixture modifications

Modification	Specimen geometry (angle/radius)	T_{max} (psi)	G_{12} (Msi)
No doublers	90/0	<4833	3.41
Rectangular bars	90/0	>23013	3.52

doublers, the specimens were completely crushed under the loading cylinders at very low loads. With rectangular bars glued to the edges, it was found that the bars bent and deformed under the load cylinders as the test progressed, introducing ambiguous loading forces into the specimen. The shear moduli for the specimens compared favorably with the results given on Table 6.4 but the modifications themselves were completely useless. Obviously, doublers placed on the specimen were the best way to test for the shear properties.

Finite element studies were conducted to determine the effects of non-symmetric loading or bending on the stress state in the notch region. Ideally, the moment through the center of the notch of an Iosipescu Shear specimen should be zero, but in reality this may not always be possible due to bending if the specimen is not machined properly or if the specimen is not accurately aligned in the fixture.

The analysis was conducted by off-setting the load edges by 0.1 inches for a specimen with a 0.05-inch notch radius. The results of a specimen tested in a Wyoming fixture are given on Figs. 7.1 and 7.2, and in an AFPB fixture on Figs. 7.3 and 7.4. Note that the results are presented from notch tip to notch tip. Contour plots of the stresses are shown on Figs. 7.5 and 7.6.

The detrimental effects on the stress state can clearly be seen. Both specimens follow the same trends for σ_x, σ_y and T_{xy}. The magnitude of the bending stress at the notch tips is greater for the AFPB specimen than for the Wyoming specimen, but the transverse stresses are much lower for the AFPB specimen. These effects are due to the greater loading distance for the AFPB specimen. The shear stress distributions for the two specimens are identical. They indicate that a

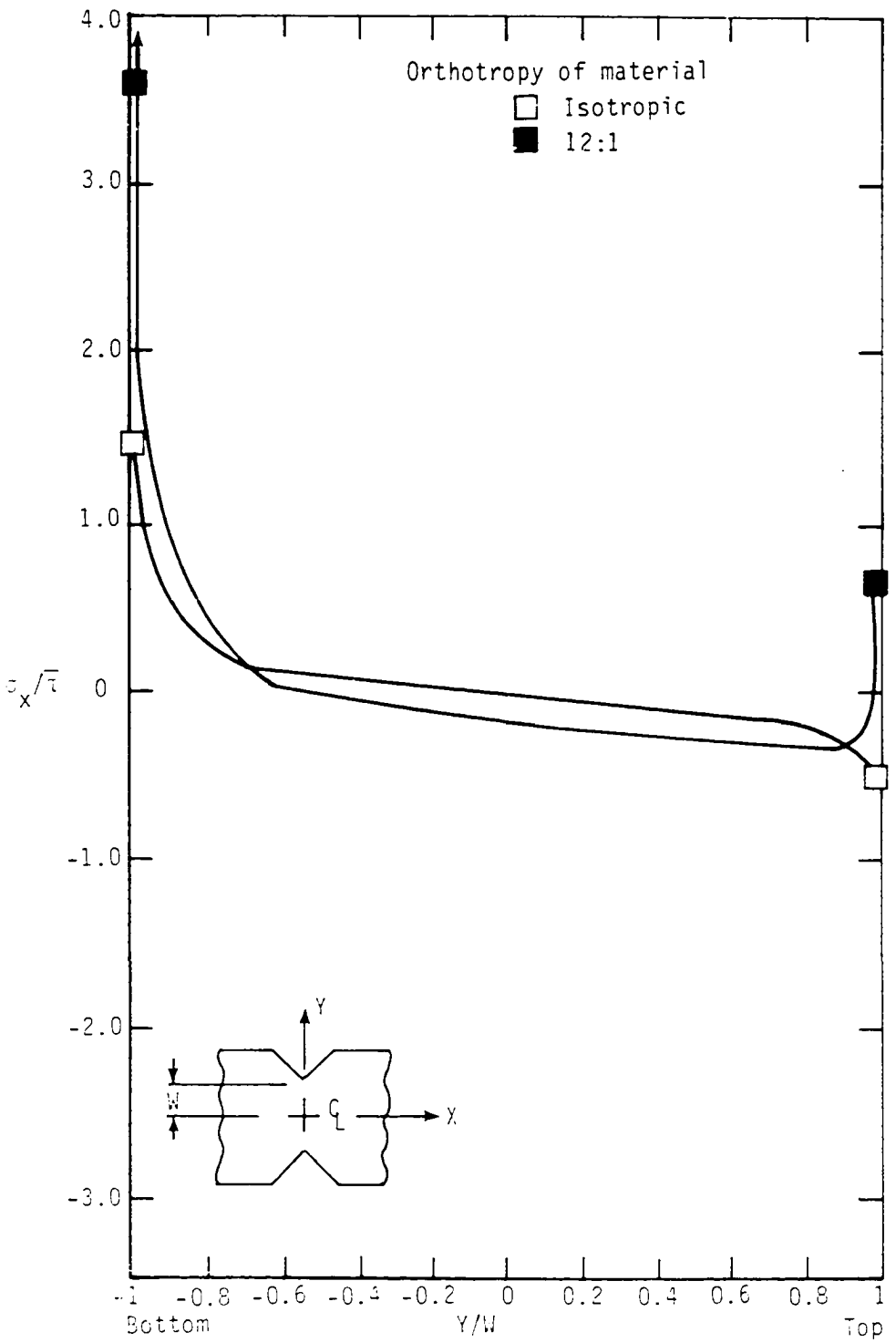

Fig. 7.1. Variation of σ_x in various materials with a notch radius of 0.05 inches due to non-symmetric loading in the Wyoming fixture.

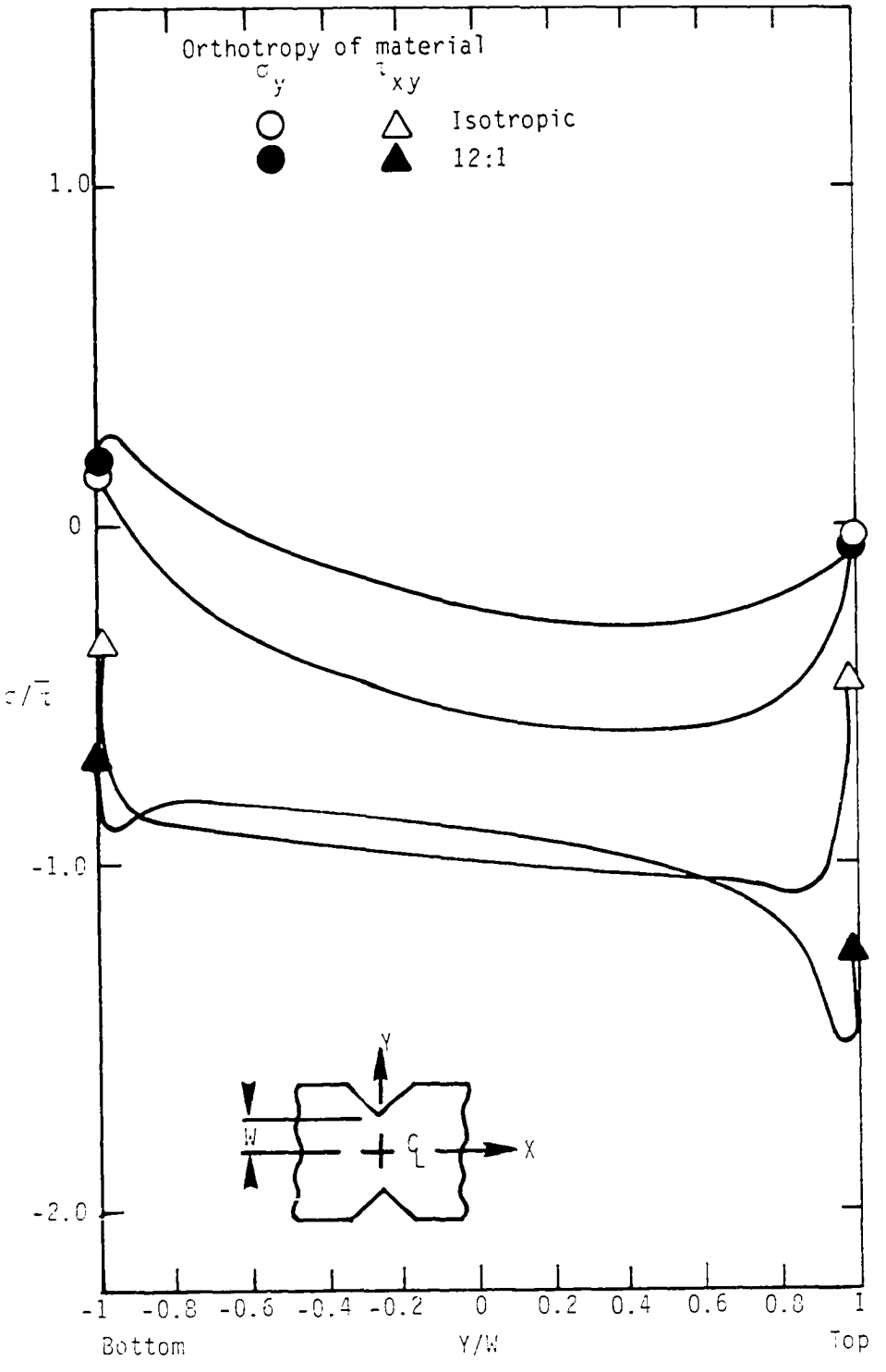

Fig. 7.2. Variation of σ_y and τ_{xy} in various materials with a notch radius of 0.05 inches due to non-symmetric loading in the Wyoming fixture.

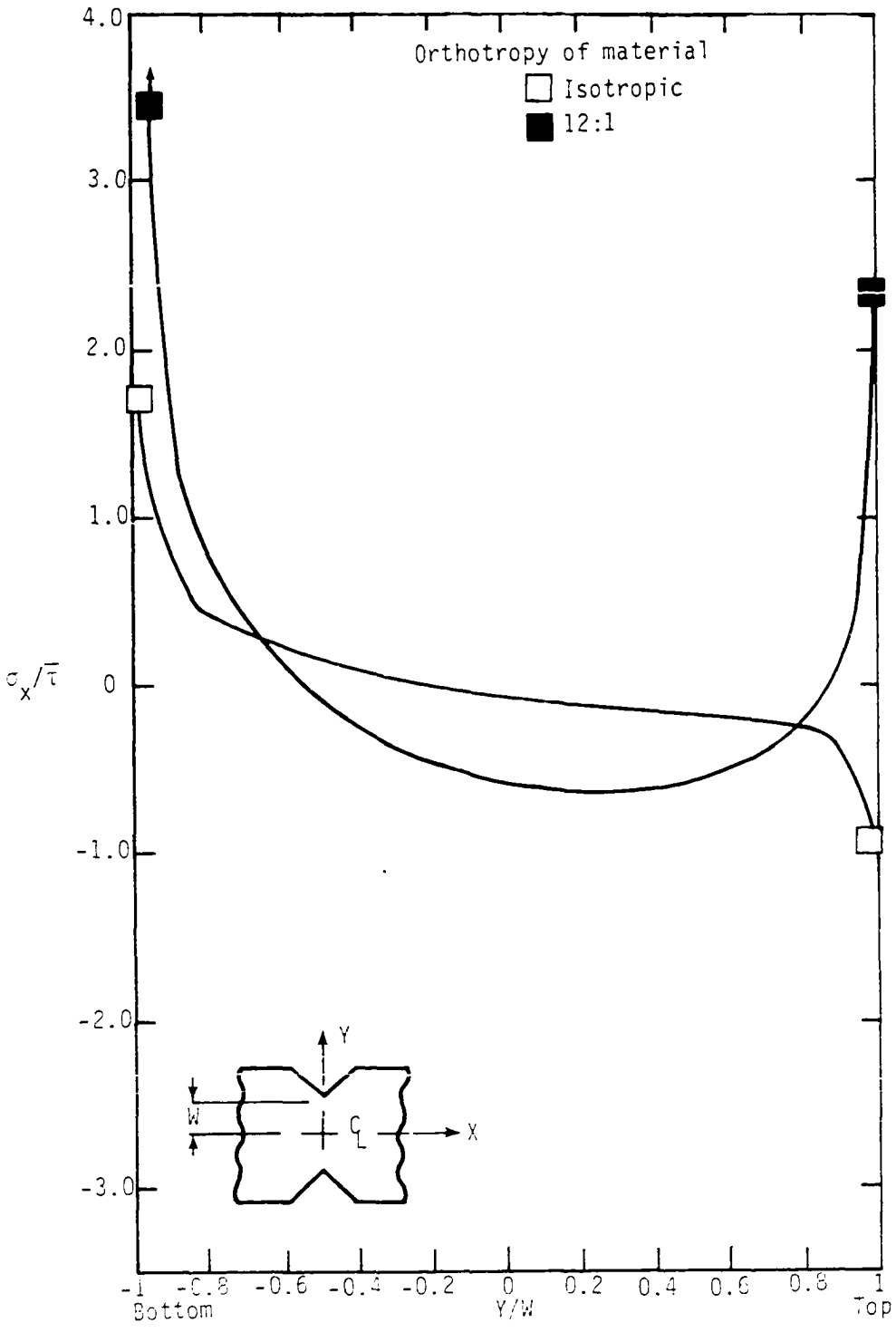

Fig. 7.3. Variation of σ_y in various materials with a notch radius of 0.05 inches due to non-symmetric loading in the AFPB fixture.

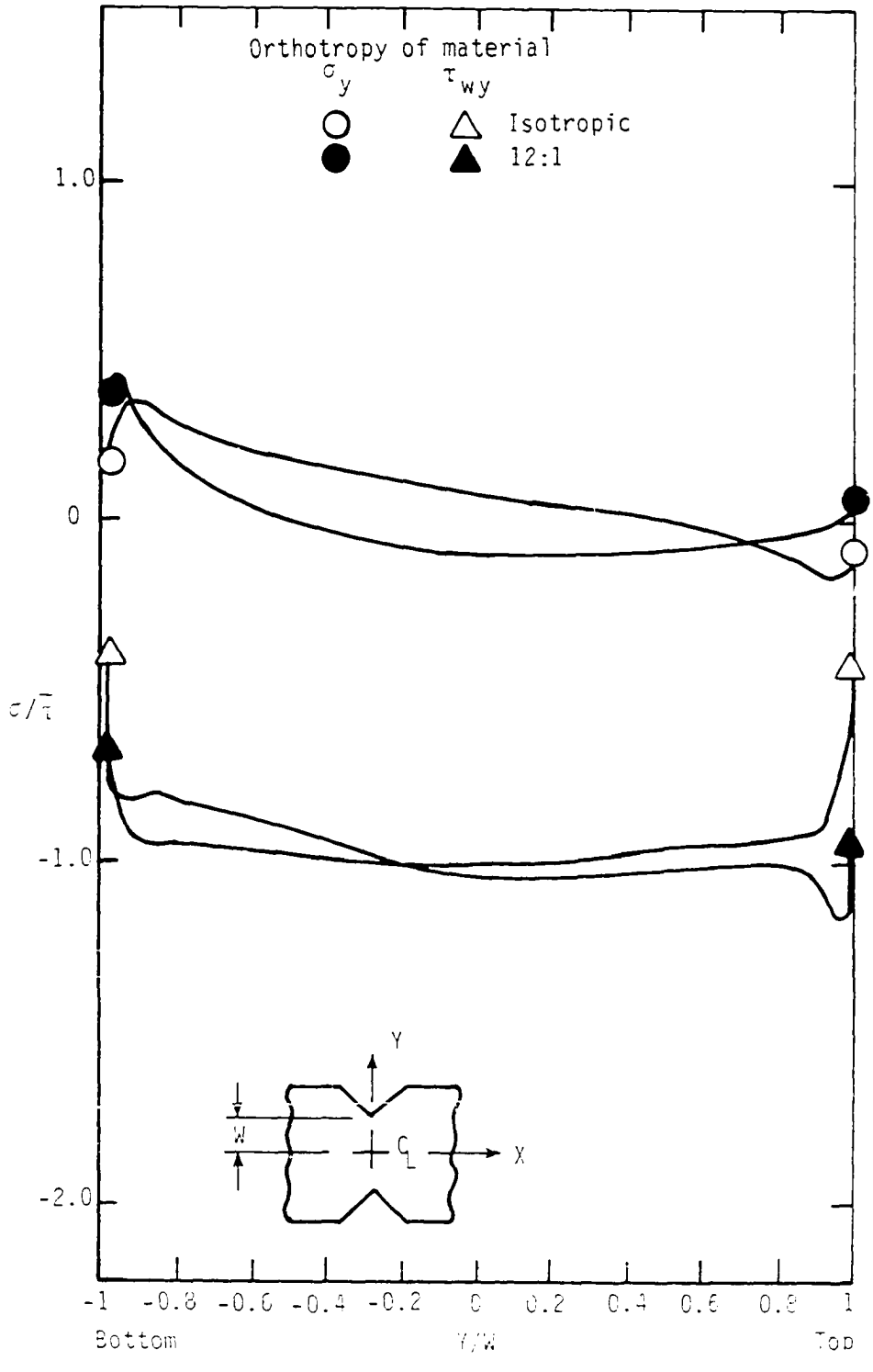

Fig. 7.4. Variation of σ_y and τ_{xy} in various materials with a notch radius of 0.05 inches due to non-symmetric loading in the AFPB fixture.

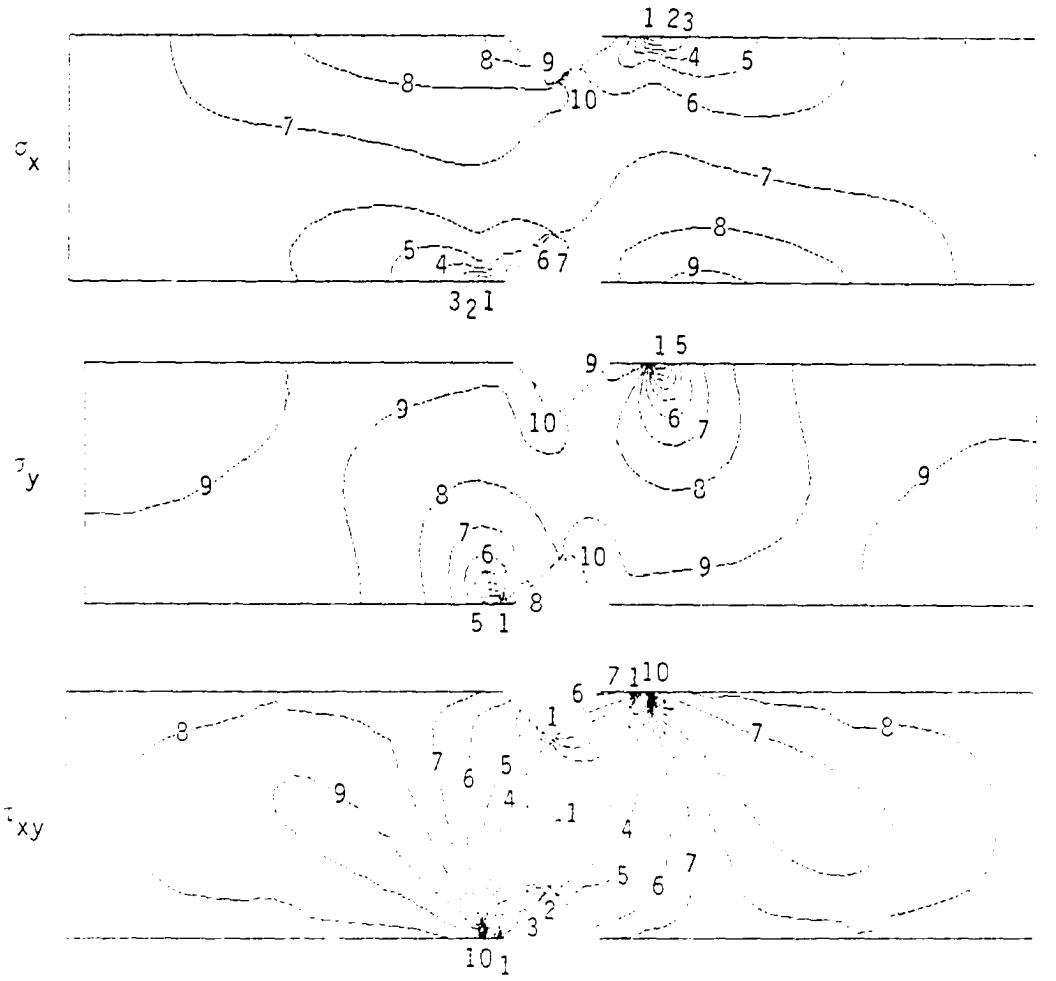

Contour number	Stress σ_x	σ_y	τ_{xy}
1	-3.2	-4.4	-1.2
2	-2.6	-3.9	-1.0
3	-2.1	-3.4	-0.8
4	-1.5	-2.8	-0.6
5	-1.0	-2.3	-0.5
6	-0.4	-1.7	-0.3
7	0.1	-1.2	-0.1
8	0.7	-0.6	0.1
9	1.2	-0.1	0.3
10	1.8	0.5	0.5

Fig. 7.5. Contour plots of an isotropic specimen due to non-symmetric loading in the Wyoming fixture.

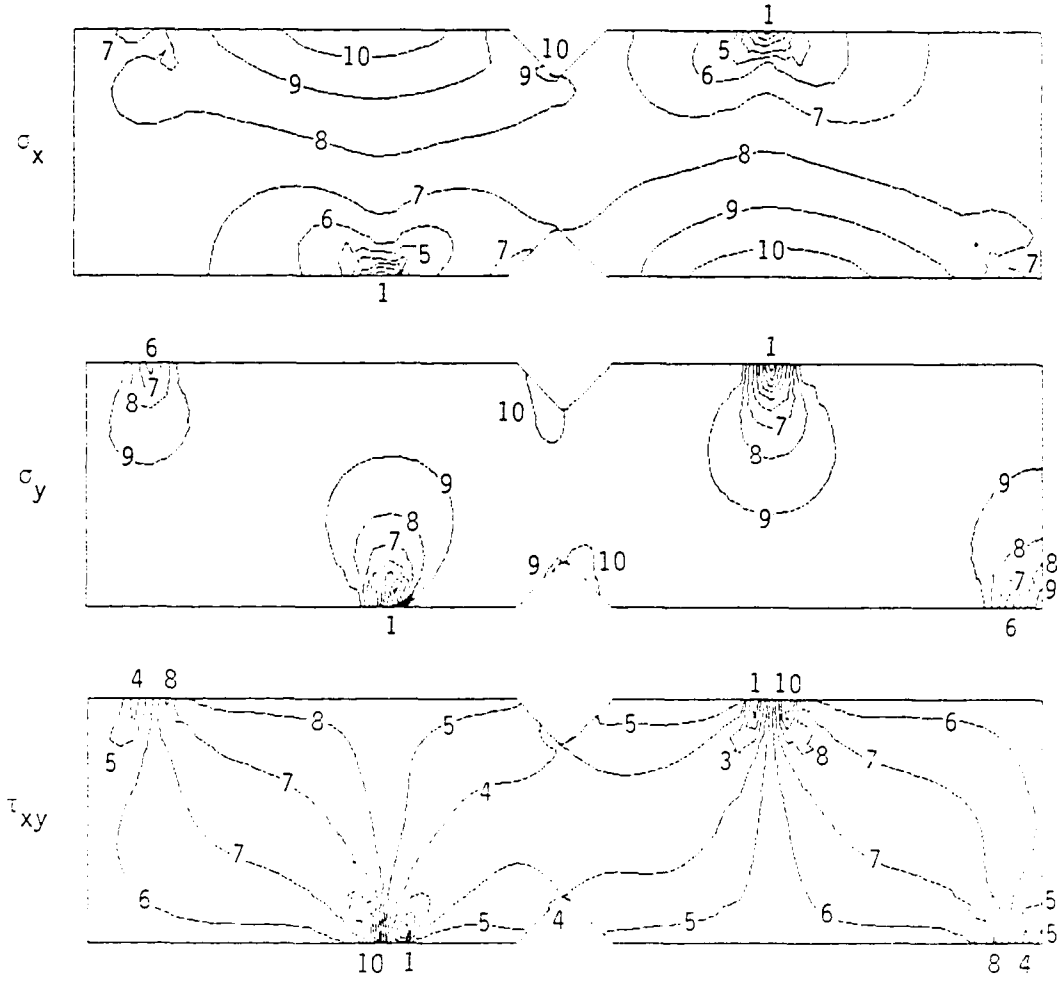

Contour number	Stress σ_x	σ_y	τ_{xy}
1	-5.5	-7.7	-2.1
2	-4.6	-6.8	-1.6
3	-3.8	-5.9	-1.2
4	-3.0	-5.0	-0.7
5	-2.2	-4.1	-0.3
6	-1.4	-3.2	0.2
7	-0.6	-2.3	0.6
8	0.2	-1.5	1.1
9	1.0	-0.6	1.5
10	1.8	0.3	1.9

Fig. 7.6. Contour plots of an isotropic specimen due to non-symmetric loading in the AFPB fixture.

non-symmetric loading of 0.1 inch will result in a 5 percent gradient through the center of the specimen for an isotropic material and a 20 percent gradient for an orthotropic material, excluding the results at the notch tip.

Based upon the problems described above, it appears that the AFPB fixture is superior to the Wyoming apparatus for use in a laboratory setting. The time involved in bonding and grinding the doublers on the AFPB specimen is insignificant when compared to the alignment problems associated with the Wyoming fixture. One can be assured of reasonable results with the AFPB fixture even though a point loading is used, and the fact that the shear stress is a function of the loading point location is only a minor nuisance to the experimentalist. It is known that Walrath and Adams are currently modifying their test fixture [39], but it remains to be seen if the alignment problems and the requirements for strict dimensional tolerances can be adequately resolved in order to make this test fixture reliable in the laboratory.

Chapter 8

CONCLUSIONS

A linear elastic finite element analysis has shown that the Iosipescu Shear test produces a region of uniform shear stress in the test section. Effects attributed to notch geometry and loading location significantly influenced the magnitude and the purity of the shear stress in the notched region. The analysis showed that a specimen should be loaded at least 0.5 to 0.9 inches from the notch edges in order to prevent load transfer mechanisms from dominating the stress state in the gage section. These loading distances are applicable to either isotropic or orthotropic materials, though one must be aware that a loading distance of 0.5 inches may result in high transverse stresses and a loading distance of 0.9 inches may result in high bending stresses. The choice of loading distance is dependent upon the material and the material properties that one is seeking, but it is suggested that a loading distance of 0.9 inches be used for determining the shear properties of most composite materials. The analysis also showed that a notch radius of at least 0.05 inches will significantly reduce the magnitude of the normal and shear stress concentrations.

The experimental results were to verify the conclusions of the finite element analysis. However the trends demonstrated by the experimental data appear to have been influenced by free edge effects. The failures of the quasi-isotropic specimens exhibit evidence of matrix cracks propagating from the free edge into the interior of the specimen, particularly along the interface between the +45-degree and -45-degree laminae where the interlaminar shear stresses are at a maximum.

This matrix failure was probably triggered by the discontinuity of the fibers in the notch region. As the notch angle or notch radius increased, the number of discontinuous fibers increased, and the failure strengths of the specimens deteriorated accordingly. The shear modulus also degraded as the number of discontinuous fibers increased, substantiating previous suppositions that free edge effects reduce the material stiffness in addition to the material strength.

The practicality of the Iosipescu Shear test in the laboratory was clearly demonstrated. Examinations of two loading fixtures were conducted, and despite minor disadvantages with both, it was concluded that the Asymmetrical Four-Point Bend test fixture was simpler in application and less costly to utilize in the laboratory setting.

In summary, the Iosipescu Shear test is but the latest in a long series of test methods that have attempted to induce an unambiguous state of pure shear in a composite material. Refinement of this test technique is still required and further research into the stress/strain fields in the notched region is of paramount importance. Such inquiries should determine if the Iosipescu Shear test can produce a state of pure shear, or if indeed any test method can induce pure, uniform shear in a composite material.

REFERENCES

1. Pagano, N. J., "Observations on Shear Test Methods of Composite Materials," Technical Memorandum MAN 67-16, Air Force Materials Laboratory, September 1967.

2. Prosen, S. P., "Composite Materials Testing," Composite Materials: Testing and Design, ASTM STP 460, 1969, pp. 5-12.

3. Lyle, D. P., "Shear Testing of Continuous Fiber Reinforced Plastics," 37th Annual Conference, Reinforced Plastics/Composites Institute, The Society of the Plastics Industry, January 1982, pp. 1-7.

4. Chiao, C. C., Moore, R. L., and Chiao, T. T., "Measurement of Shear Properties of Fibre Composites, Part 1. Evaluation of Test Methods," Composites, Vol. 8, No. 3, July 1977, pp. 161-169.

5. Terry, G., "A Comparative Investigation of Some Methods of Unidirectional, In-Plane Shear Characterization of Composite Materials," Composites, Vol. 10, No. 4, October 1979, pp. 233-237.

6. Slepetz, J. M., Zageski, T. F., and Novello, R., "In-Plane Shear Test for Composite Materials," AMMRC TR 78-30, Army Materials and Mechanics Research Center, July 1978.

7. Markham, M. F. and Dawson, D., "Interlaminar Shear Strength of Fibre-Reinforced Composites," Composites, Vol. 6, No. 4, July 1975, pp. 173-176.

8. Berg, C. A., Tirosh, J., and Israeli, M., "Analysis of Short Beam Bending of Fiber Composites," Composite Materials: Testing and Design, ASTM 497, 1972, pp. 206-218.

9. Phillips, D. C. and Scott, J. M., "The Shear Fatigue of Unidirectional Fiber Composites," Composites, Vol. 8, No. 4, October 1977, pp. 233-238.

10. Stinchcomb, W. W., Henneke, E. G., and Price, H. L., "Use of the Short-Beam Shear Test for Quality Control of Graphite Polymide Laminates," Reproducibility and Accuracy of Mechanical Tests, ASTM 626, 1977, pp. 96-109.

11. Werren, F. and Heebink, G., "Interlaminar Shear Strength of Glass-Fiber-Reinforced Plastic Laminates," Report No. 1848, Forest Products Laboratory, September 1955.

12. Zabora, R. F. and Bell, J. E., "A Test Technique to Study Interlaminar Shear Phenomena of Laminated Composites," Technical Report AFFDL-TR-71-67, Air Force Flight Dynamics Laboratory, July 1971.

13. Iosipescu, N., "New Accurate Procedure of Single Shear Testing of Metals," Journal of Materials, Vol. 2, No. 3, September 1967, pp. 537-566.

14. Peters, P. W. M., "The Interlaminar Shear Strength of Unidirectional Boron Aluminum Composites," Journal of Composite Materials, Vol. 12, January 1978, pp. 53-62.

15. Bergner, H. W., Davis, J. G., and Herakovich, C. T., "Analysis of Shear Test Method for Composite Laminates," Report VPI-E-77-14, Virginia Polytechnic Institute and State University, April 1977.

16. Loveless, H. S. and Ellis, J. H., "A Comparison of Methods for Determining the Shear Properties of Glass/Resin Unidirectional Composites," Journal of Testing and Evaluation, Vol. 5, No. 5, September 1977, pp. 369-374.

17. Romstad, K., "Methods for Evaluating Shear Strength of Plastic Laminates Reinforced with Unwoven Glass Fibers," Report FPL-033, Forest Products Laboratory, May 1964.

18. Whitney, J. M., Stansbarger, D. L., and Howell, H. B., "Analysis of the Rail Shear Test-Applications and Limitations," Journal of Composite Materials, Vol. 5, January 1971, pp. 24-34.

19. Duggan, M. F., "An Experimental Evaluation of the Slotted-Tension Shear Test for Composite Materials," Experimental Mechanics, Vol. 20, No. 7, July 1980, pp. 233-239.

20. Weisshar, T. A. and Garcia, R., "Analysis of Graphite/Polymide Rail Shear Specimens Subjected to Mechanical and Thermal Loading," NASA Contractor Report 3106, March 1979.

21. Yeow, Y. T. and Brinson, H. F., "A Comparison of Simple Shear Characterization Methods for Composite Laminates," Composites, Vol. 9, No. 1, January 1978, pp. 49-55.

22. Sims, D. F., "In-Plane Shear Stress-Strain Response of Unidirectional Composite Materials," Journal of Composite Materials, Vol. 7, January 1973, pp. 124-128.

23. Adsit, N. R., McCutchen, H., and Forest, J. D., "Shear Testing of Advanced Composites," Composite Materials in Engineering Design, Proceedings of the Sixth Symposium, May 1972, pp. 448-460.

24. Kadotani, K. and Aki, F., "Analysis of the Interlaminar Shear Strength of Mica/Epoxy Insulations," Composites, Vol. 5, No. 1, January 1984, pp. 57-60.

25. Bush, H. G. and Weller, T., "A Biaxial Method for Inplane Shear Testing," NASA Technical Memorandum 74070, April 1978.

26. Arcan, M., Hashin, Z., and Voloshin, A., "A Method to Produce Uniform Plane-Stress Strain with Applications to Fiber-Reinforced Materials," Experimental Mechanics, Vol. 18, No. 4, April 1978, pp. 141-146.

27. Hadcock, R. N. and Whiteside, J. B., "Special Problems Associated with Boron-Epoxy Mechanical Test Specimens," Composite Materials: Testing and Design, ASTM STP 460, 1969, pp. 27-36.

28. Farley, G. L. and Baker, D. J., "In-Plane Shear Test of Thin Panels," Experimental Mechanics, Vol. 23, No. 1, March 1983, pp. 81-88.

29. Greszczuk, L. B., "Shear Modulus Determination of Isotropic and Composite Materials," Composite Materials: Testing and Design, ASTM STP 460, 1969, pp. 140-149.

30. Duggan, M. F., McGrath, J. T., and Murphy, M. A., "Shear Testing of Composite Materials by a Simple Combined-Loading Technique," AIAA Paper 78-50B, AIAA/ASME 19th Structures, Structural Dynamics and Materials Conference, April 1978, pp. 311-319.

31. Petit, P. H., "A Simplified Method of Determining the Inplane Shear Stress-Strain Response of Unidirectional Composites," Composite Materials: Testing and Design, ASTM STP 460, 1969, pp. 83-93.

32. Rosen, B. W., "A Simplified Procedure for Experimental Determination of the Longitudinal Shear Modulus of Unidirectional Composites," Journal of Composite Materials, Vol. 6, October 1972, pp. 552-554.

33. Hahn, H. T., "A Note on Determination of the Shear Stress-Strain Response of Unidirectional Composites," Journal of Composite Materials, Vol. 7, July 1973, pp. 383-386.

34. Chamis, C. C. and Sinclair, J. H., "Ten-deg Off-Axis Test for Shear Properties in Fiber Composites," Experimental Mechanics, Vol. 17, No. 9, September 1977, pp. 339-346.

35. Nemeth, M. P., Herakovich, C. T., and Post, D., "On the Off-Axis Tension Test for Unidirectional Composites," Composites Technology Review, Vol. 5, No. 2, Summer 1983, pp. 61-68.

36. Greszczuk, L. B., "Experimental Determination of Shear Moduli of Fiber-Reinforced Anisotropic Laminates," Society for Experimental Stress Analysis, Spring Meeting, May 1967.

37. Walrath, D. E. and Adams, D. F., "The Iosipescu Shear Test as Applied to Composite Materials," Experimental Mechanics, Vol. 23, No. 1, March 1983, pp. 105-110.

38. Adams, D. F. and Walrath, D. E., "Iosipescu Shear Properties of SMC Composite Materials," Composite Materials: Testing and Design, ASTM STP 787, American Society for Testing and Materials, 1982, pp. 9-33.

39. Walrath, D. E. and Adams, D. F., "An Analysis of the Stress State in an Iosipescu Shear Test Specimen," Report UWME-DR-301-102-1, Dept. of Mechanical Engineering, University of Wyoming, June 1983.

40. Arcan, M. and Goldenberg, N., "On a Basic Criterion for Selecting a Shear Testing Standard for Plastic Materials," ISO/TC 61-WG 2 Sp. 171, Burgenstock-Switzerland, 1957.

41. Goldenberg, N., Arcan, M., and Nicolau, E., "On the Most Suitable Specimen Shape for Testing Shear Strength of Plastics," International Symposium on Plastics Testing and Standards, ASTM STP 247, American Society for Testing and Materials, 1958, pp. 115-121.

42. Voloshin, A. and Arcan, M., "Pure Shear Moduli of Unidirectional Fibre-Reinforced Materials (FRM)," Fibre Science and Technology, Vol. 13, March-April 1980, pp. 125-134.

43. Marloff, R. H., "Finite Element Analysis of Biaxial Stress Test Specimen for Graphite/Epoxy and Glass Fabric/Epoxy Composites," Composite Materials: Testing and Design, ASTM STP 787, 1982, pp. 34-49.

44. Arcan, M., "The Iosipescu Shear Test as Applied to Composite Materials: Discussion," Experimental Mechanics, Vol. 24, No. 1, March 1984, pp. 66-67.

45. Popov, E. P., Mechanics of Materials, Second Edition, Prentice-Hall, Englewood Cliffs, N.J., 1976, pp. 570-571.

46. Communication with Lockheed-Georgia, February 8, 1982.

47. Whitney, J. M., "Free Edge Effects in the Characterization of Composite Materials," Analysis of the Test Methods for High Modulus Fibers and Composites, ASTM STP 521, American Society for Testing and Materials, 1973, pp. 167-180.

48. Pipes, R. B., Kaminski, B. E., and Pagano, N. J., "Influence of the Free Edge upon the Strength of Angle-Ply Laminates," Analysis of the Test Methods for High Modulus Fibers and Composites, ASTM STP 521, American Society for Testing and Materials, 1973, pp. 218-228.

49. Wang, A. S. D. and Crossman, F. W., "Some New Results on Edge Effect in Symmetric Composite Laminates," Journal of Composite Materials, Vol. 11, January 1977, pp. 92-106.